Mediterranean algal mariculture potential under global climate change

Zvy Dubinsky

Faculty of Life Sciences,Bar-Ilan University, Israel.

Solar radiation and the underwater light field

The sun as the source of energy for life on Earth

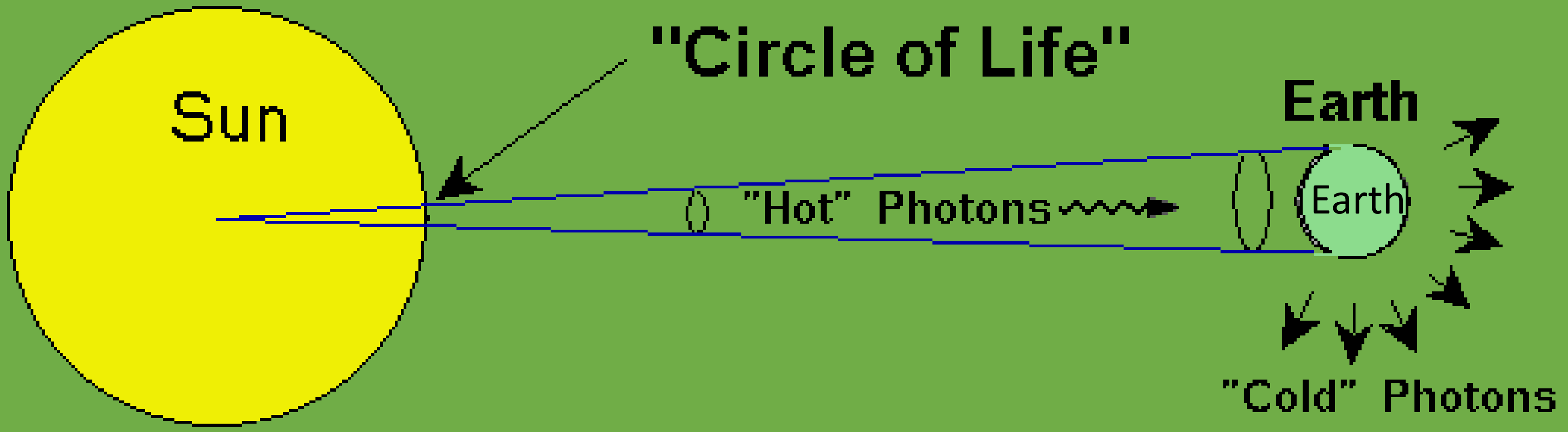

The energy needed to sustain life on Earth arrives as sunlight, through the process of PHOTOSYNTHESIS, by which light energy is converted into energy in organic compounds supporting all of life processes. That energy is then converted to heat, and dissipated in space.

The flow of energy through the biosphere

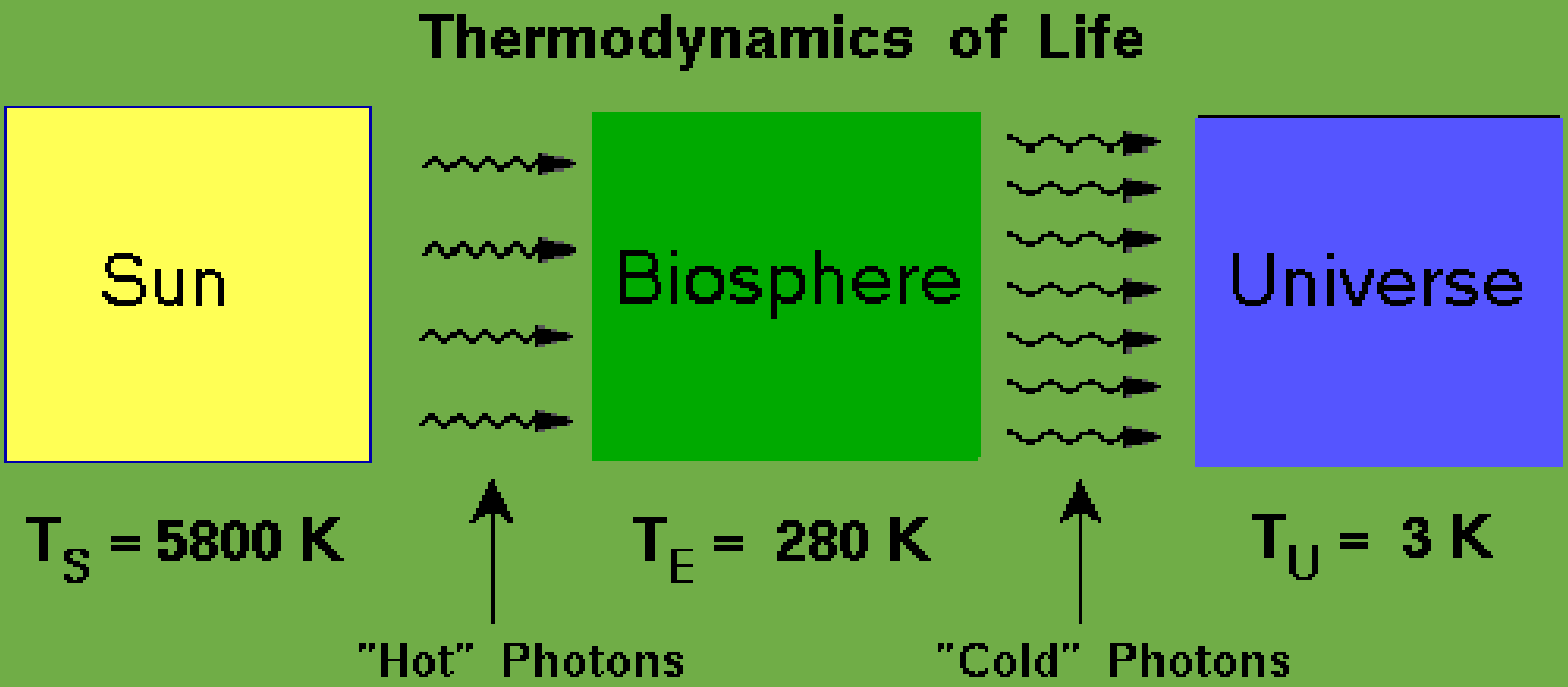

Radiation and temperature

- **The temperature of the sun's core is 20,000,000 degrees, but the radiation of any body depends on its surface temperature, which for the sun is 5760 ^{0}K,**

- The Stefan–Boltzmann constant

- **$\sigma = 5.673 X 10^{-8}$ $Js^{-1}m^{-2}K^{-4}$**

- The radiation emitted by a square meter of the body surface (flux) is

- **$\mathfrak{R} = \sigma K^4$ Js^{-1} (W)m^{-2}**

- **$\mathcal{R}= \sigma \times T^4\ Wm^{-2}$**

$\mathcal{R}= 5.673X10^{-8} \times 5760^4\ Wm^{-2}$

- For the entire sun

$\mathcal{R}= 5.673X10^{-8} \times 5760^4\ [Wm^{-2}] \times 4\pi\ r^2\ [m^2]\ W$

- The radius of the sun is $r = 6.965 \times 10^8$

Wein's law

$$\lambda_{max}[m] = \frac{289.7 \times 10^{-5}\ {}^{o}K\ [m]}{T[{}^{o}K]}$$

For the sun whose surface is at 5760 ^{o}K

$\lambda_{max} = 5.18X10^{-7}$ m = 518 nm

Spectral curves of radiating bodies

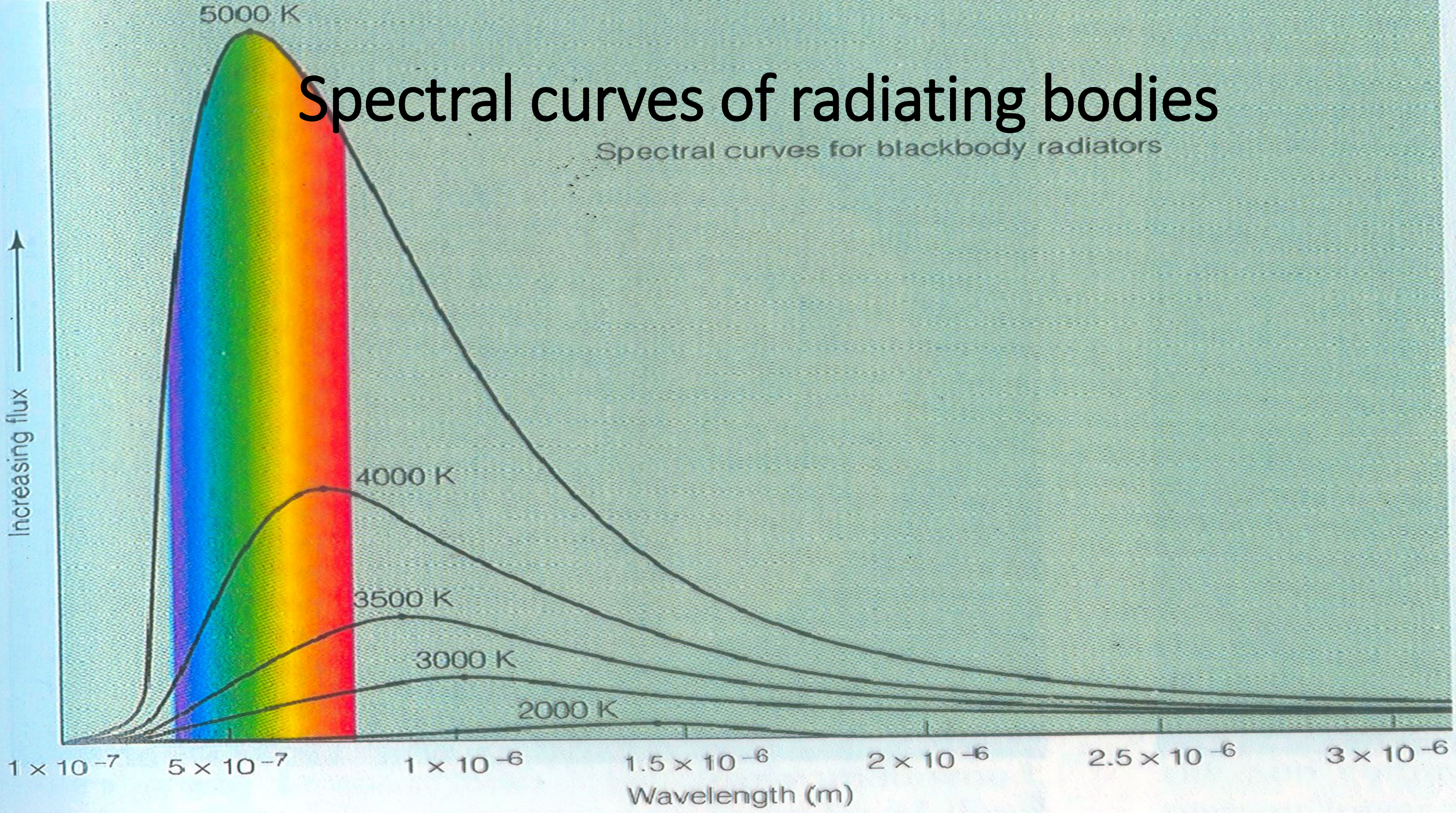

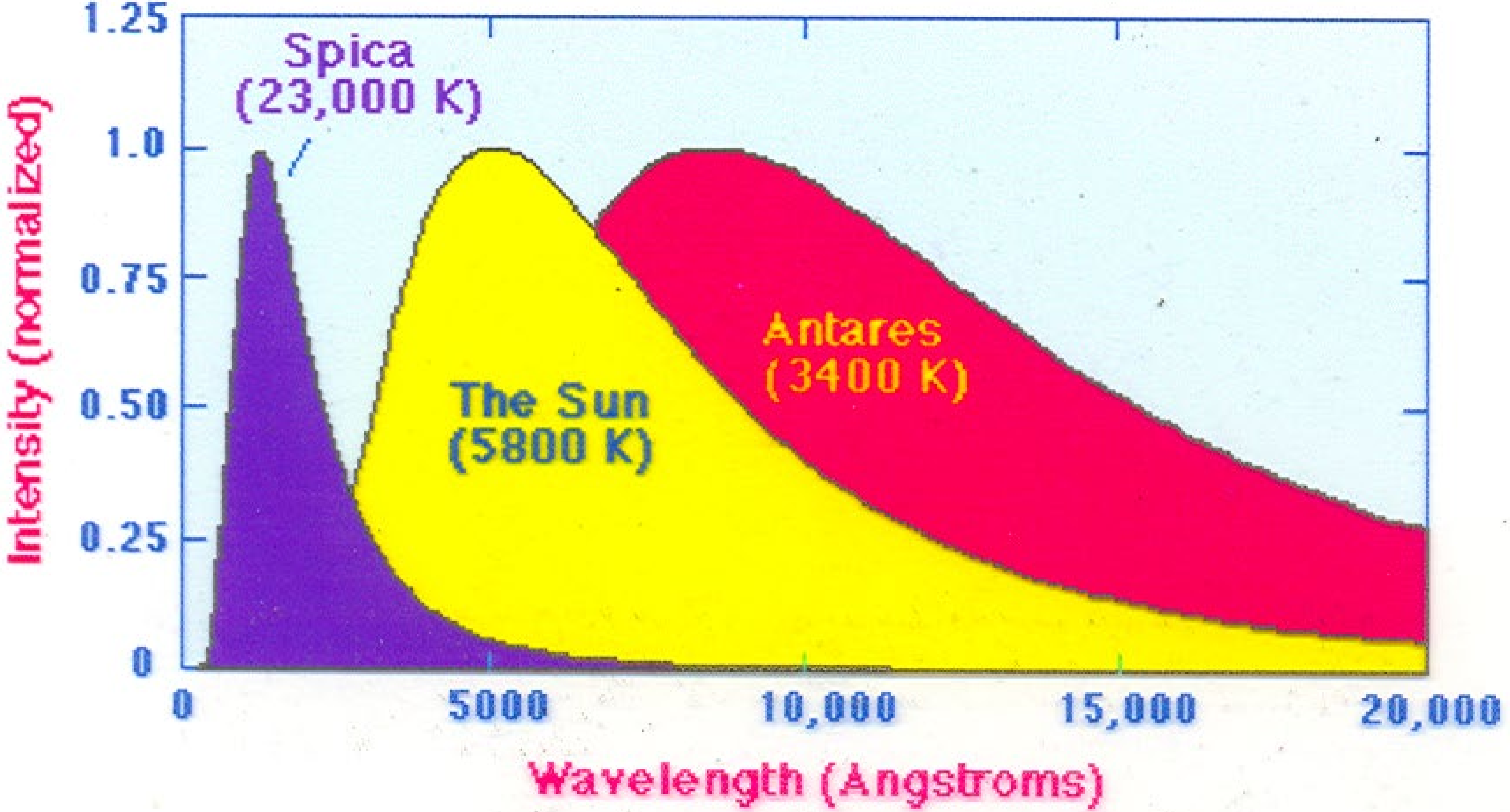

Spica
(23,000 K)
The Sun
(5800 K)
Antares
(3400 K)
Intensity (normalized)
1.25
1.0
0.75
0.50
0.25
0
0
5000
10,000
15,000
20,000
Wavelength (Angstroms)

Total solar energy reaching Earth depends on

Sun's .1

K ,temperature

Sun's surface .2

area $\underline{4\pi r^2}$

Earth's .3

distance from the sun, d

Earth's Projected area .4

of Earth's shadow

$\underline{\pi a^2}$

Earth's surface .5

area $\underline{4\pi a^2}$

Earth's radius

$a = 6.37 \times 10^6 m$

וכל m^2 של פניו יקבל בממוצע

$$S = \frac{\sigma\ {}^{o}K^4 \times 4\pi r^2 \times \pi a^2}{4\pi d^2 \times 4\pi a^2}$$

$$S = \frac{\sigma\ {}^{o}K^4 \times (r^2/d^2) \times \pi a^2}{4\pi a^2}$$

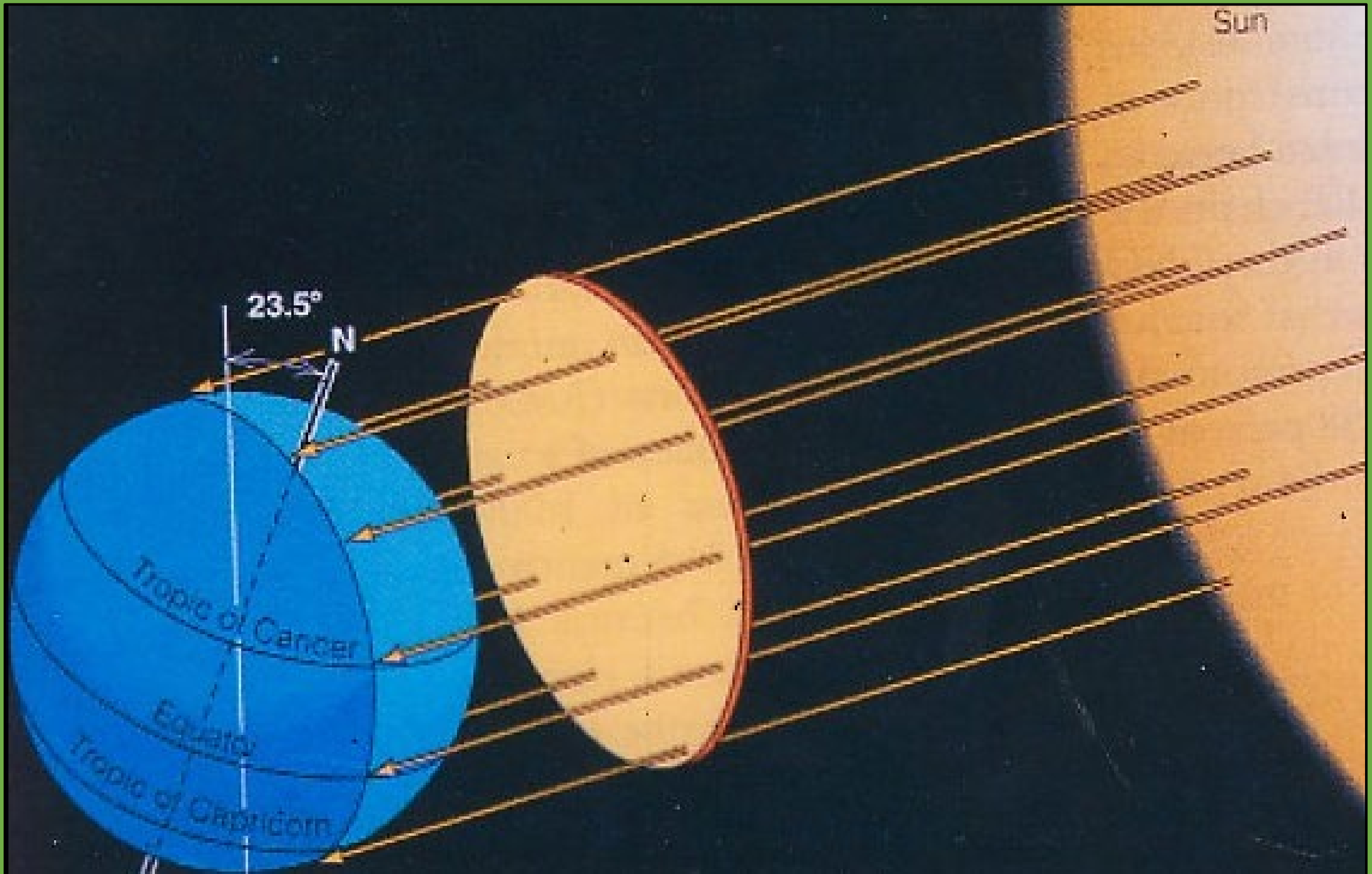

Albedo of the Earth = 0.39

Of that, part, the albedo (between 1 and 0, for Earth 0.4), is reflected back to space.

Thus the surface temperature of any planet assuming no atmosphere and no residual internal heat can be calculated as follows.

$Energy_{in} = Energy_{out}$

$\sigma\ {}^{o}K_{SUN}{}^{4} \times (r^2/d^2)/4 \times (1- 0.4)= \sigma\ {}^{o}K^4{}_{surface}$

${}^{o}K^4{}_{surface}=0.6\ {}^{o}K_{SUN}{}^{4} \times (r^2/d^2)/4$

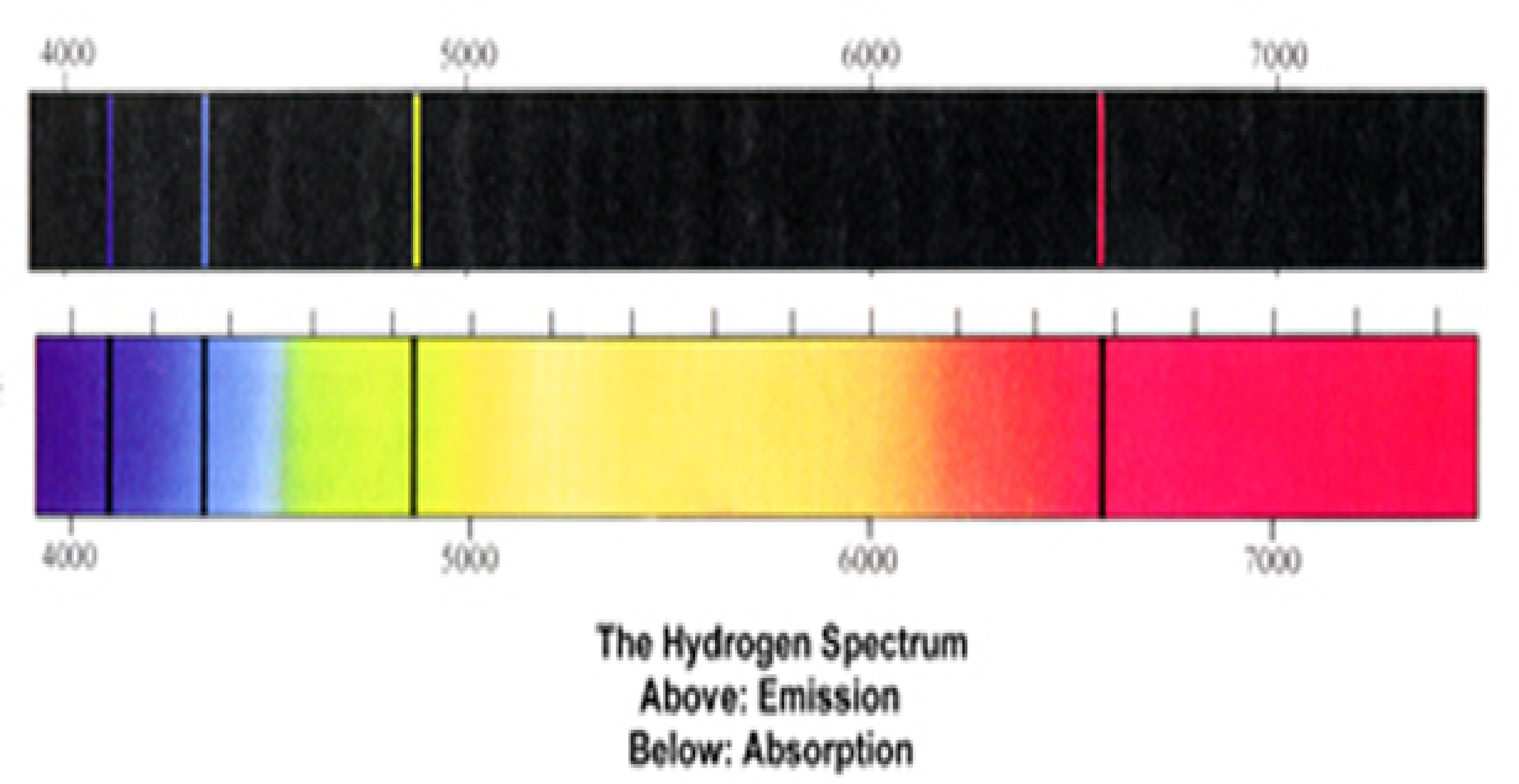

- Of the red shift we know from the position of the hydrogen absorption and emission lines

Star spectra contain information of the elements in it

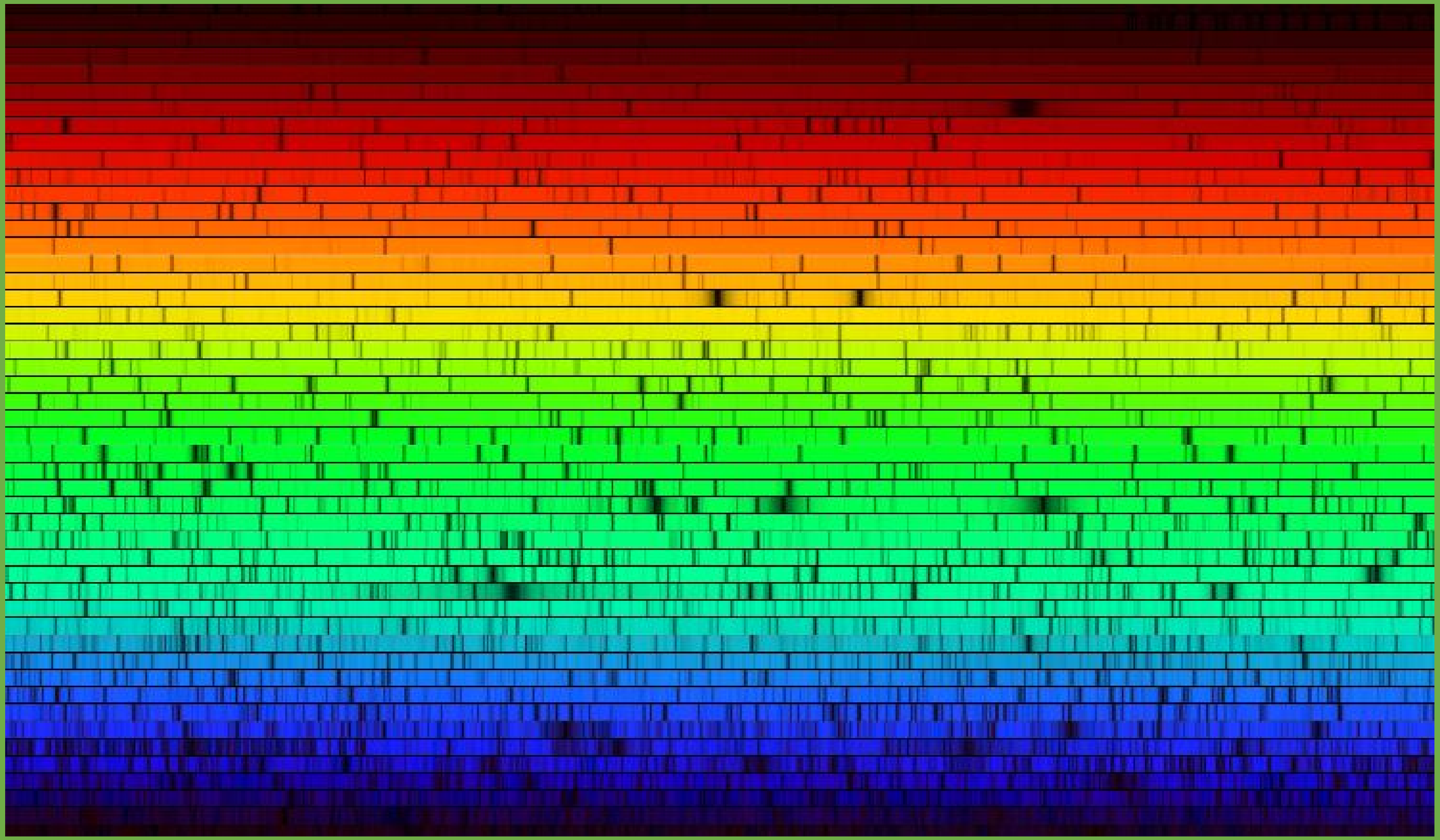

- **<u>UV radiation includes</u> UV-A**, the least dangerous form of UV radiation, with a wavelength range between 315nm to 400nm, **UV-B** with a wavelength range between 280nm to 315nm, and **UV-C** which is the most dangerous between 100nm to 280nm. UV-C is unable to reach Earth's surface due to stratospheric ozone's ability to absorb it. (Last, 2006)

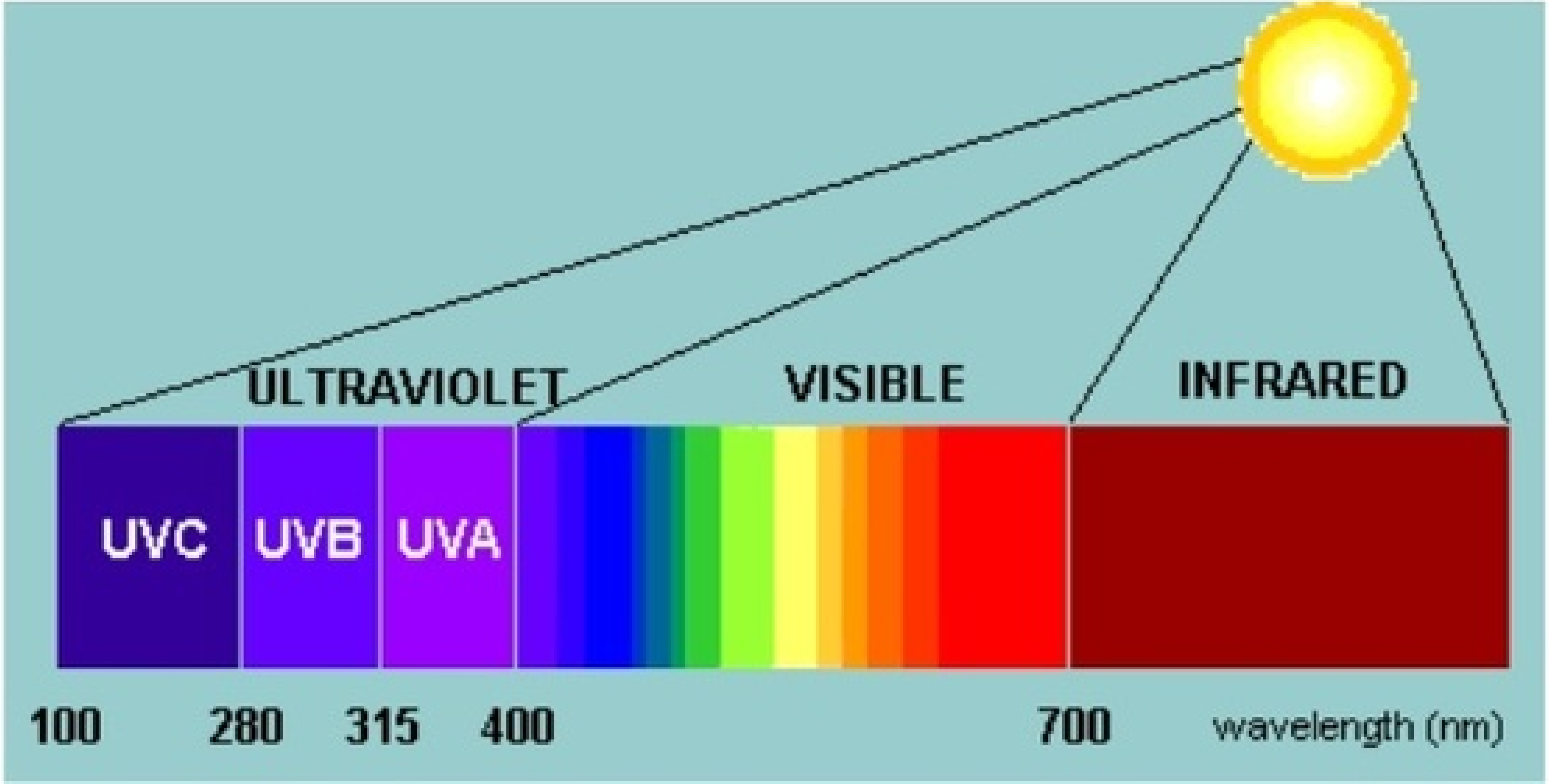

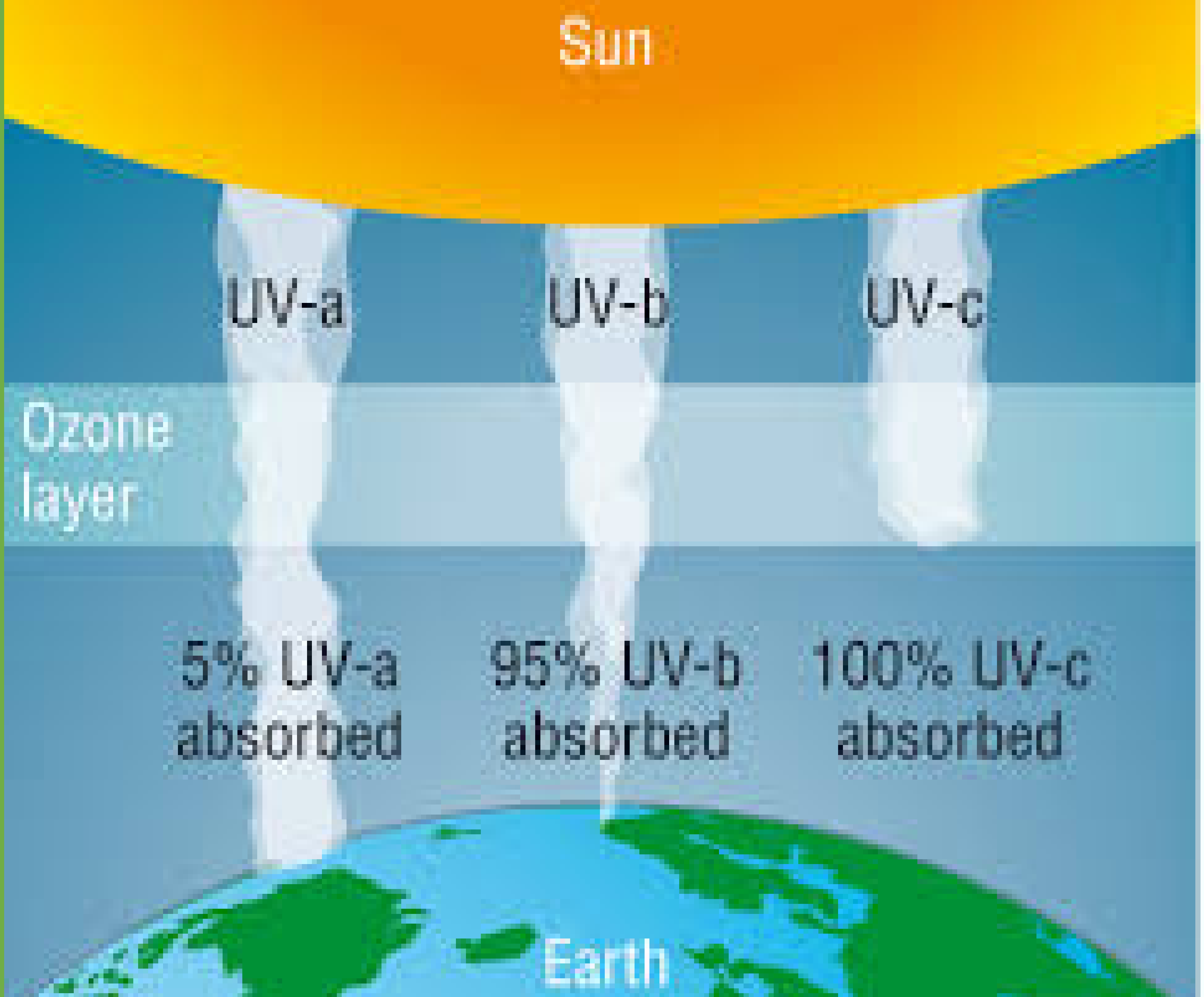
Sun
UV-a
UV-b
UV-c
Ozone layer
5% UV-a absorbed
95% UV-b absorbed
100% UV-c absorbed
Earth

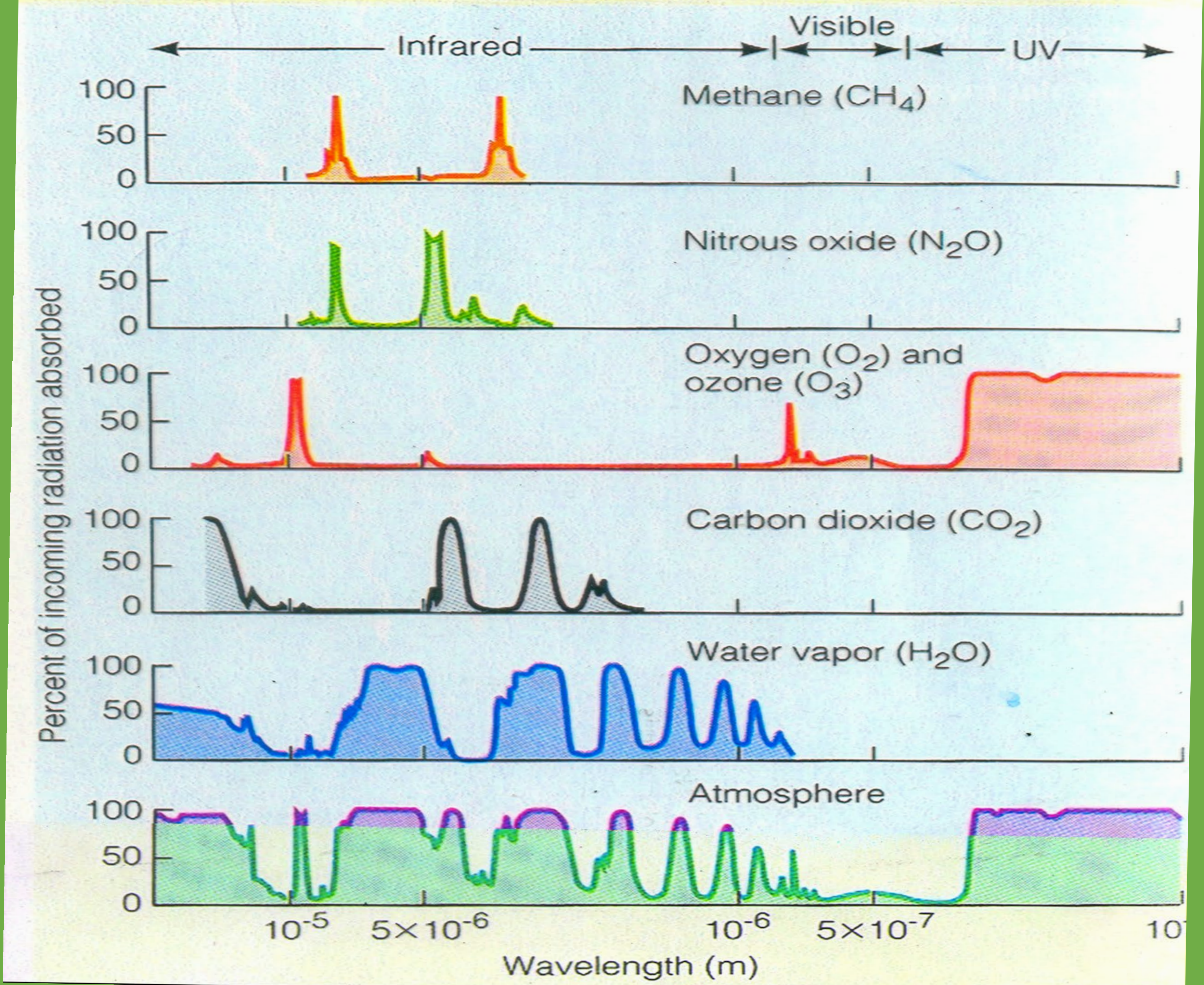

Infrared
Visible
UV
Methane (CH_4)
Nitrous oxide (N_2O)
Oxygen (O_2) and ozone (O_3)
Carbon dioxide (CO_2)
Water vapor (H_2O)
Atmosphere
Percent of incoming radiation absorbed
100
50
0
10^{-5}
5×10^{-6}
10^{-6}
5×10^{-7}
Wavelength (m)

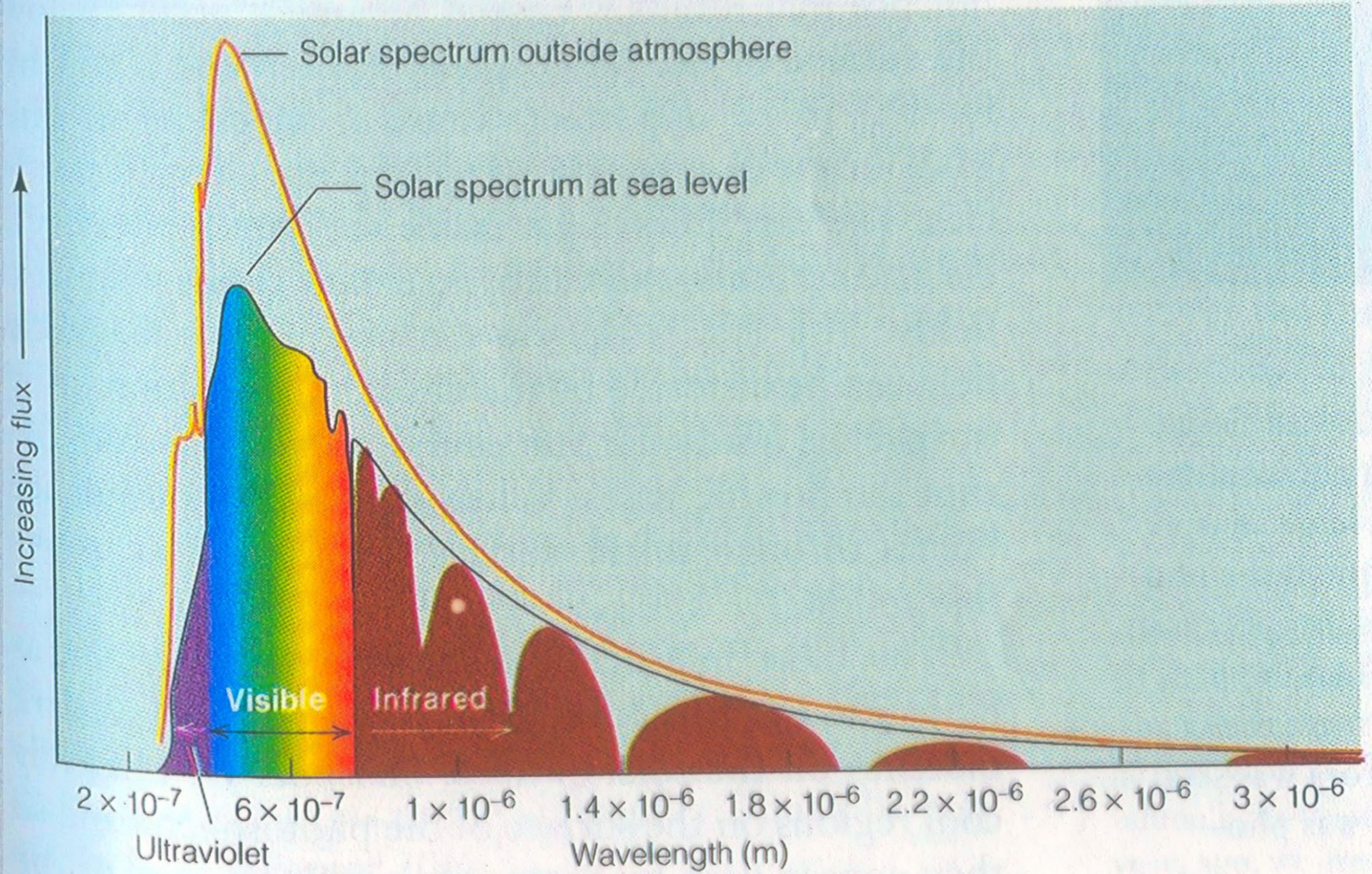
Solar spectrum outside atmosphere
Solar spectrum at sea level
Increasing flux
Visible
Infrared
2 × 10⁻⁷
6 × 10⁻⁷
1 × 10⁻⁶
1.4 × 10⁻⁶
1.8 × 10⁻⁶
2.2 × 10⁻⁶
2.6 × 10⁻⁶
3 × 10⁻⁶
Ultraviolet
Wavelength (m)

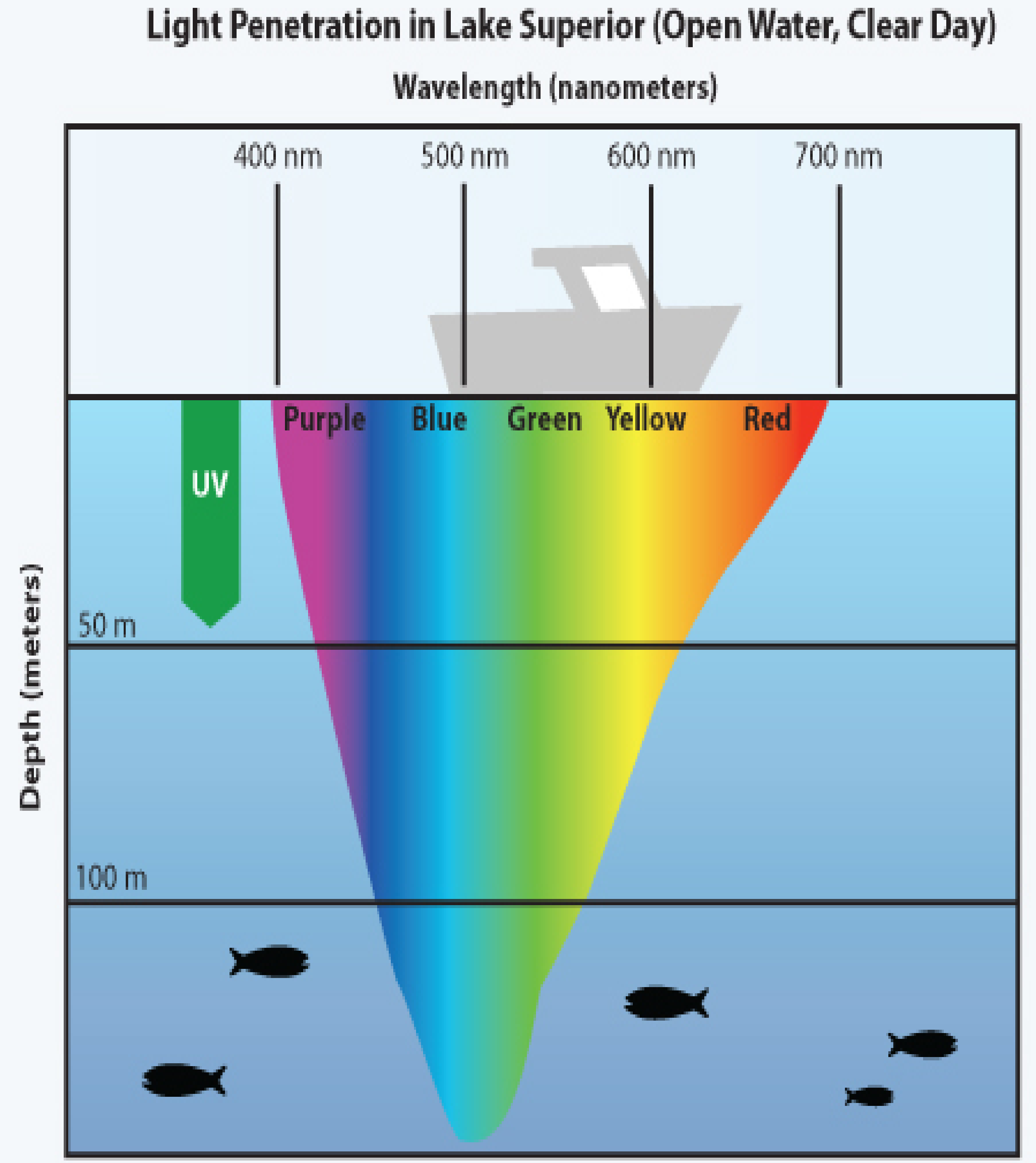
Light Penetration in Lake Superior (Open Water, Clear Day)
Wavelength (nanometers)
400 nm
500 nm
600 nm
700 nm
Purple
Blue
Green
Yellow
Red
UV
Depth (meters)
50 m
100 m

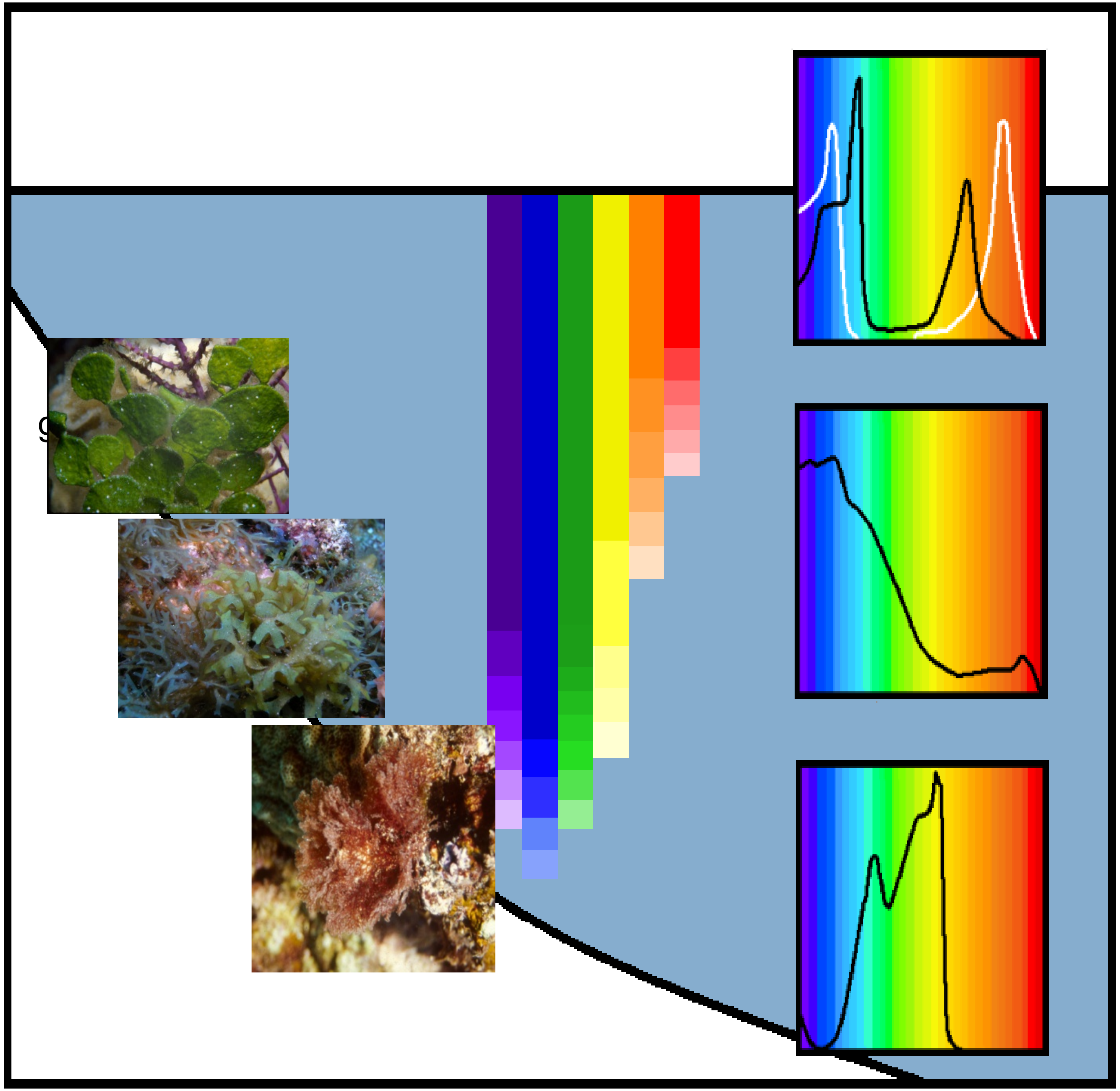

All algae have chlorophyll *a* (white line in top graph)

Green algae also have chlorophyll b and are generally limited to shallow turbid water.

Brown algae have auxiliary pigments such as fucoxanthin that expand absorption into the green wavelengths and allow them to proliferate at intermediate depths

Red algae can survive at the deepest depths as auxiliary pigments such as phycoerythrin absorb blue and green light

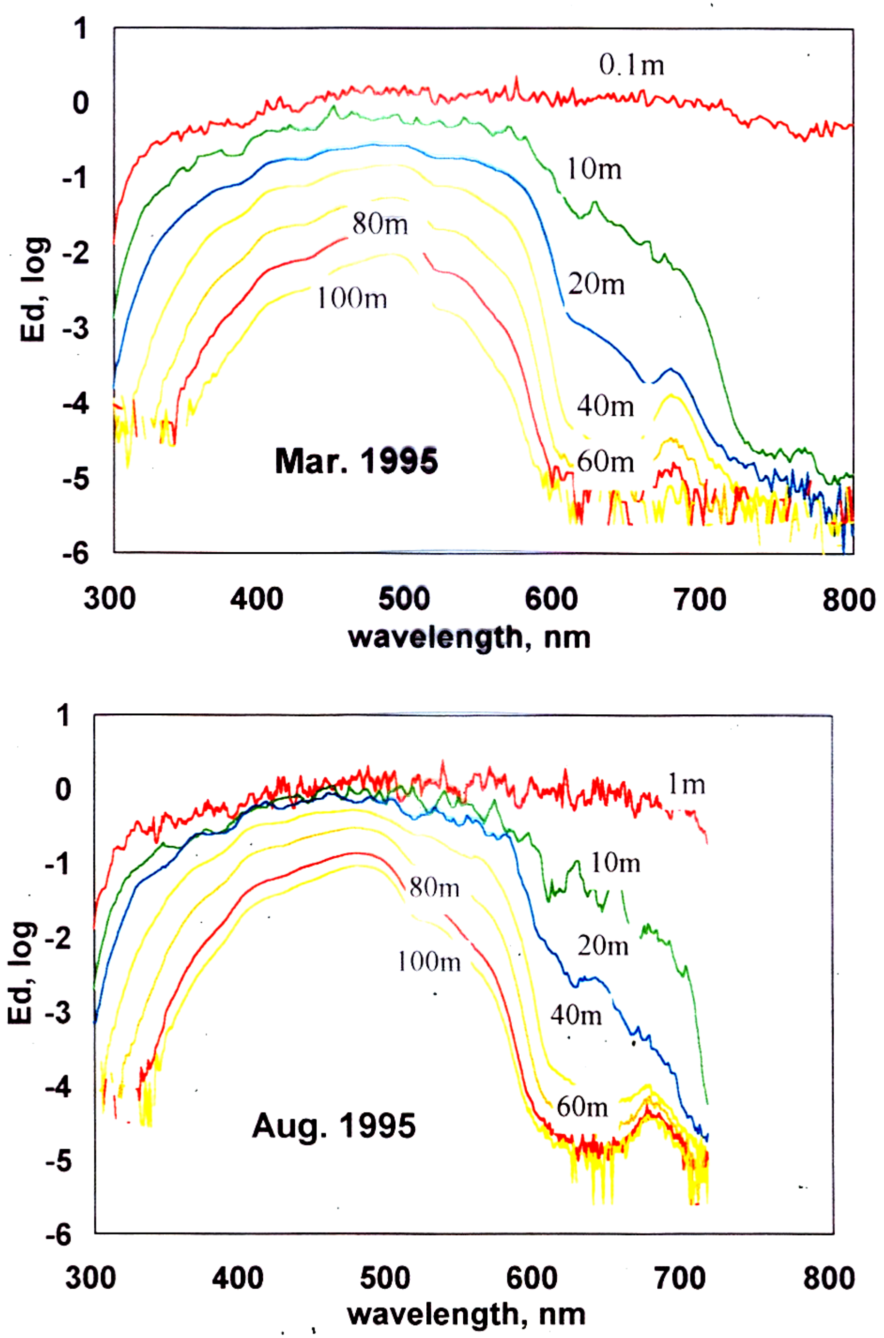

Spectral distribution of underwater light in spring and summer in the oligotrophic Gulf of Eilat (Red Sea)

Spectral distribution of underwater light in spring and summer in the eutrophic Lake Kinneret

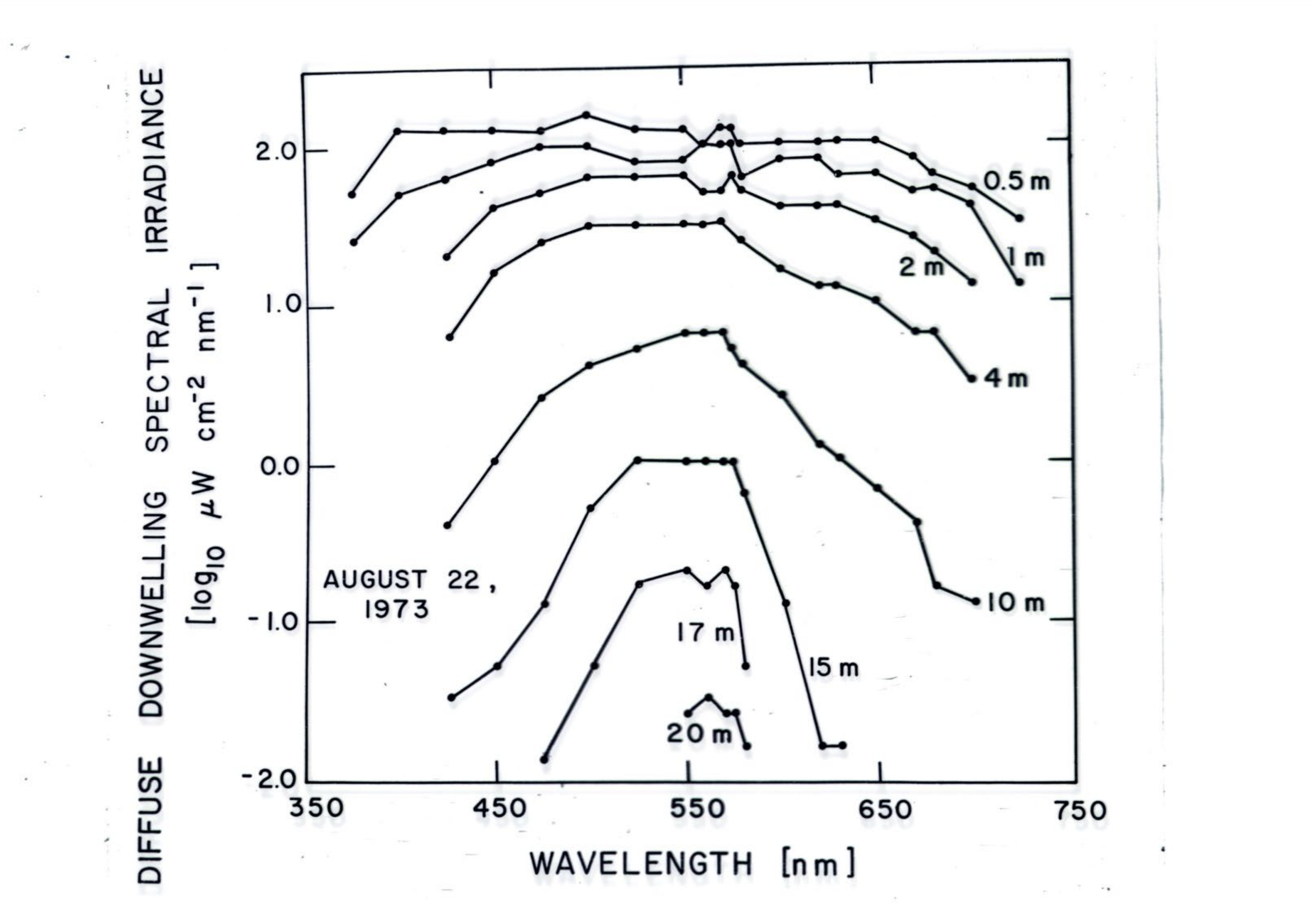

Light and chlorophyll in Lake Kinneret

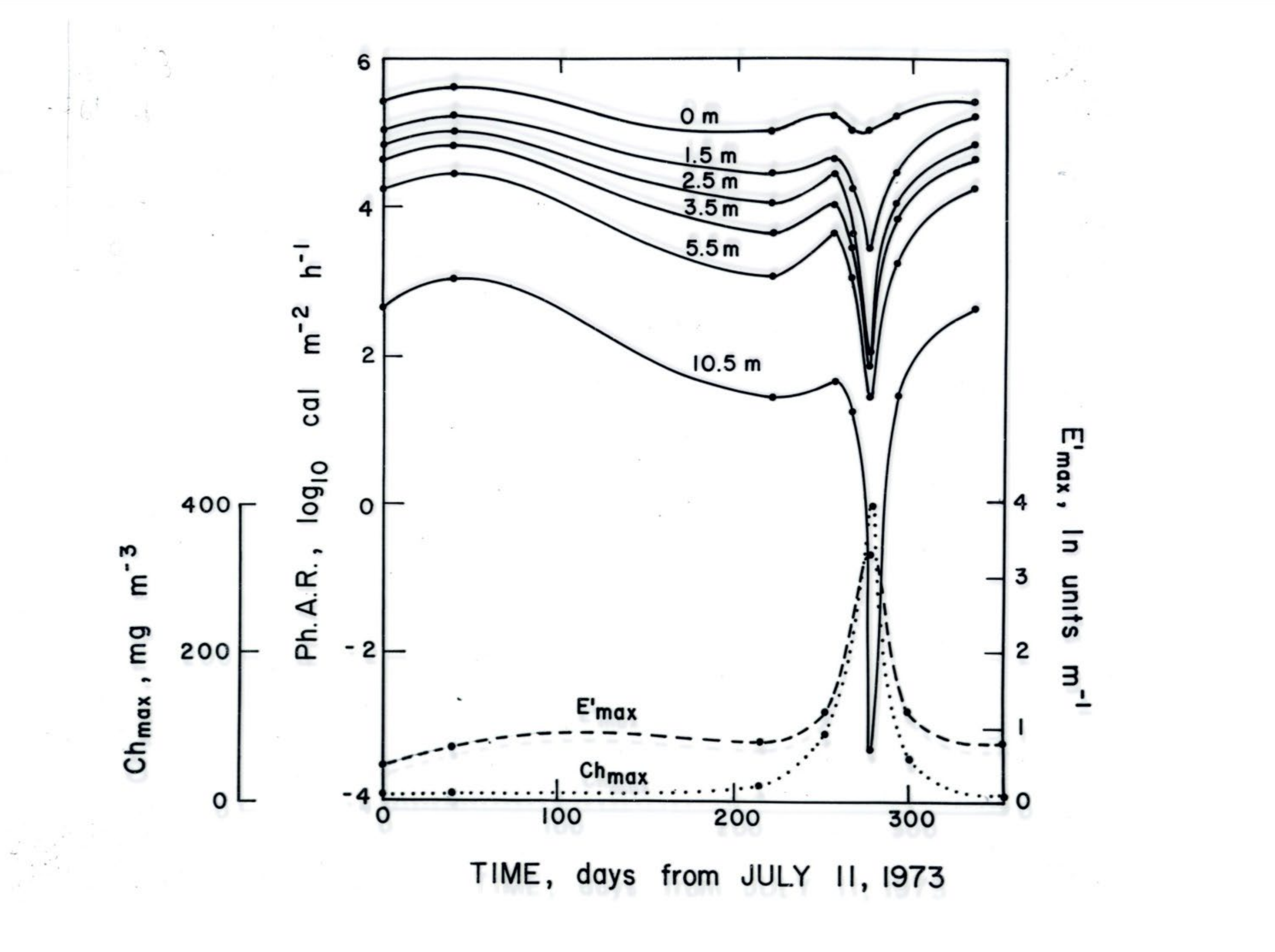

Each wavelength is absorbed differently with depth

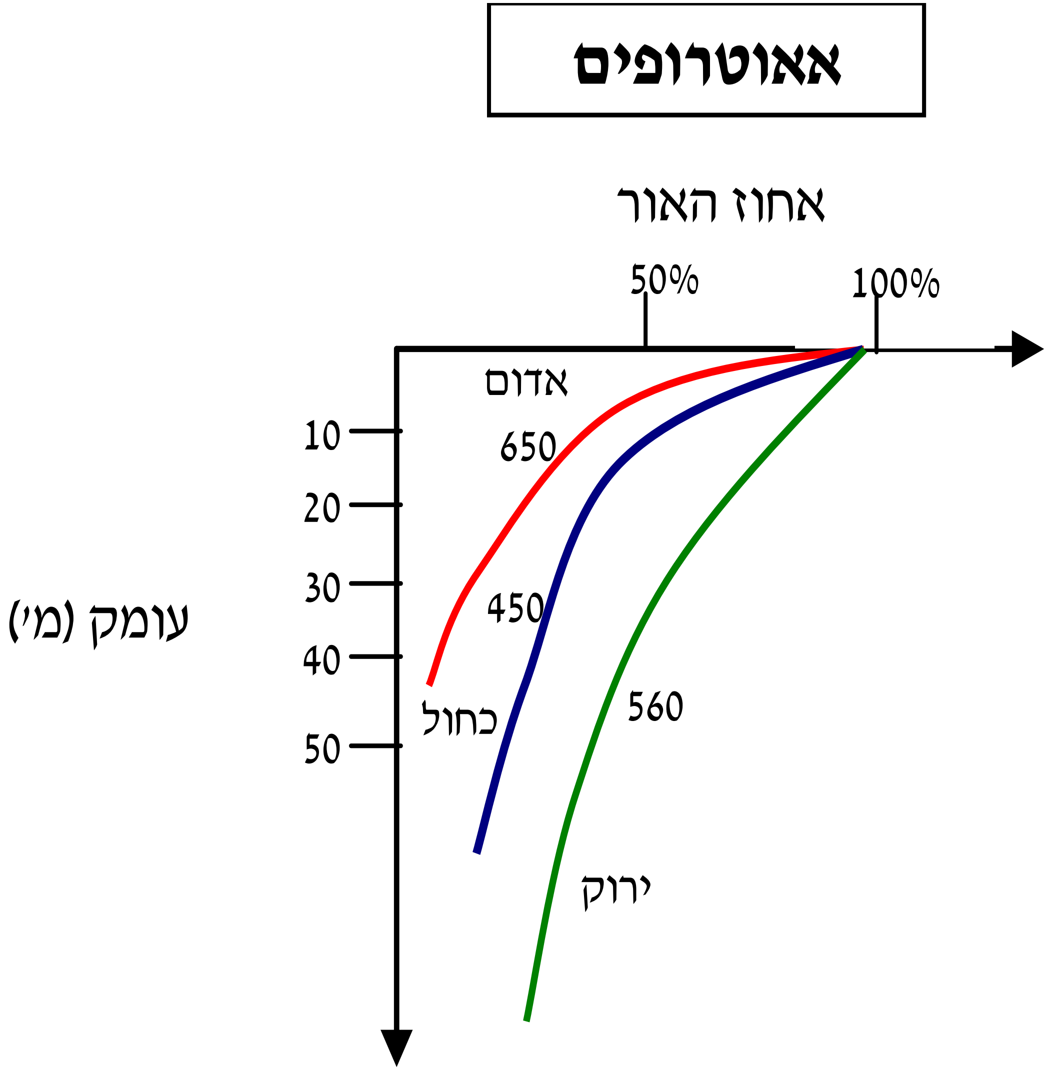

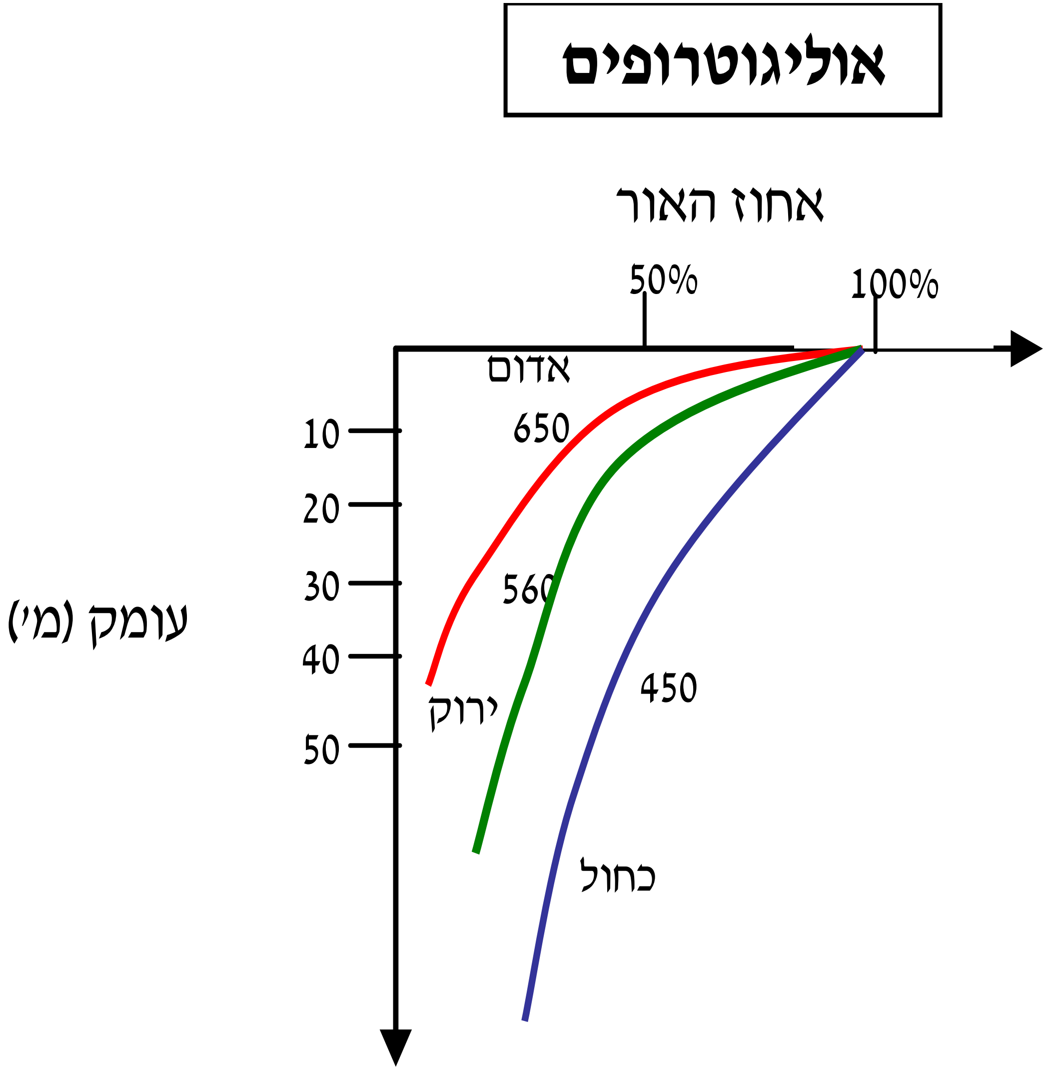

Light in water

- Light is absorbed with depth:
  - $E_z = E_0 e^{-kdz}$
- E_z is the light intensity at z meters
- E_0 is the light intensity at 0 meters
- k_d is the light attenuation coefficient

- $E_z/E_0 e^{-kdz}$
- $\ln(E_z/E_0) = -k_d z$
- $k_d = -\ln(E_z/E_0)/z$ [m]

The euphotic depth z_{eu}

- z_{eu} Is the depth at which light is 1% of its surface intensity
  - $E_z=1\%E_0$
  - $E_z=0.01E_0$
  - $0.01E_0=E_0e^{-kd\ zeu}$
  - $0.01= e^{-kd\ zeu}$
  - $\ln 0.01= -k_d\ z_{eu}$
  - $z_{eu}[m]= -\ln 0.01/\ k_d$

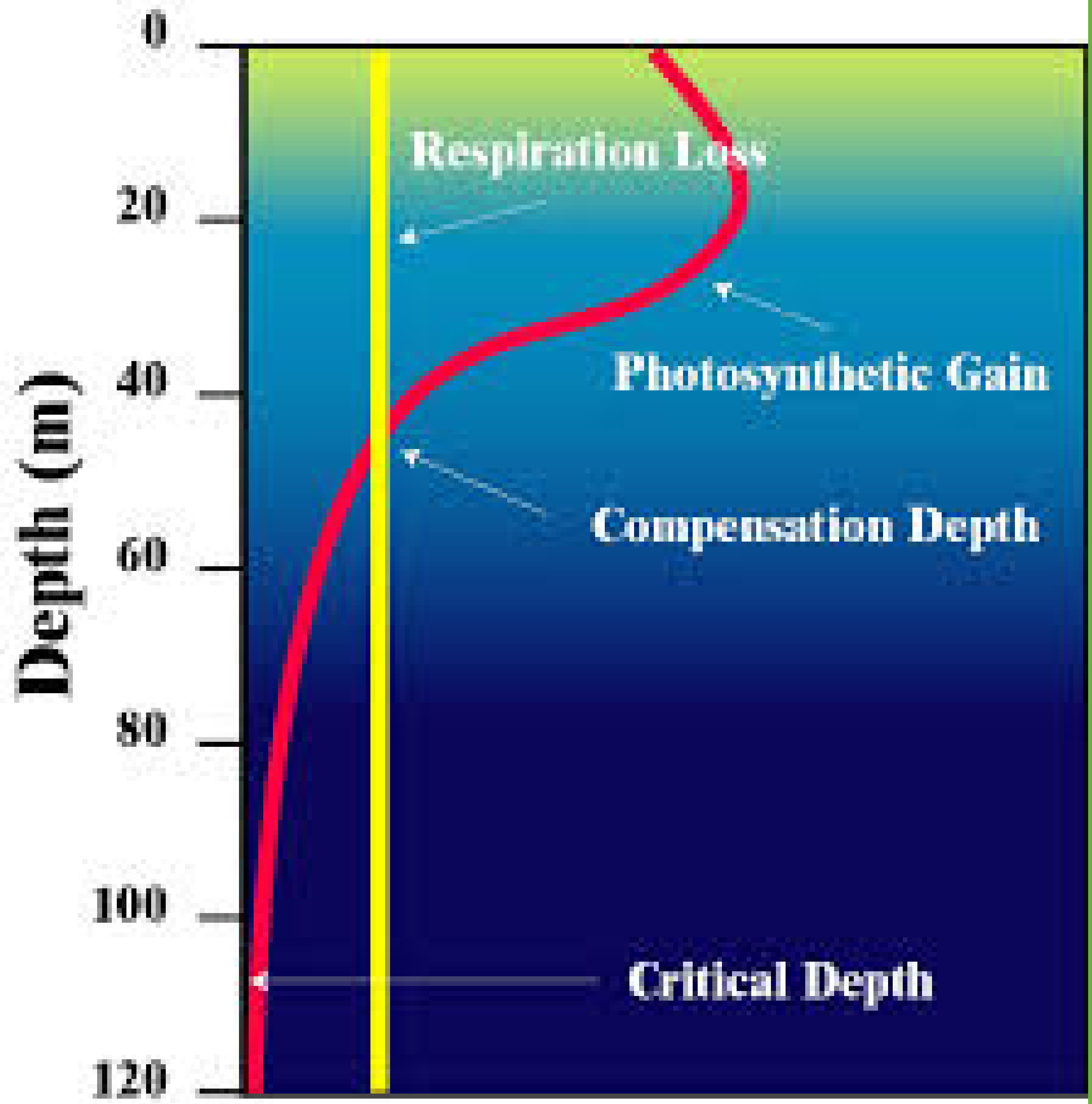

Respiration Loss
Photosynthetic Gain
Compensation Depth
Critical Depth
Depth (m)
0
20
40
60
80
100
120

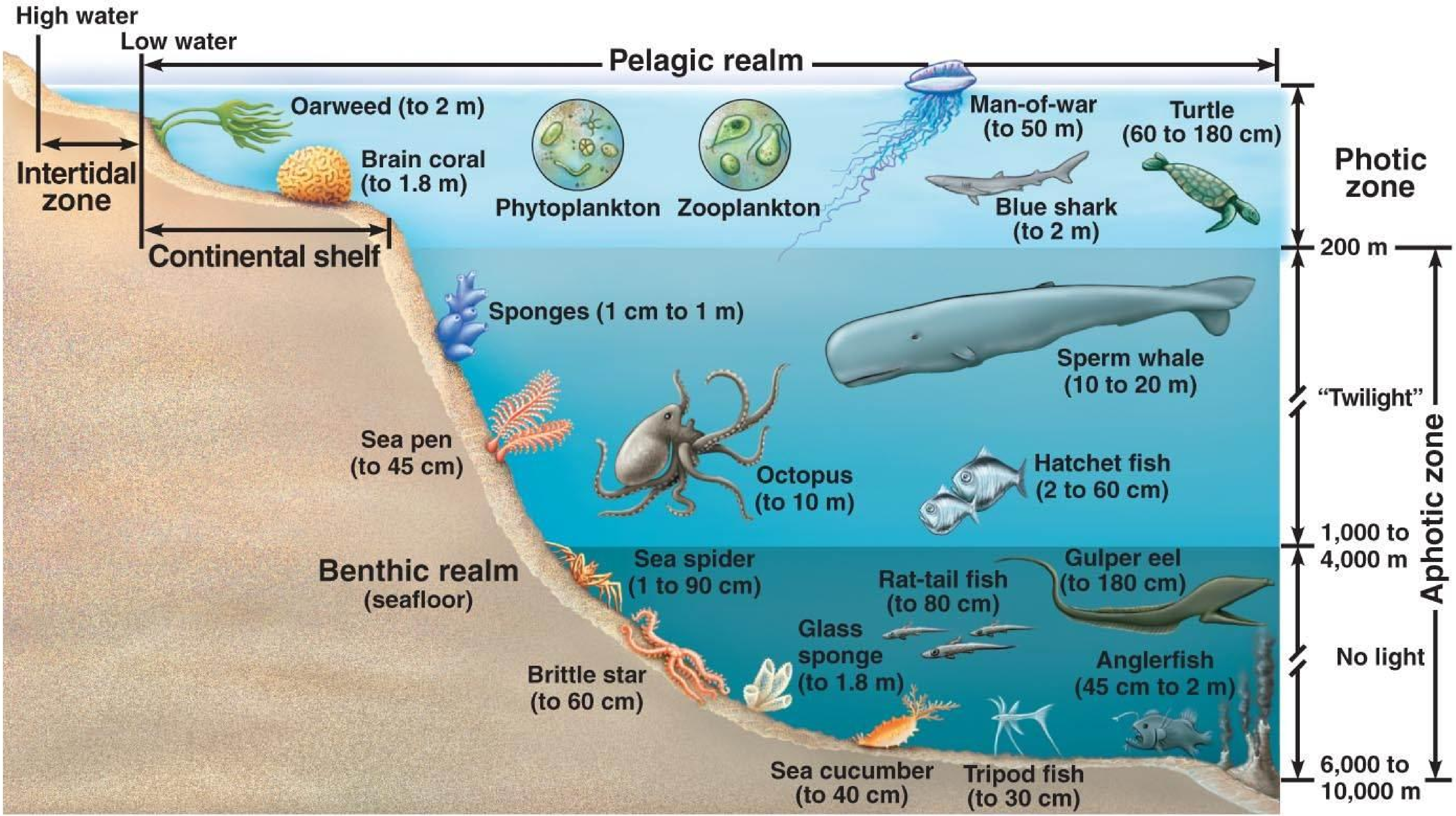

Copyright © 2009 Pearson Education, Inc.

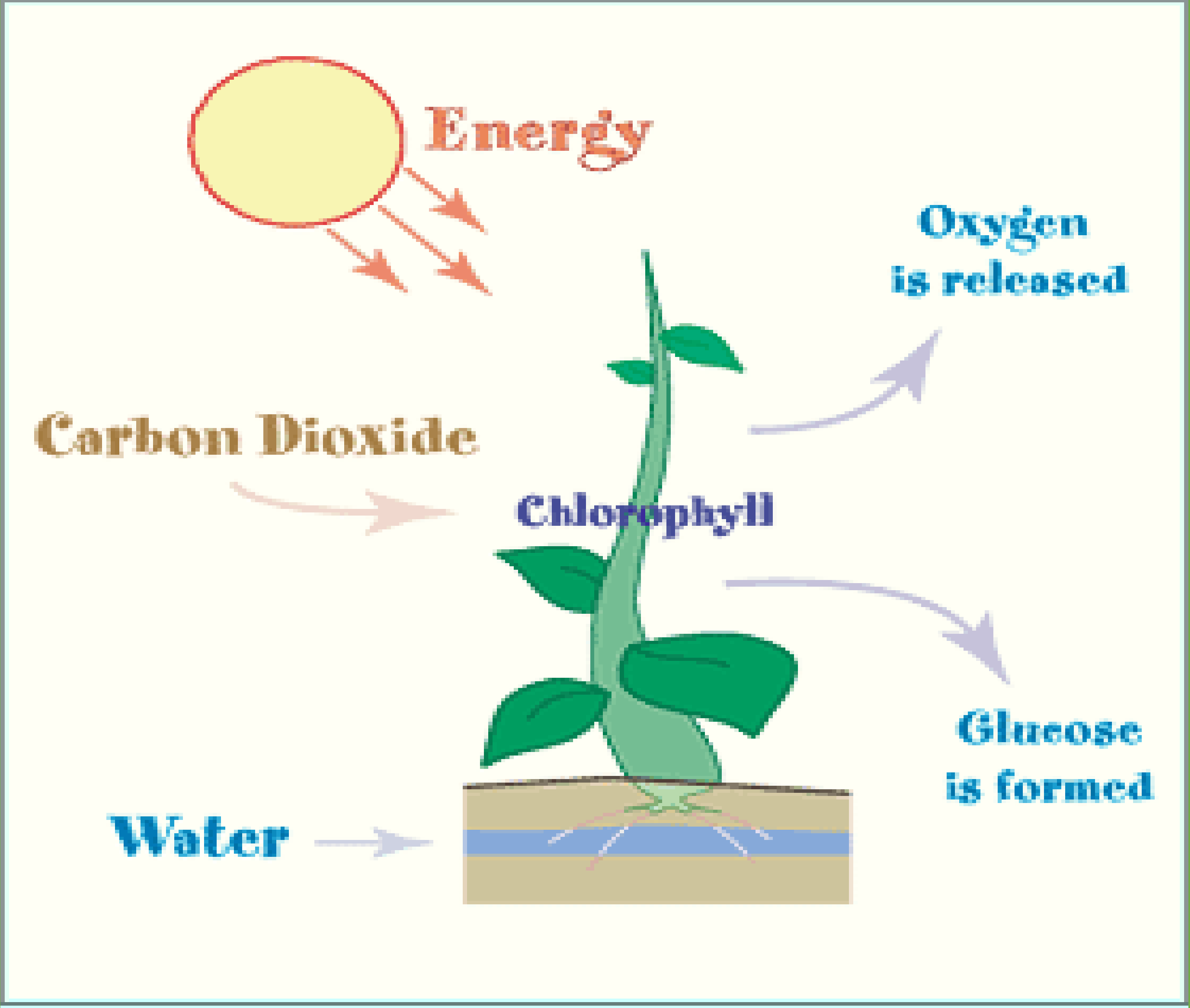

Photosynthesis

Photosynthesis

- $6CO_2 + 6H_2O \leftrightarrow C_6H_{12}O_6 + 6O_2\uparrow$
- $P_G - R = P_N$
- $P_G = P_N + R$

הפוטוסינתזה

- $6CO_2 + 6H_2O <-> C_6H_{12}O_6 + 6O_2\uparrow$
- P_G-R=P_N
- R נשימה
- פוטוסינתזה ברוטו (כולל הפסדי נשימה)
- P_G
- P_N פוטוסינתזה נטו

Photosynthesis

- $6CO_2 + 6H_2O$ -> $C_6H_{12}O_6 + 6O_2$↑
-
- $6C^{18}O_2 + 6H_2O$ -> $C_6H_{12}{}^{18}O_6 + 6O_2$↑
-
- $6CO\ _2 + 6H_2{}^{18}O$ -> $C_6H_{12}O_6$ + ?$6^{18}O_2$↑
-
- $6CO\ _2 + 12H_2{}^{18}O$ -> $C_6H_{12}O_6 + 6^{18}O_2$↑ $+6H_2O$

Antarctic photosynthesis and daylength

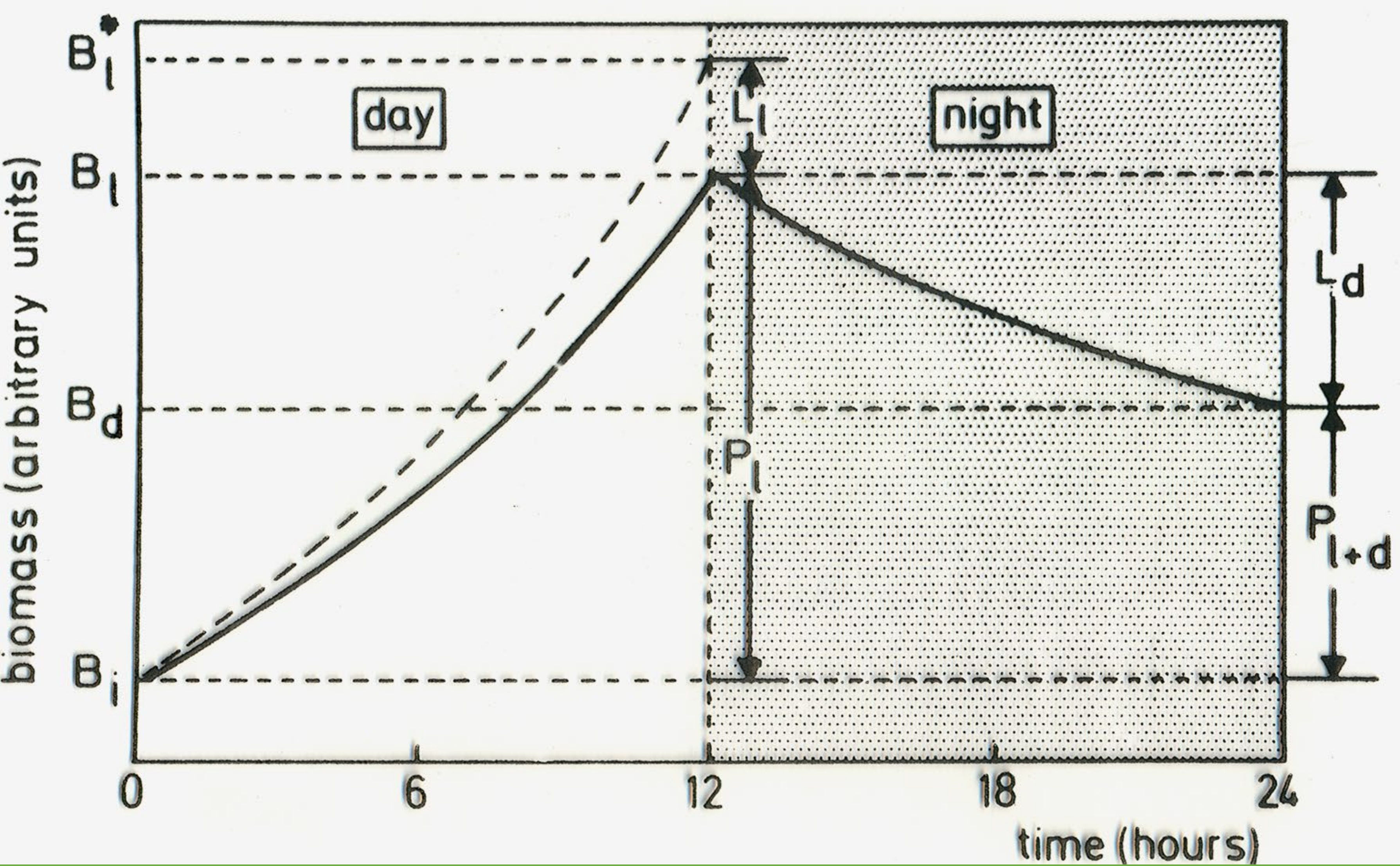

Dashed line represents gross photosynthesis

measuring photosynthesis

$6CO2 + 6H_2O \rightarrow {}^{14}C_6H_{12}O_6 + 6O_2\uparrow$

fluorescence

photoacoustics

$P_G - R = P_N$

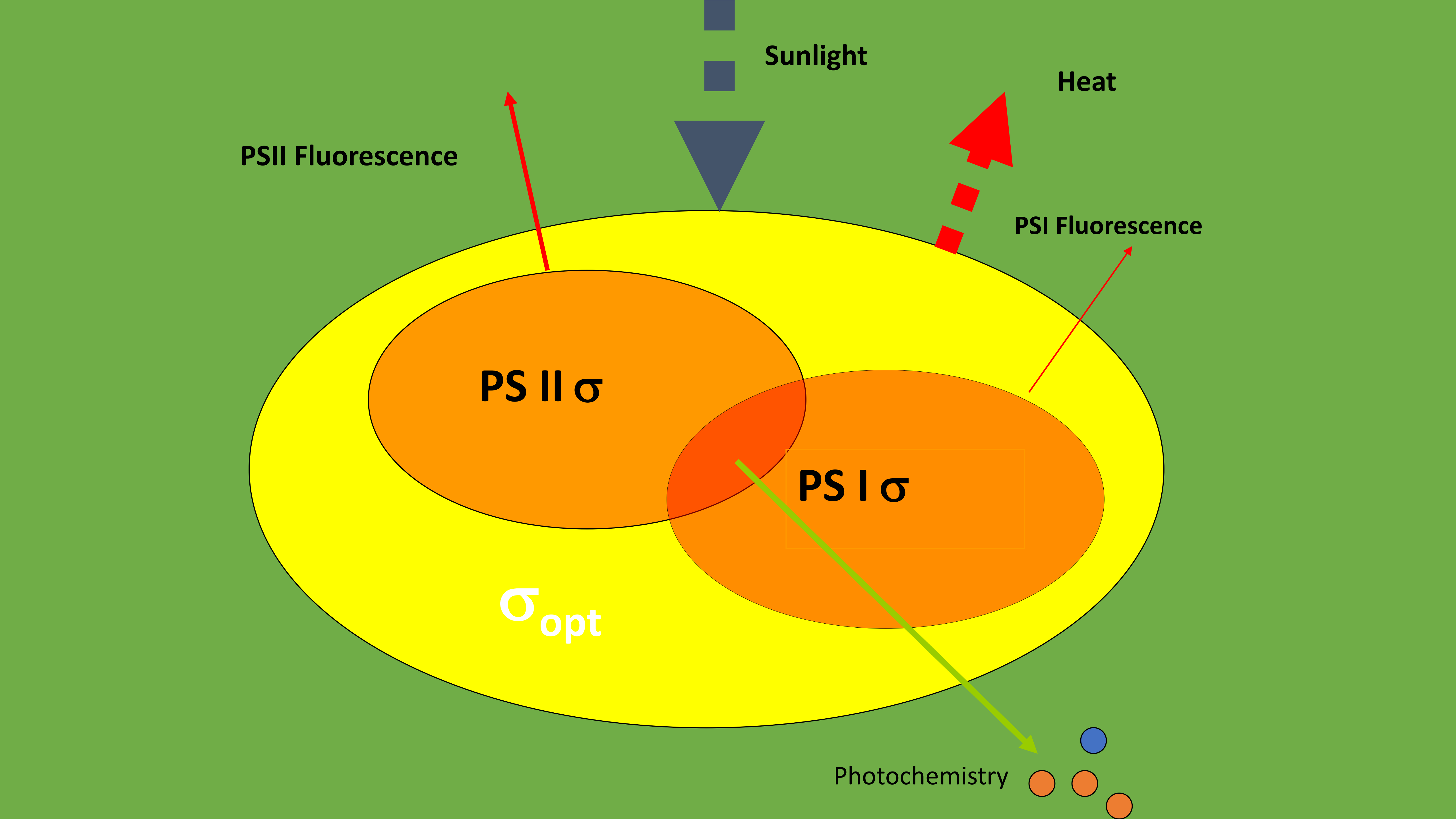

Sunlight
Heat
PSII Fluorescence
PSI Fluorescence
PS II σ
PS I σ
σopt
Photochemistry

Radioactive carbon labelling of high and low light *Stylophora pistillata* branches under a range of light intensities

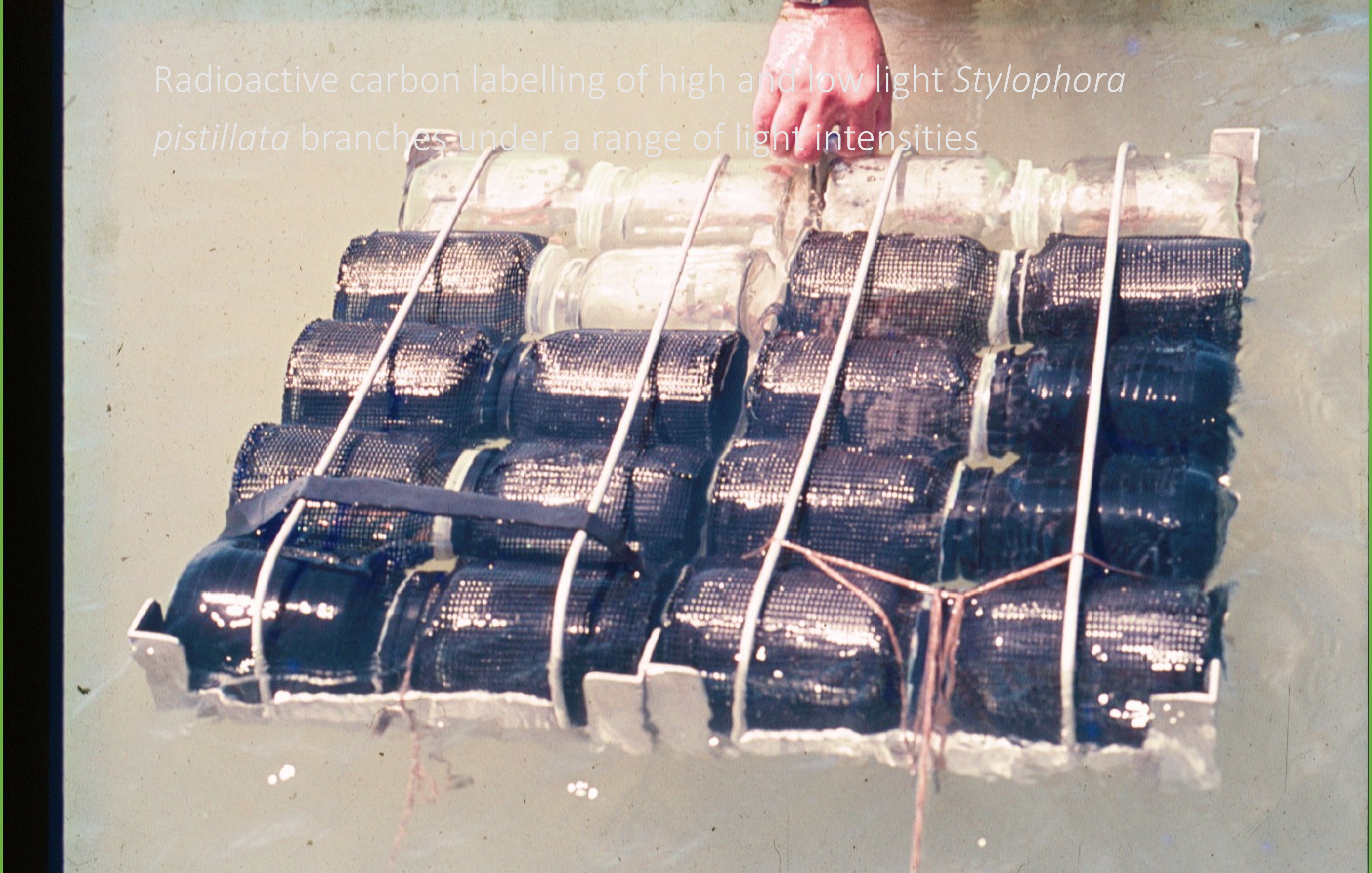

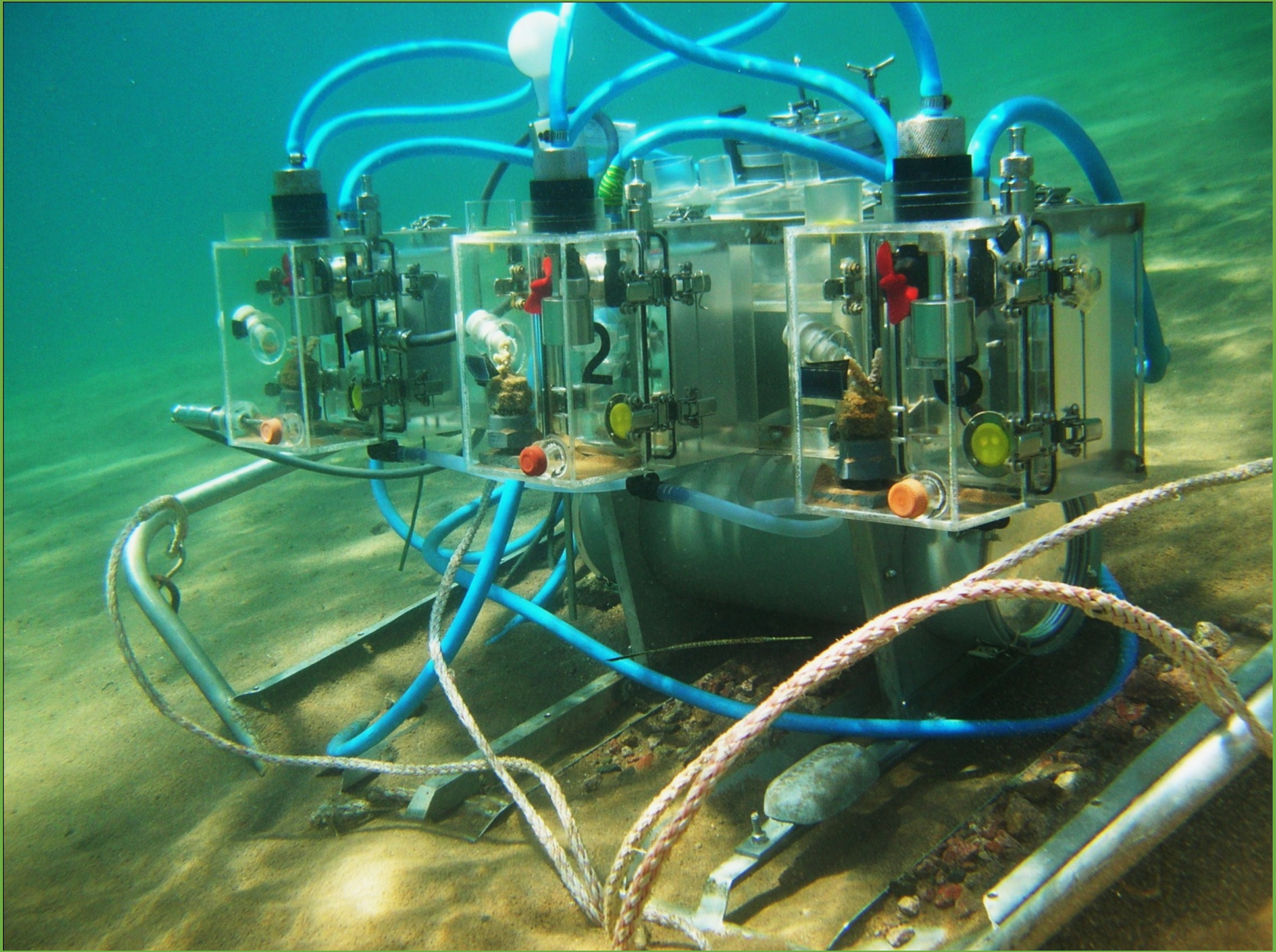
1
2

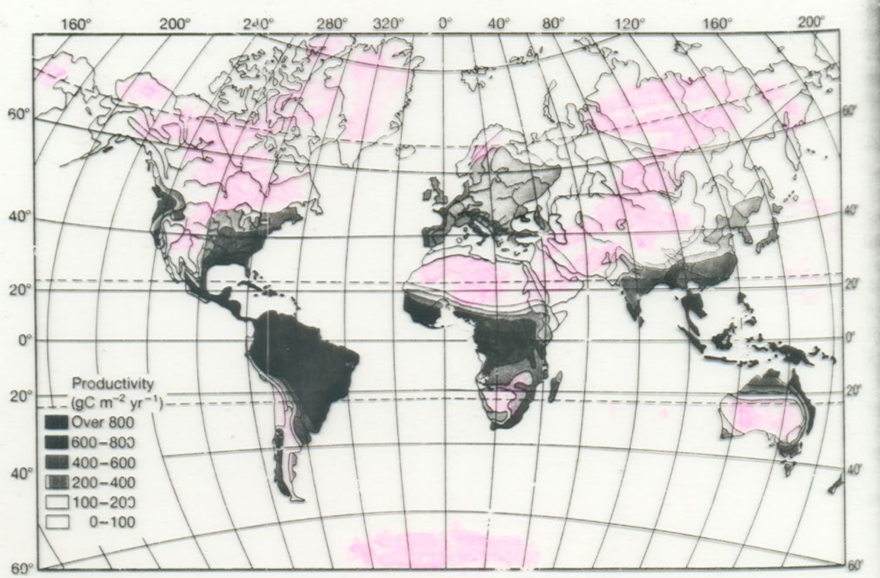

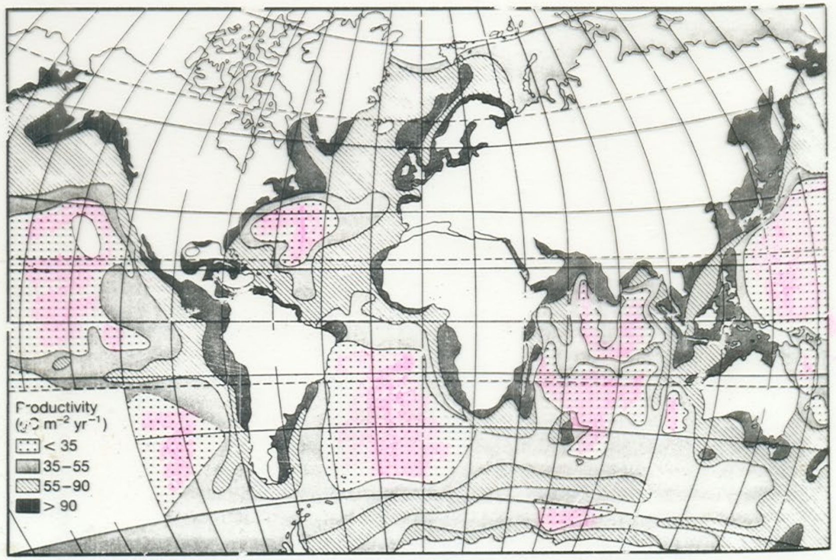

Figure 17.1. Top: Worldwide pattern of net primary productivity on land (from Reichle, 1970). Bottom: Worldwide pattern of net primary productivity in the oceans (from Koblentz-Mishke *et al.*, 1970).

Table 18.1 Annual net primary productivity (NPP) and standing crop biomass estimates for contrasting communities of the world. (After Whittaker, 1975.)

Ecosystem type	Area (10^6 km^2)	NPP, per unit area (g m^{-2} *or* t km^{-2}) y^{-1} Normal range	Mean	World NPP (10^9 t)	Biomass per unit area (kg m^{-2}) Normal range	Mean	World biomass (10^9 t)
Tropical rainforest	17.0	1000–3500	2200	37.4	6–80	45	765
Tropical seasonal forest	7.5	1000–2500	1600	12.0	6–60	35	260
Temperate evergreen forest	5.0	600–2500	1300	6.5	6–200	35	175
Temperate deciduous forest	7.0	600–2500	1200	8.4	6–60	30	210
Boreal forest	12.0	400–2000	800	9.6	6–40	20	240
Woodland and shrubland	8.5	250–1200	700	6.0	2–20	6	50
Savannah	15.0	200–2000	900	13.5	0.2–15	4	60
Temperate grassland	9.0	200–1500	600	5.4	0.2–5	1.6	14
Tundra and alpine	8.0	10–400	140	1.1	0.1–3	0.6	5
Desert and semi-desert shrub	18.0	10–250	90	1.6	0.1–4	0.7	13
Extreme desert, rock, sand and ice	24.0	0–10	3	0.07	0–0.2	0.02	0.5
Cultivated land	14.0	100–3500	650	9.1	0.4–12	1	14
Swamp and marsh	2.0	800–3500	2000	4.0	3–50	15	30
Lake and stream	2.0	100–1500	250	0.5	0–0.1	0.02	0.05
Total continental	149		773	115		12.3	1837
Open ocean	332.0	2–400	125	41.5	0–0.005	0.003	1.0
Upwelling zones	0.4	400–1000	500	0.2	0.005–0.1	0.02	0.008
Continental shelf	26.6	200–600	360	9.6	0.001–0.04	0.01	0.27
Algal beds and reefs	0.6	500–4000	2500	1.6	0.04–4	2	1.2
Estuaries	1.4	200–3500	1500	2.1	0.01–6	1	1.4
Total marine	361		152	55.0		0.01	3.9
Full total	510		333	170		3.6	1841

Primary productivity in tropical rainforest and upwelling marine zones

$gm^{-2}\, y^{-1} / 45000\ gm^{-2} \sim 1/20\ y^{-1}$ 2200

$45000\ gm^{-2} / 2200 gm^{-2}\, y^{-1} \sim 20\ y$

$500\ gm^{-2}\, y^{-1} / 20 gm^{-2} \sim 25\ y^{-1}$

$20 gm^{-2} / 500\ gm^{-2}\, y^{-1} \sim 1/25 y$

20:1/25=500!!!

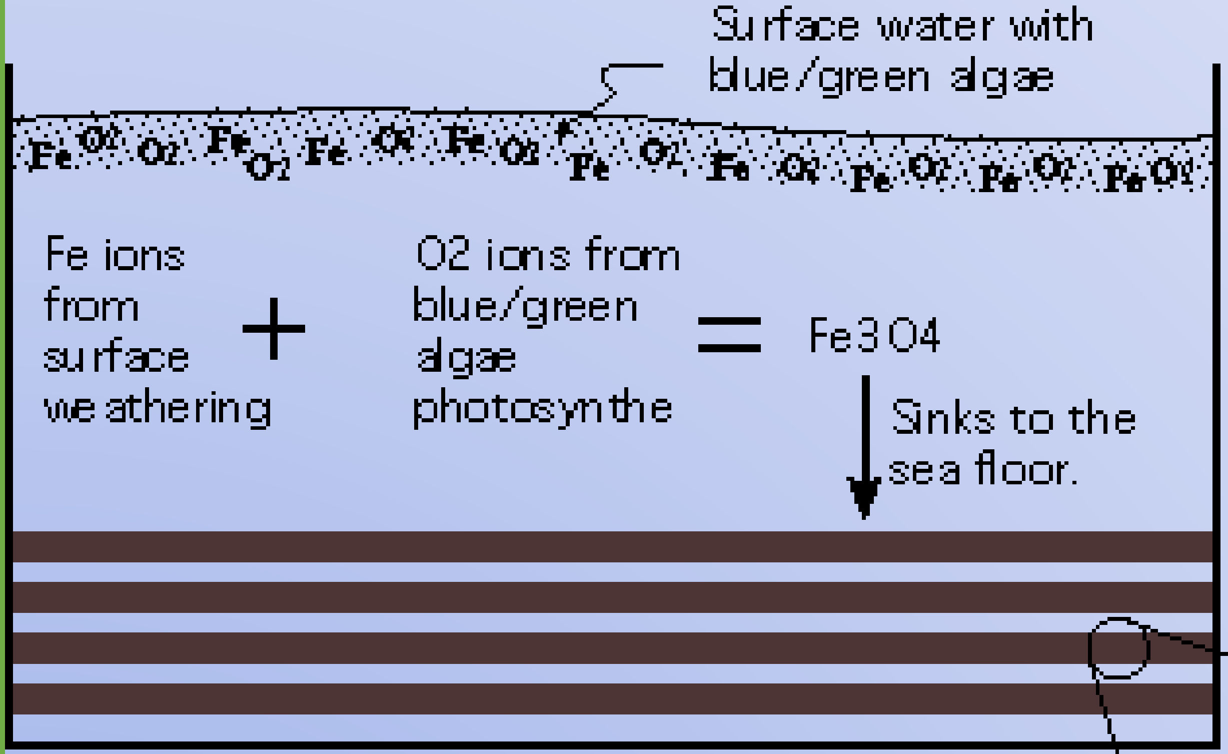

After combining the Fe and O2 ions into Magnetite (Fe_3O_4), the mineral grains sink to the sea floor, where they accumulate into iron-rich and iron-poor layers.

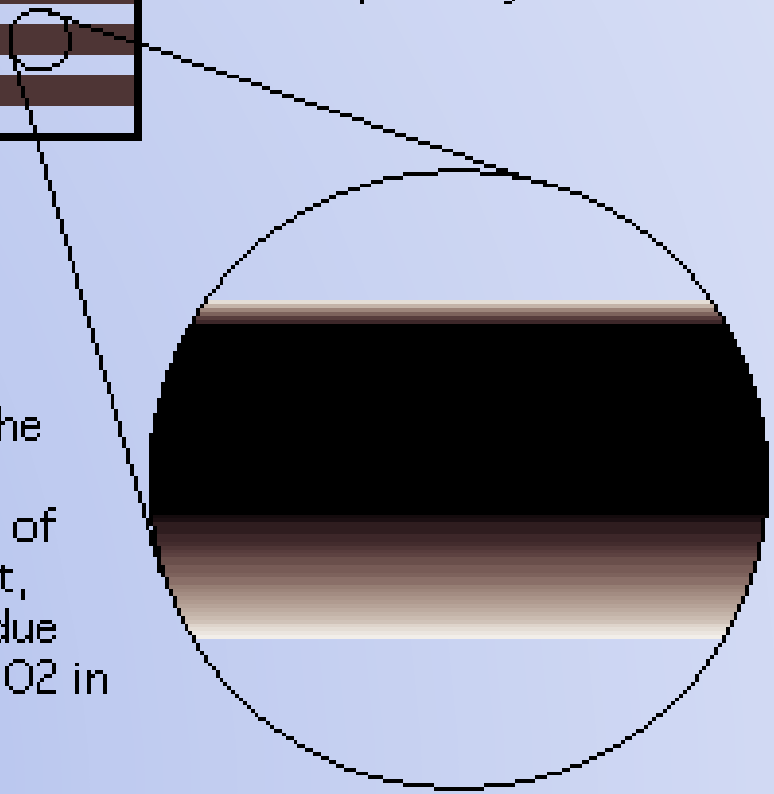

In an ideal setting, you would expect the magnetite-rich layers to exhibit a reversed graded bedding. Looking from the bottom up, this would involve a slow transition into the magnetite-rich layers, representing slowly increasing O2 levels in the upper sea water in response to the increasing population of blue/green algae. The upper contact of each magnetite-rich layer would be relatively abrupt, reflecting the sudden extinction of the population due to O2 poisoning, and the resulting loss of available O2 in the water to combine with the iron ions.

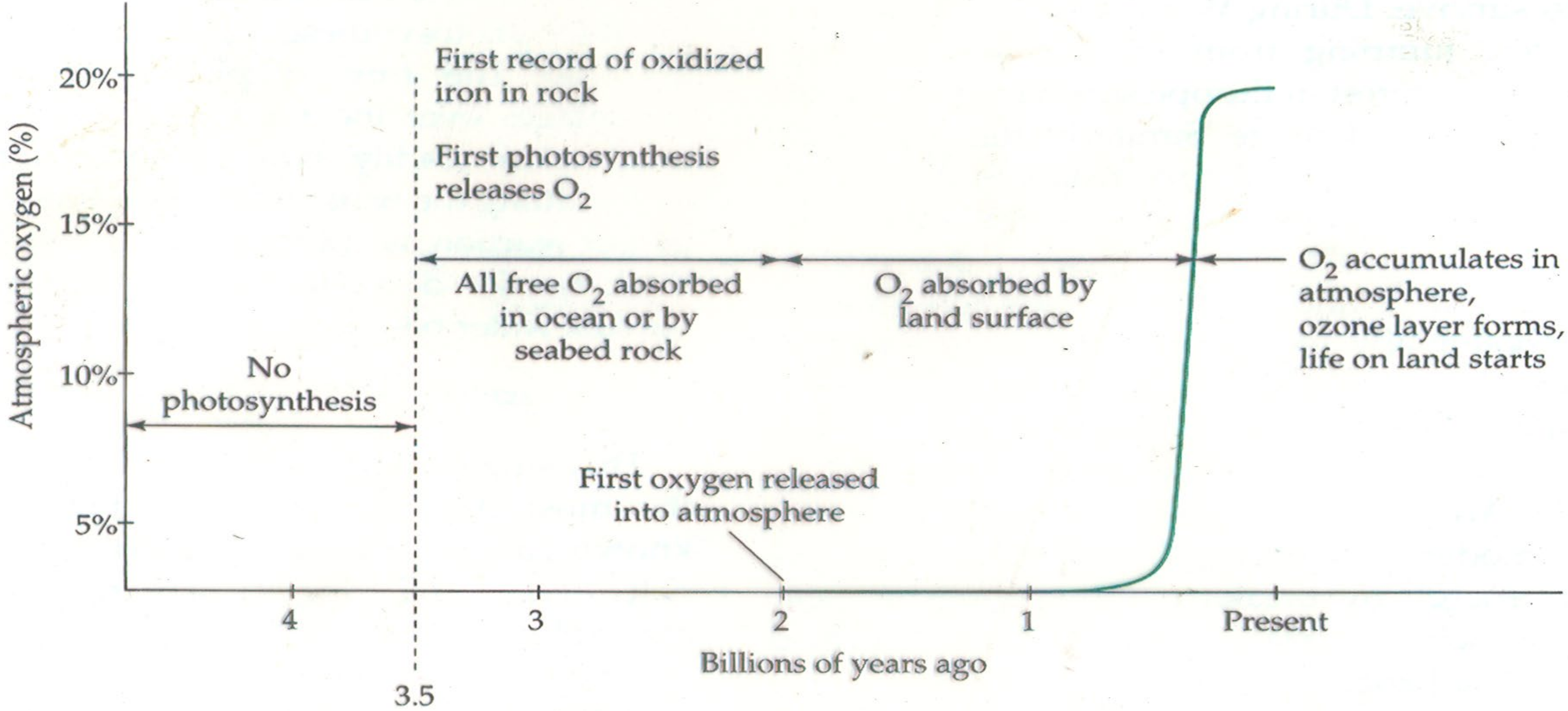

Figure 1.6 The accumulation of atmospheric oxygen through geologic time. The first oxygen produced was absorbed first by oxygen-hungry minerals that produced a banded-iron formation and later by "Red-Beds" (terrestrial rocks that absorbed atmospheric oxygen). Once these minerals had been saturated, oxygen could accumulate in the atmosphere. Modern oxygen levels were attained about 400 million years ago. (After M. Schidlowski, 1980.)

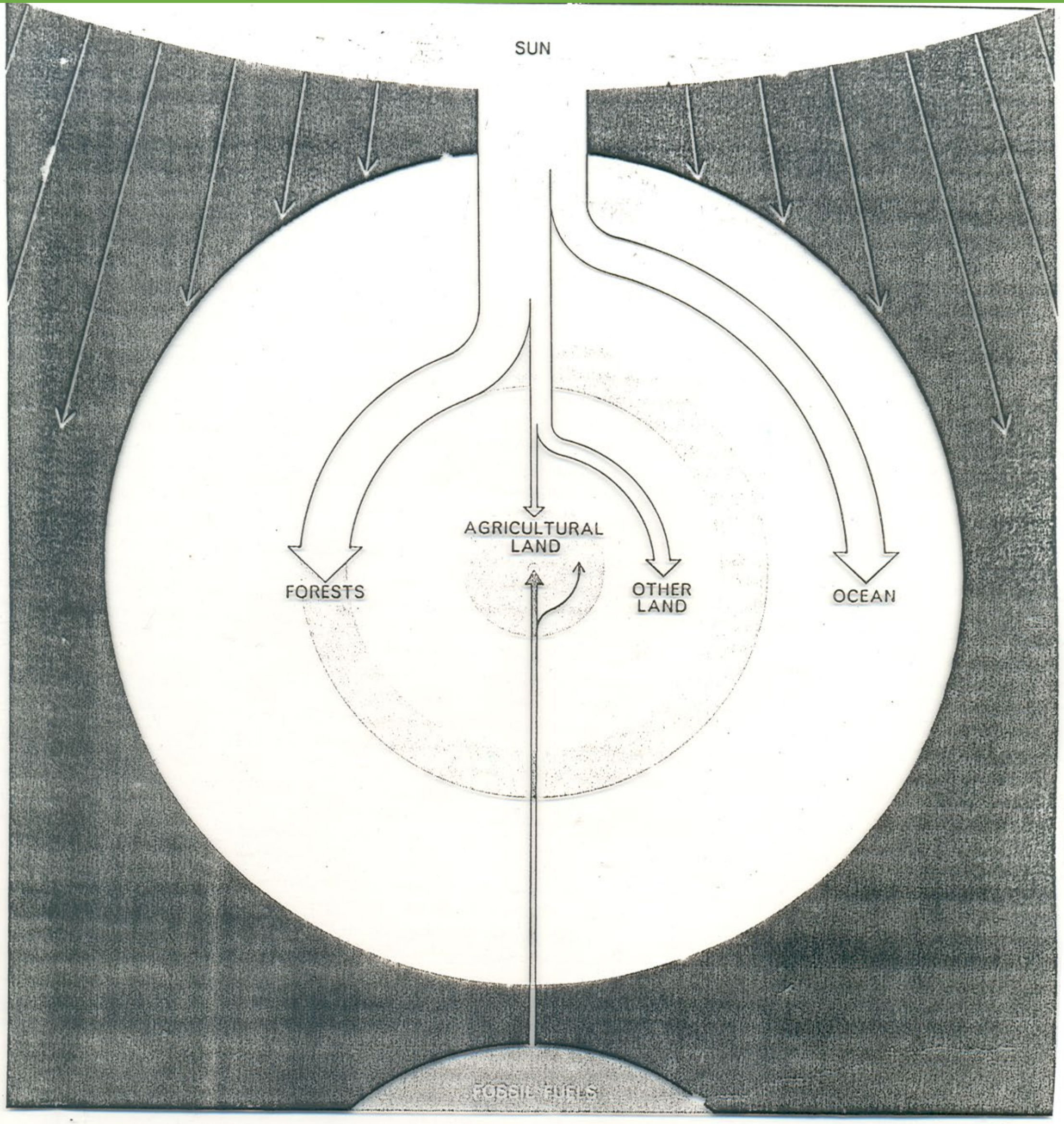

ENERGY FIXED by the earth's primary producers is equivalent to about 164 billion metric tons of dry organic matter a year, according to Robert H. Whittaker and Gene E. Likens of Cornell University. About 5 percent of the energy is fixed by agricultural ecosystems and is utilized directly by man, one species among millions. Man also draws annually on fossil fuel reserves for about the same amount of energy. In this anthropocentric view of the biosphere the area of the concentric rings is proportional to th major ecosystems' share of the surface area of the earth (indicate in millions of square kilometers). The width of the arrows is pr portional to the amount of energy fixed in each ecosystem an contributed by fossil fuels (indicated in billions of metric tons o dry matter per year). The intensity of the color in each ring sug gests the productivity (production per unit area) of each ecosystem.

פוטואקלימציה של פוטוסינטזה: *Dunaliella salina* מאוקלמת לאור גבוה (b&d) ונמוך (a & c)

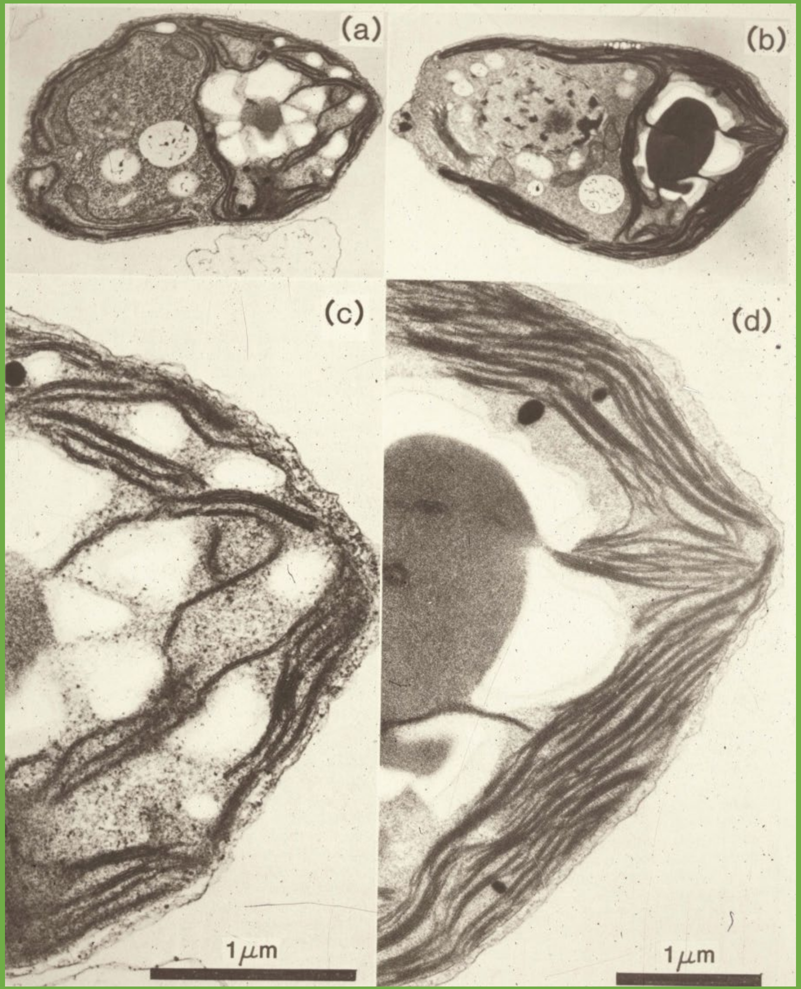

פוליפים של אלמוג ובתוכם אצות שיתופיות

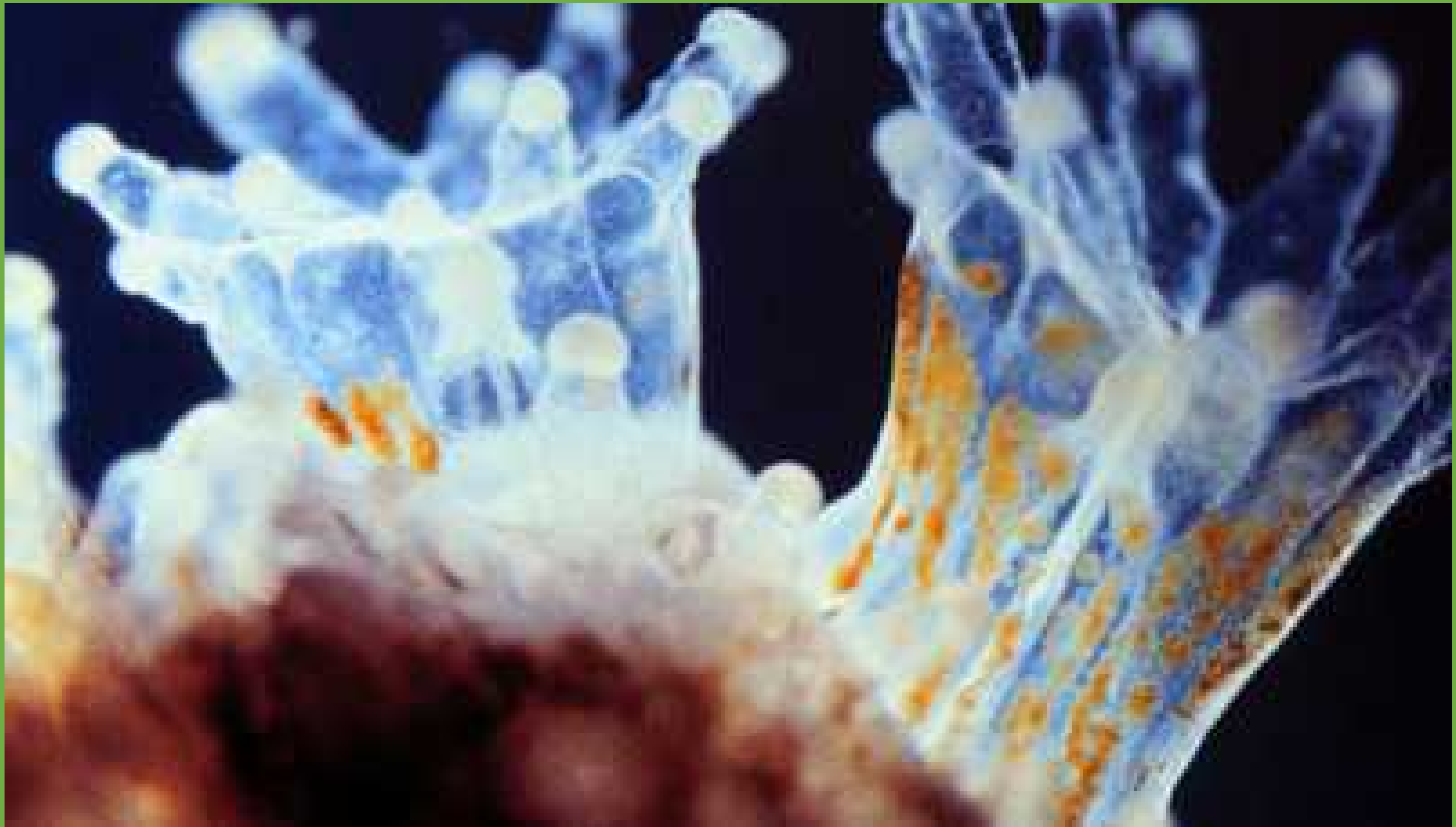

זואוקסנטלות
באלמוגים שוני

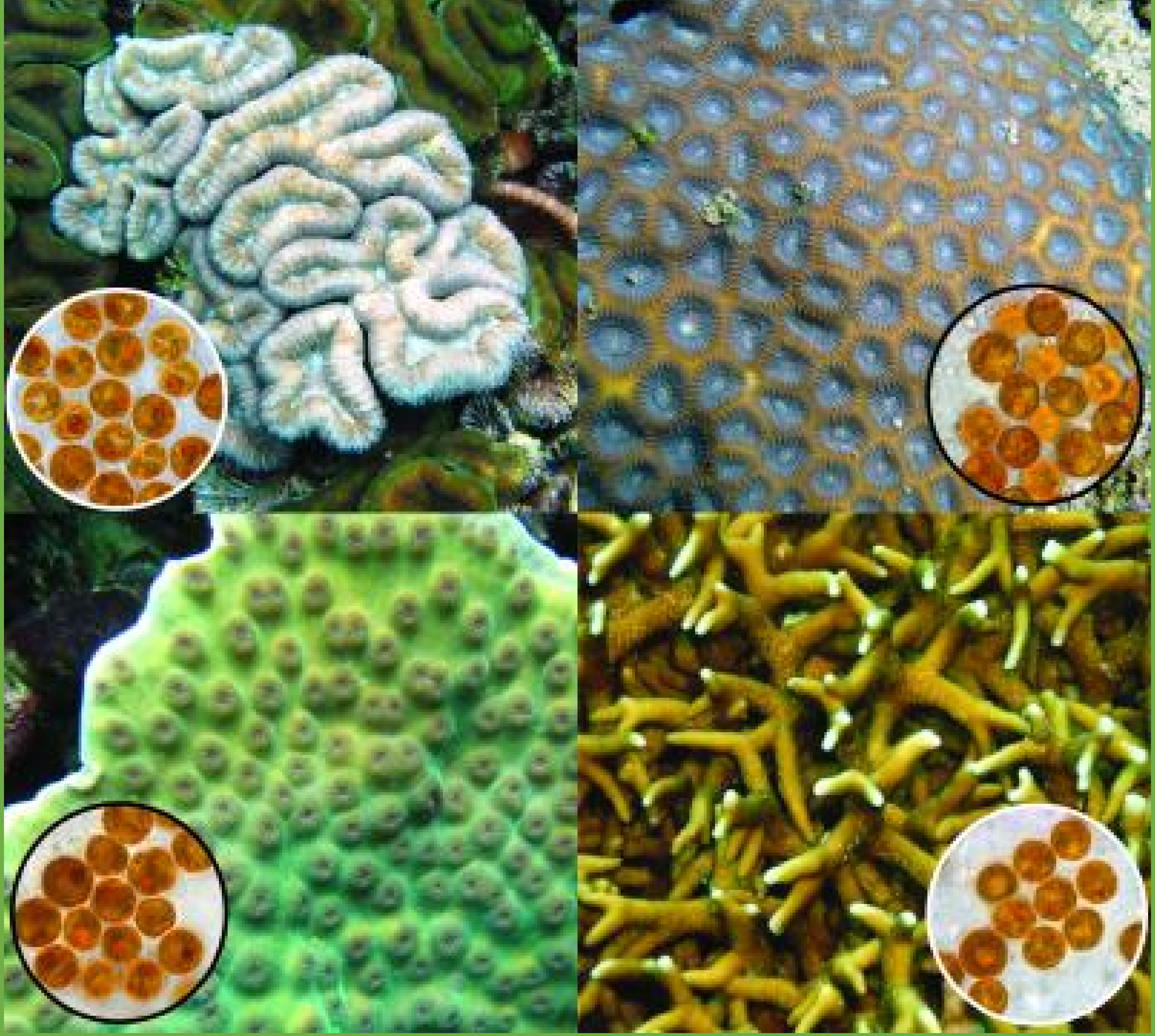

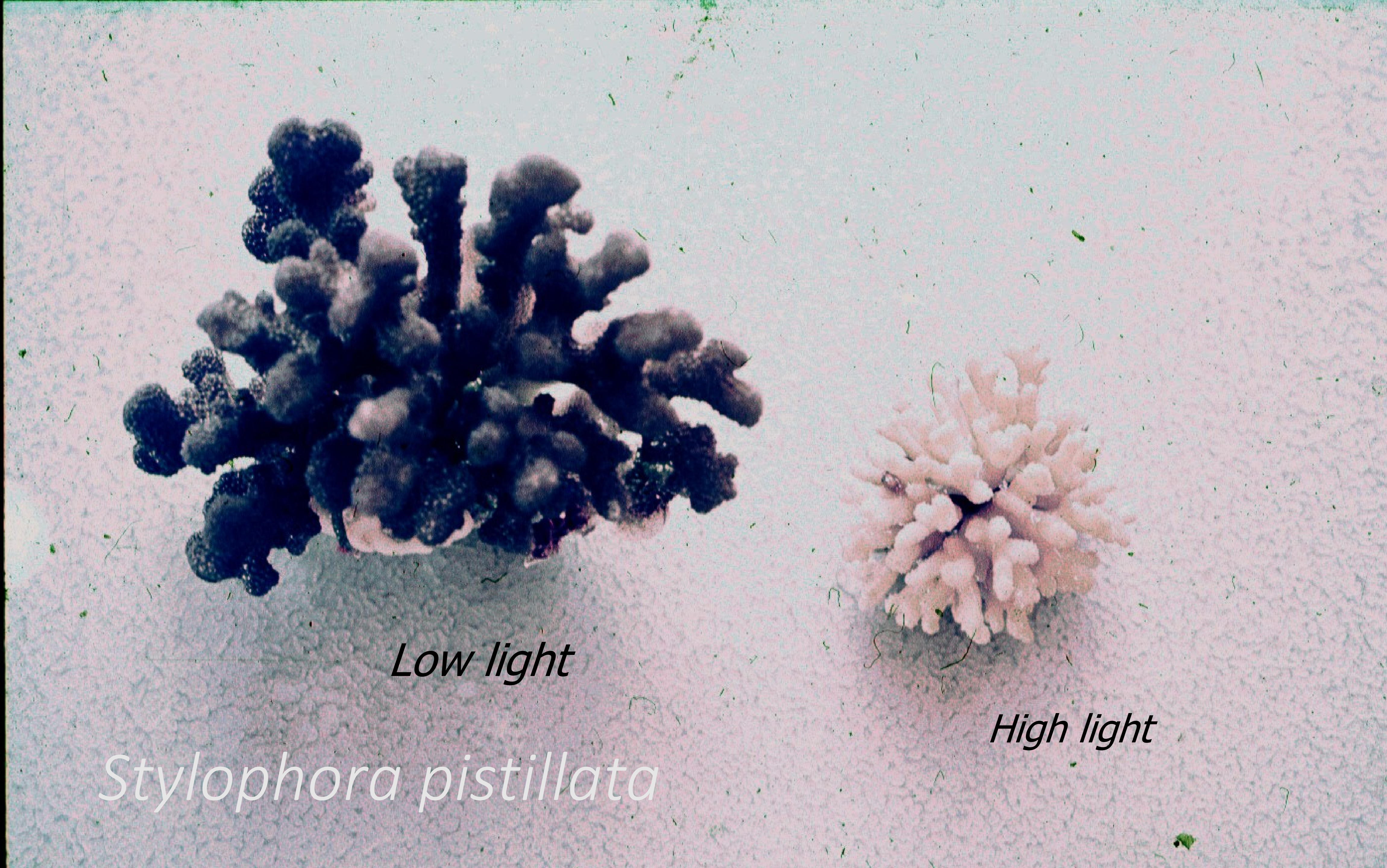
Low light
High light
Stylophora pistillata

High and low light acclimation in *Stylophora pistillata* zooxanthellae

Parameter Treatment	μg ch *a* cm^{-2}	10^6 cells cm^{-2}	pg ch *a* cell
HL	**3.6 ± 1.1**	**1.7 ± 0.3**	**2.2 ± 0.3**
LL	**14.2 ± 4**	**1.6 ± 0.1**	**8.3 ± 0.5**
LL/HL	**3.9**	**1.1**	**3.7**

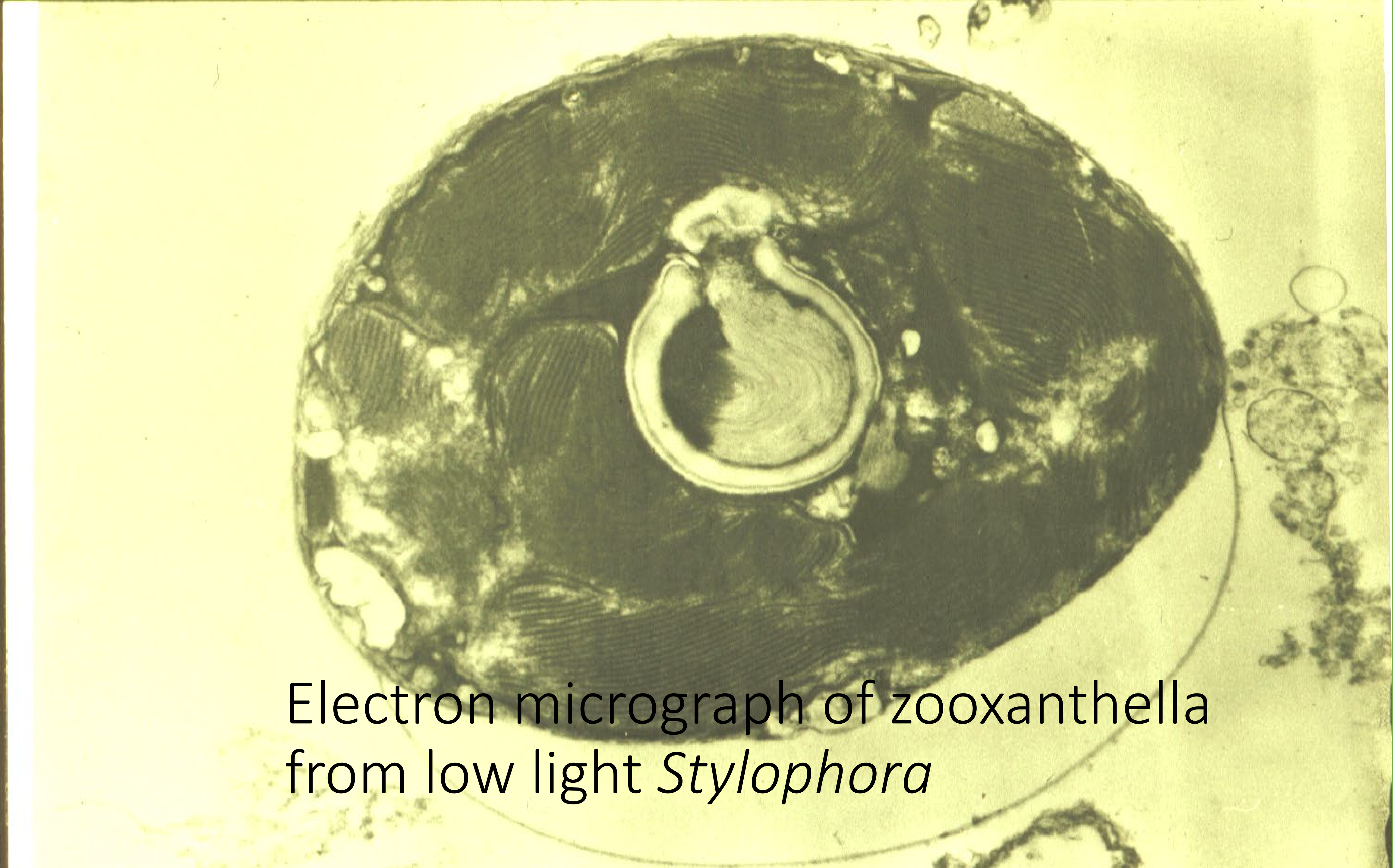

Electron micrograph of zooxanthella
from low light *Stylophora*

Electron micrograph of zooxanthella from high light *Stylophora*

Photoacclimation strategy

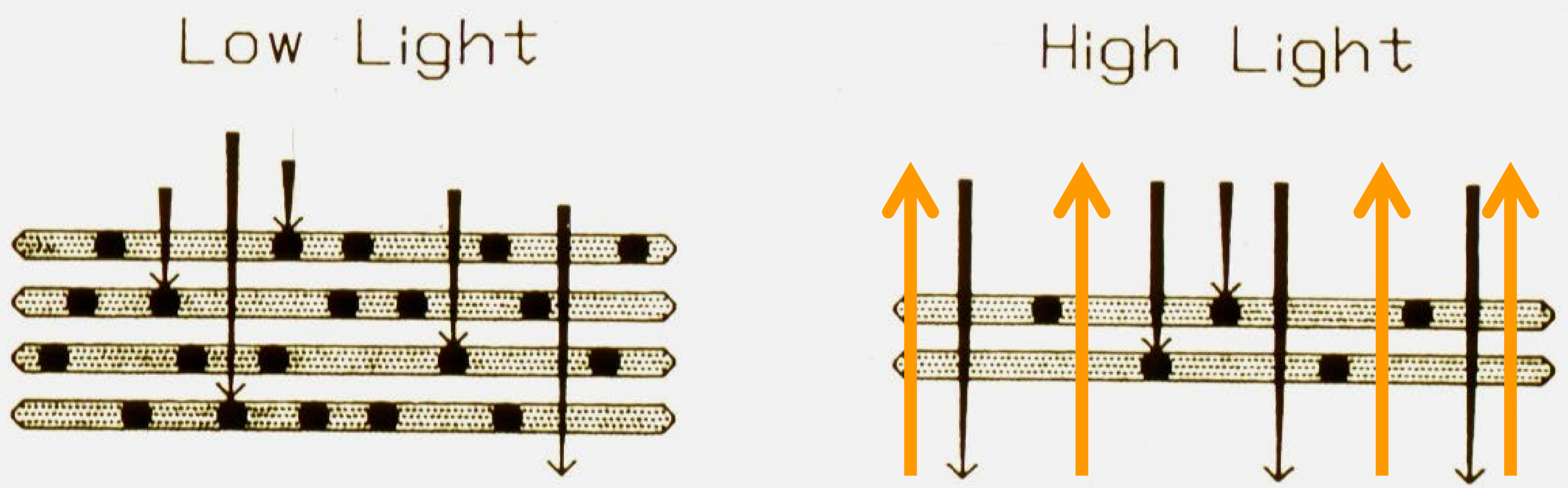

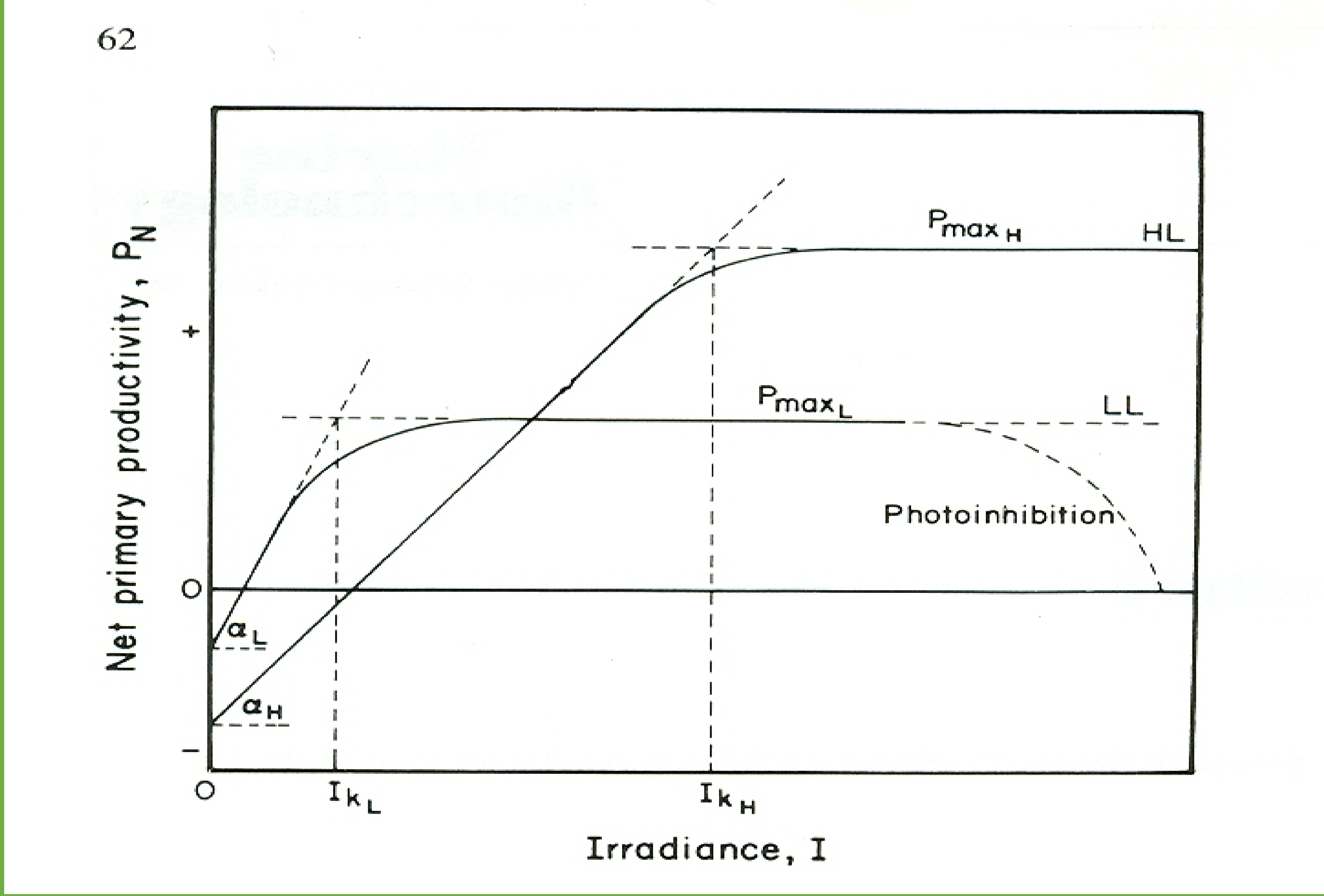

לאצות (LL) לאור גבוה ו- (HL)פוטוסינתזה ועצמת אור
מאוקלמות לאור חלש

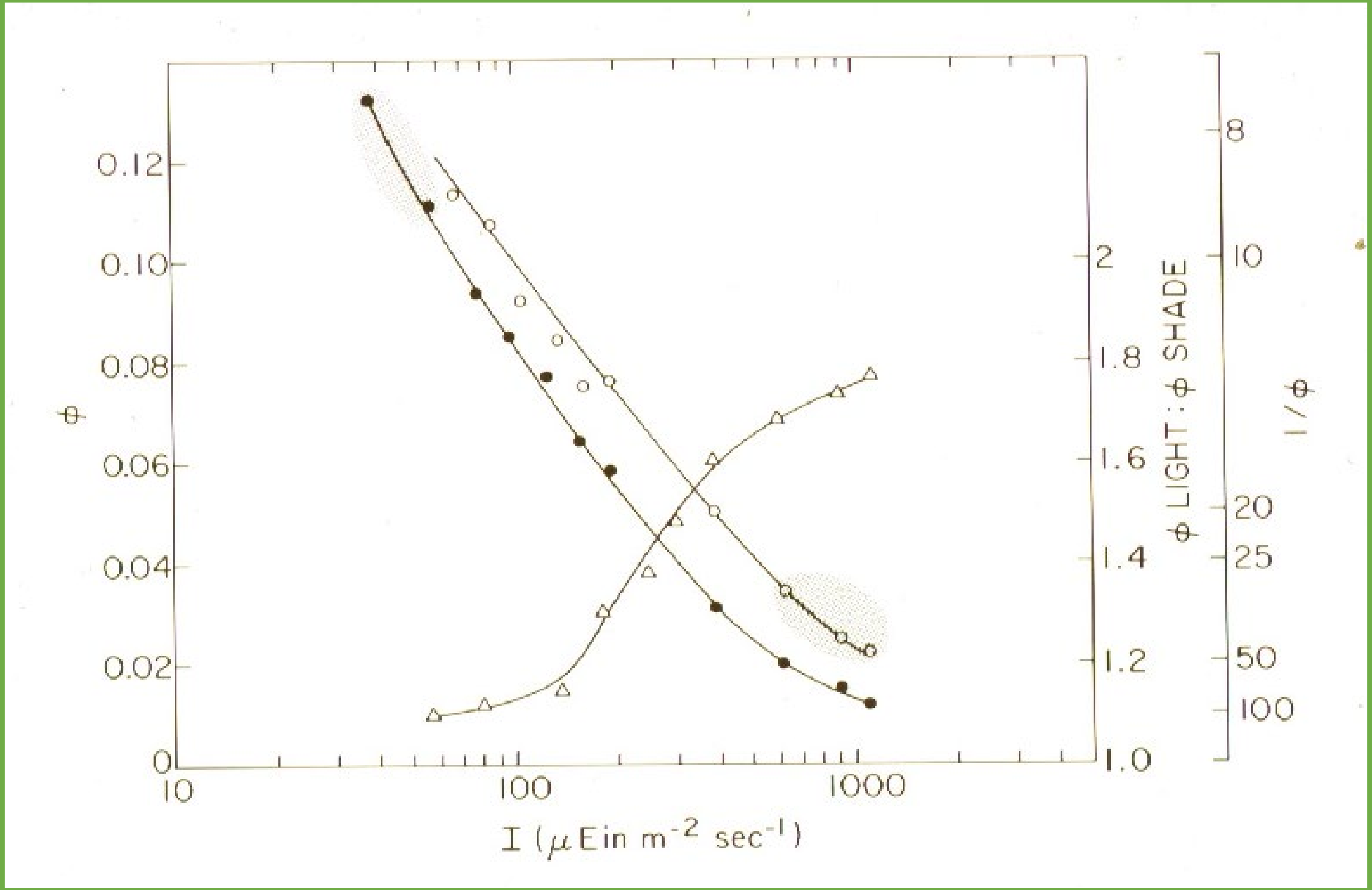

(בזואוקסנטלות ϕנצולת פוטוסינטטית)
מאלמוגי אור גבוה ונמוך

תרבית של Haematococcus pluvialis
חזק למטה ,אור חלש למעלה,

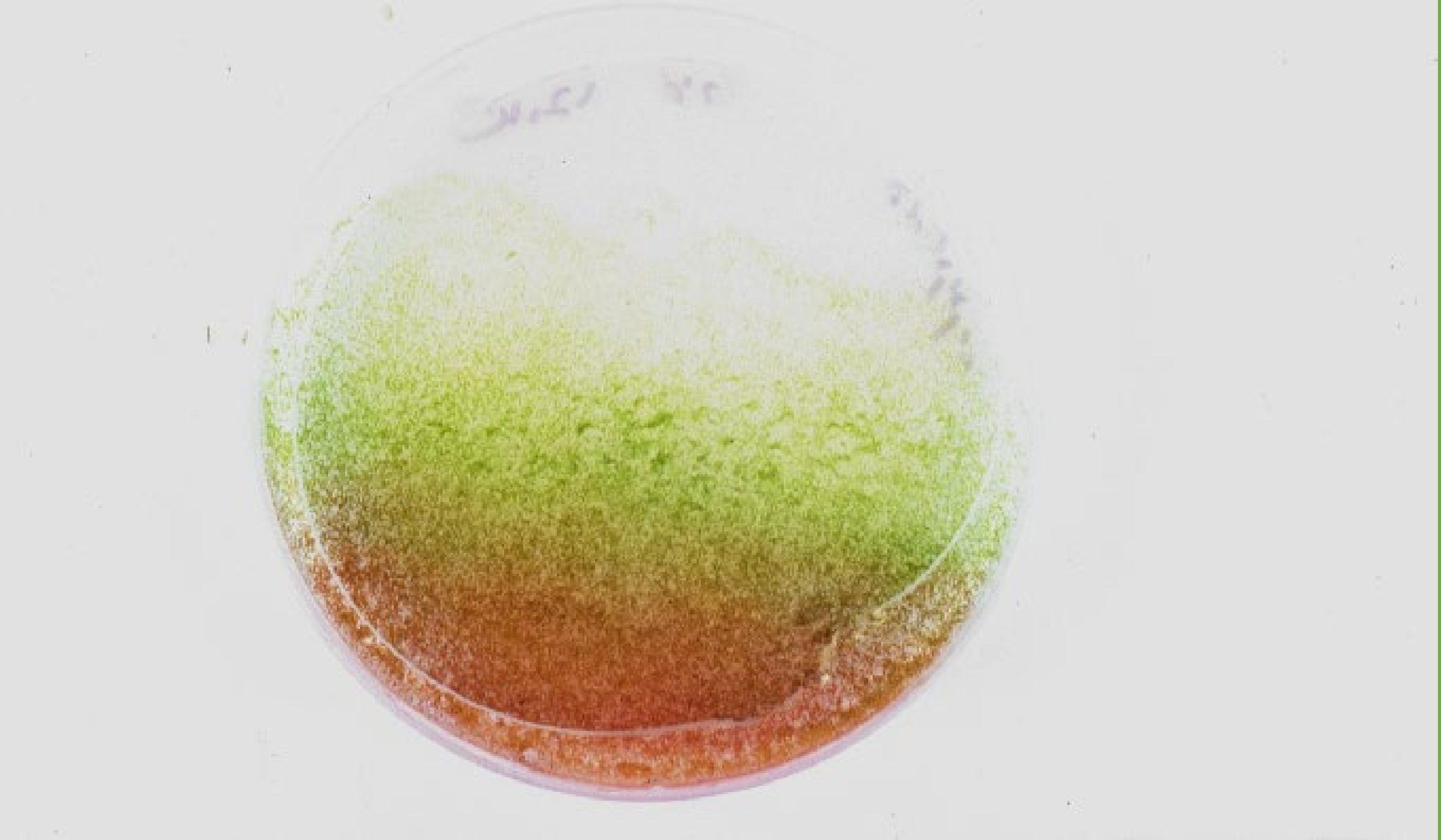

הקרוטנואידים Carotenoids

- מתחלקים ל"קוצרי אור"
- Fucoxanthine
- Peridinine
- photoprotective "ו"למגיני אור
- B carotene
- Astaxanthine
- Xanthophyll פיגמנטים של מעגל ה-

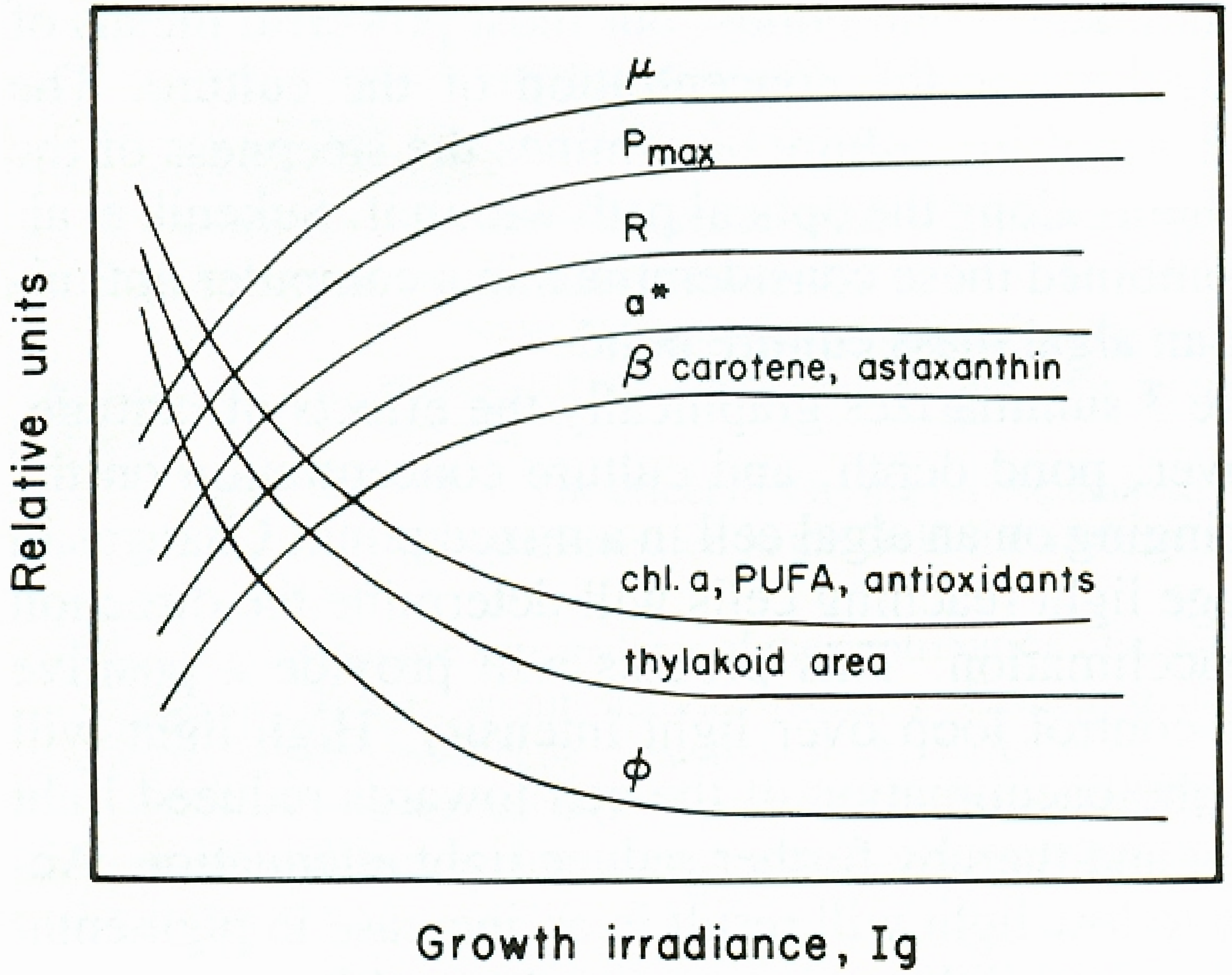

השפעת עוצמת אור גידול של אצות על קצבי הפוטוסינתזה והגדילה שלהן

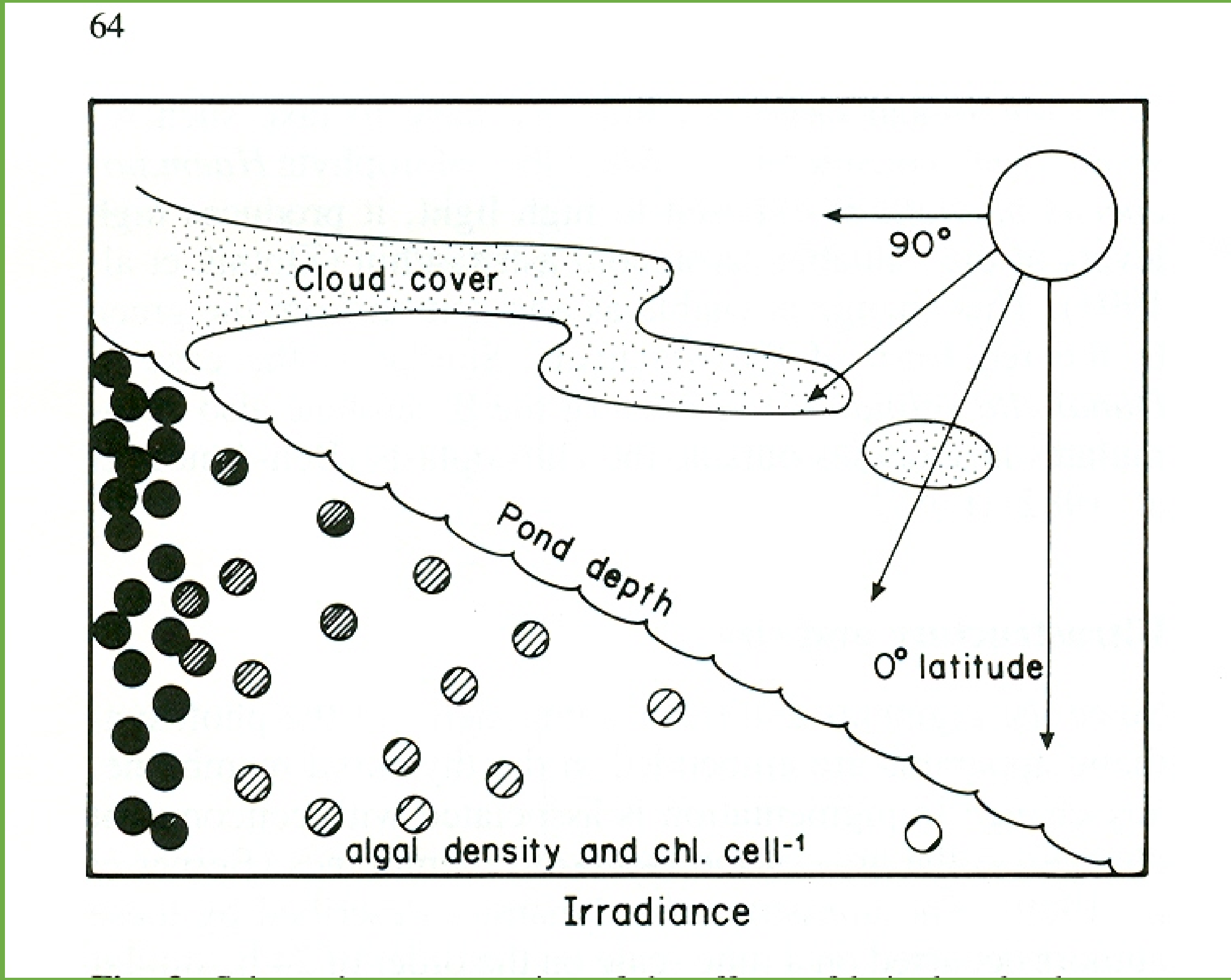

Schematic representation of the effects of latitude, cloud cover, pond depth and cellular pigment content on the time integrated average photon flux

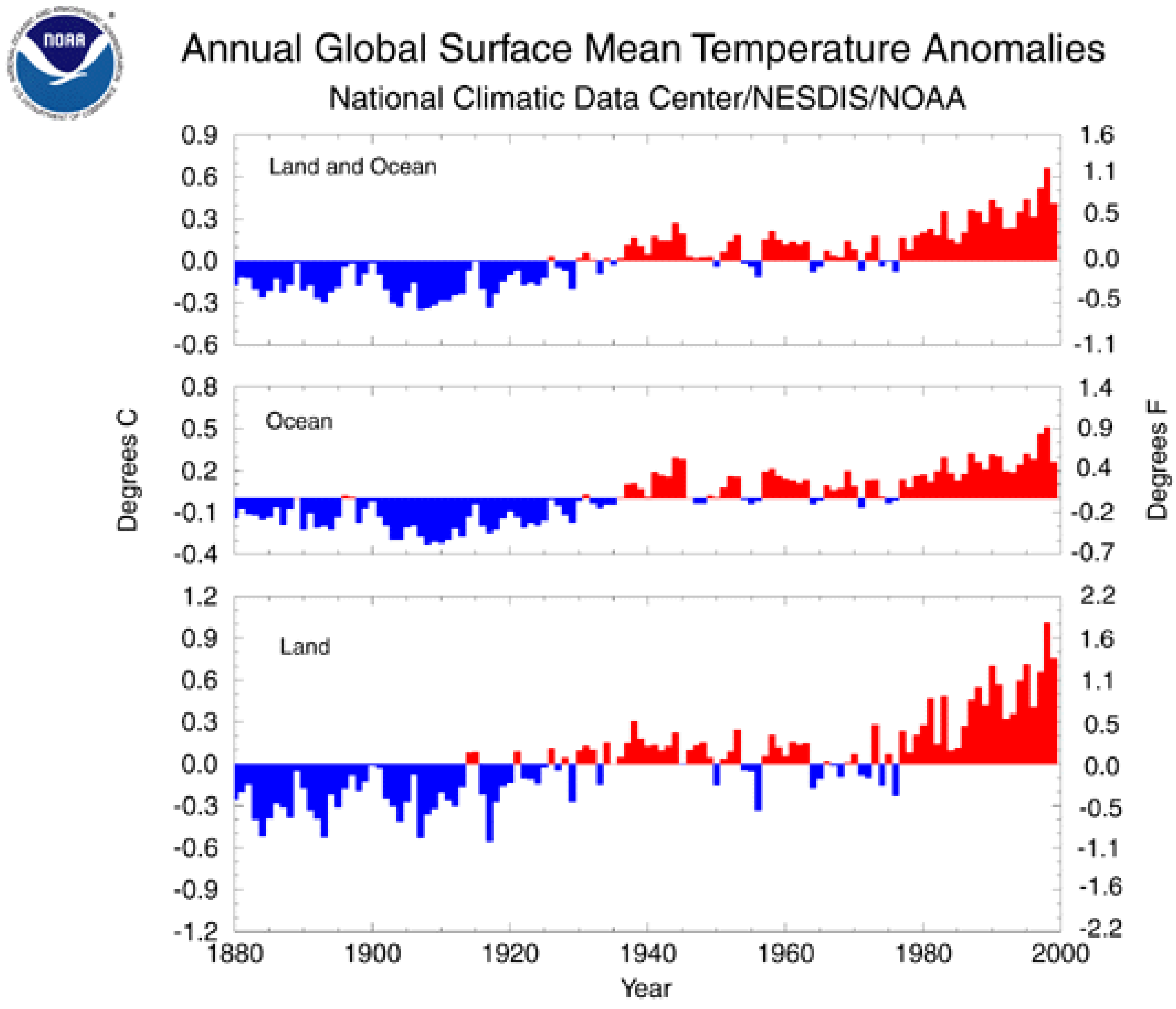

Annual Global Surface Mean Temperature Anomalies
National Climatic Data Center/NESDIS/NOAA
Land and Ocean
Ocean
Land
Degrees C
Degrees F
0.9
0.6
0.3
0.0
-0.3
-0.6
1.6
1.1
0.5
0.0
-0.5
-1.1
0.8
0.5
0.2
-0.1
-0.4
1.4
0.9
0.4
-0.2
-0.7
1.2
0.9
0.6
0.3
0.0
-0.3
-0.6
-0.9
-1.2
2.2
1.6
1.1
0.5
0.0
-0.5
-1.1
-1.6
-2.2
1880
1900
1920
1940
1960
1980
2000
Year

Temperature and CO_2 concentration in the atmosphere over the past 400 000 years (from the Vostok ice core)

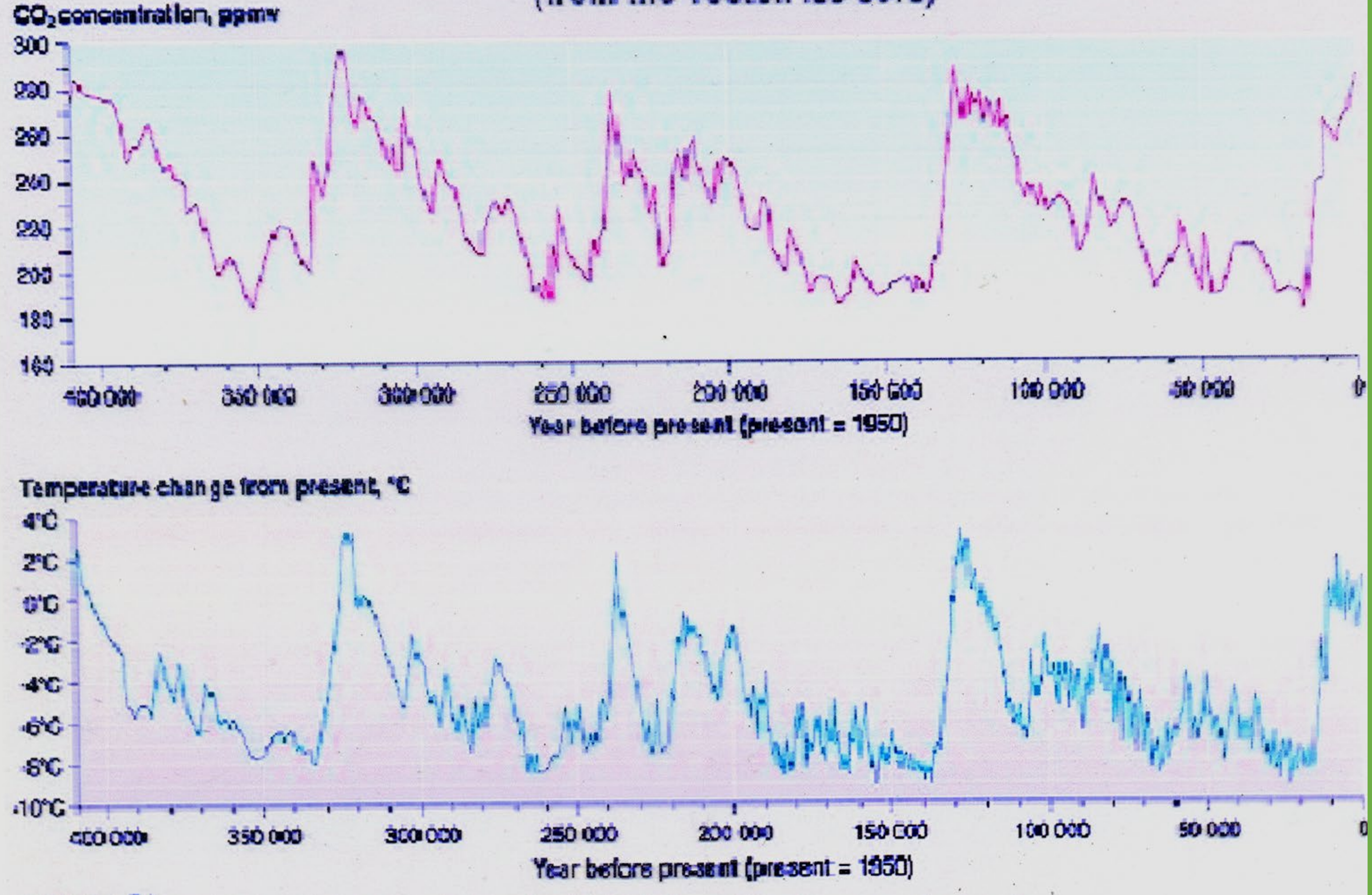

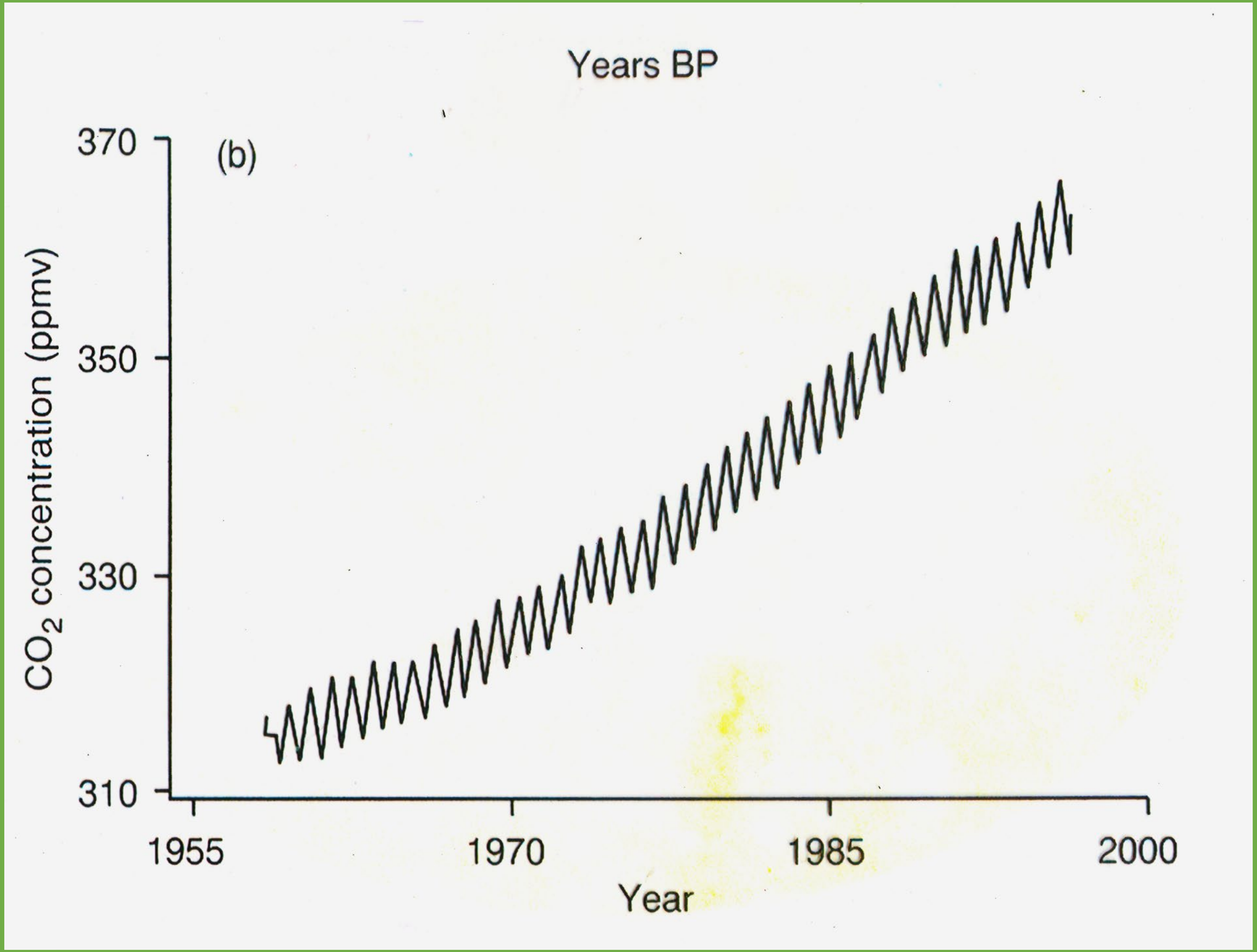
Years BP
(b)
370
350
330
310
CO_2 concentration (ppmv)
1955
1970
1985
2000
Year

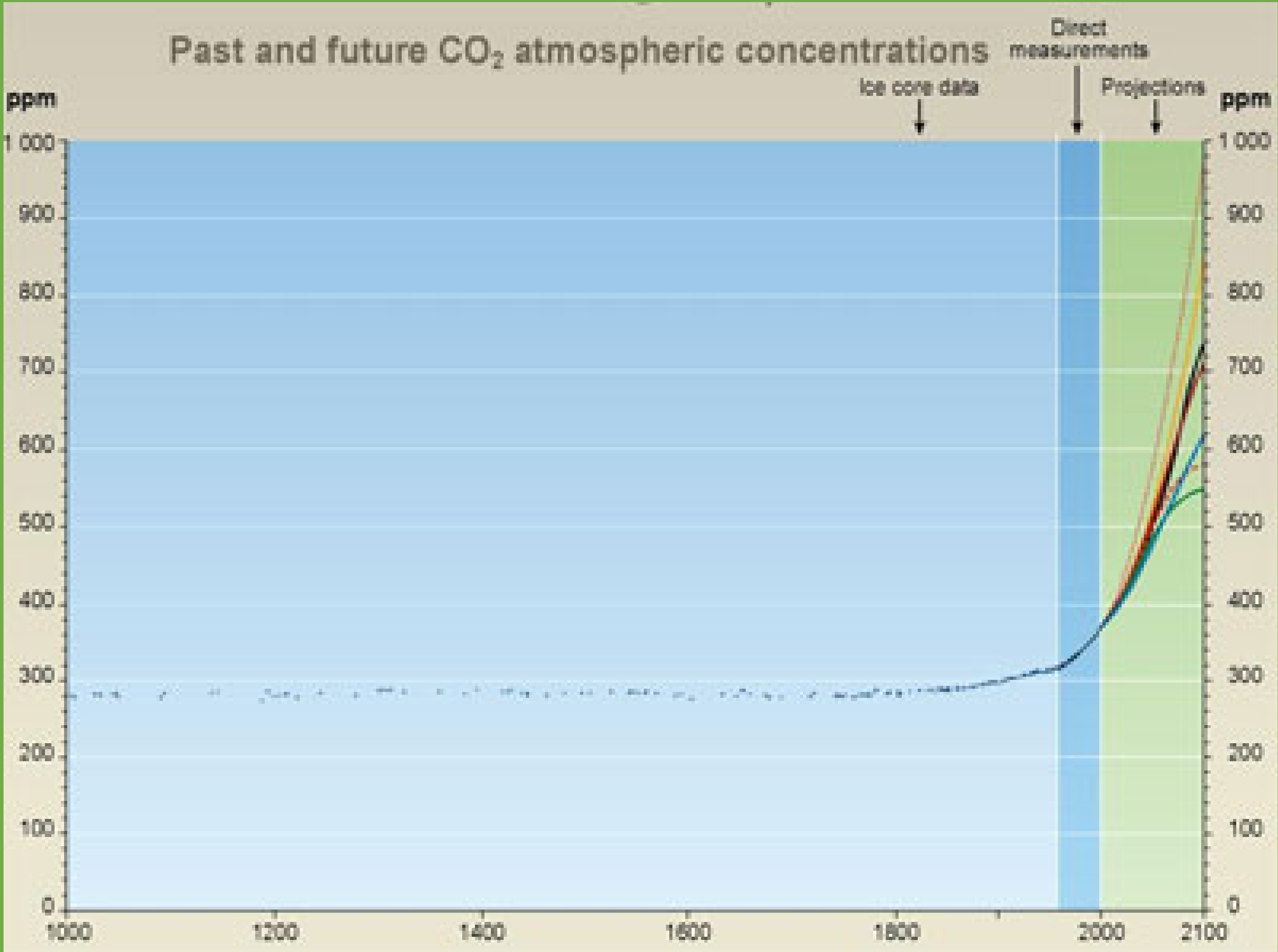

Past and future CO2 atmospheric concentrations
Direct measurements
Ice core data
Projections
ppm
ppm
1 000
900
800
700
600
500
400
300
200
100
0
1000
1200
1400
1600
1800
2000
2100

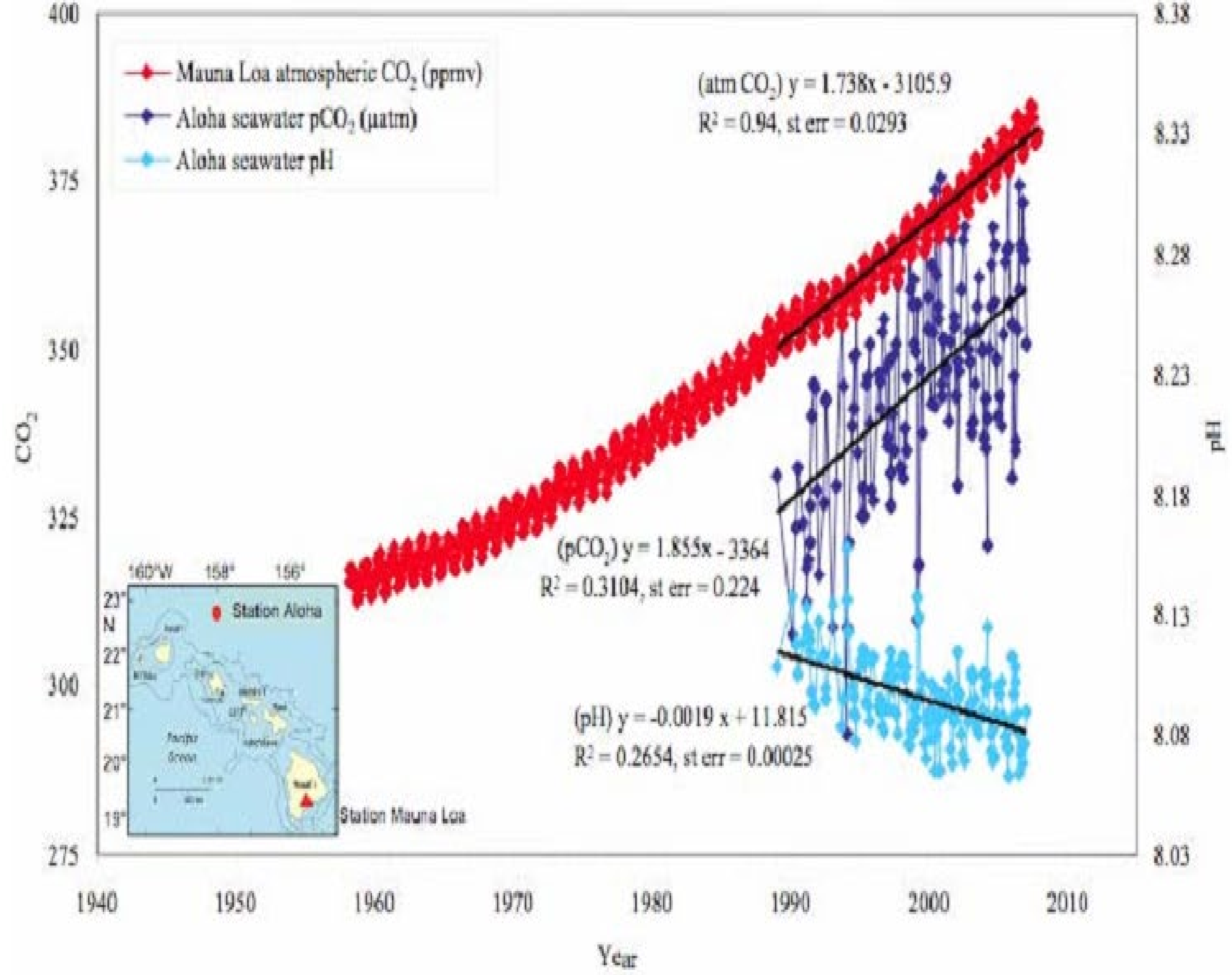

Fig. 1 Time series of atmospheric CO_2 at Mauna Loa (ppmv) and surface ocean pH and pCO_2 (µatm) at Ocean Station Aloha in the subtropical Nor Pacific Ocean. Note that the increase in oceanic CO_2 over the last 17 years is consistent with the atmospheric increase within the statistical limits of the measurements. Mauna Loa data: Dr. Pieter Tans, NOAA/ESRL (http://www.esrl.noaa.gov/gmd/ccgg/trends); HOTS/Aloha data: Dr. David Karl, University of Hawaii (http://hahana.soest.hawaii.edu).

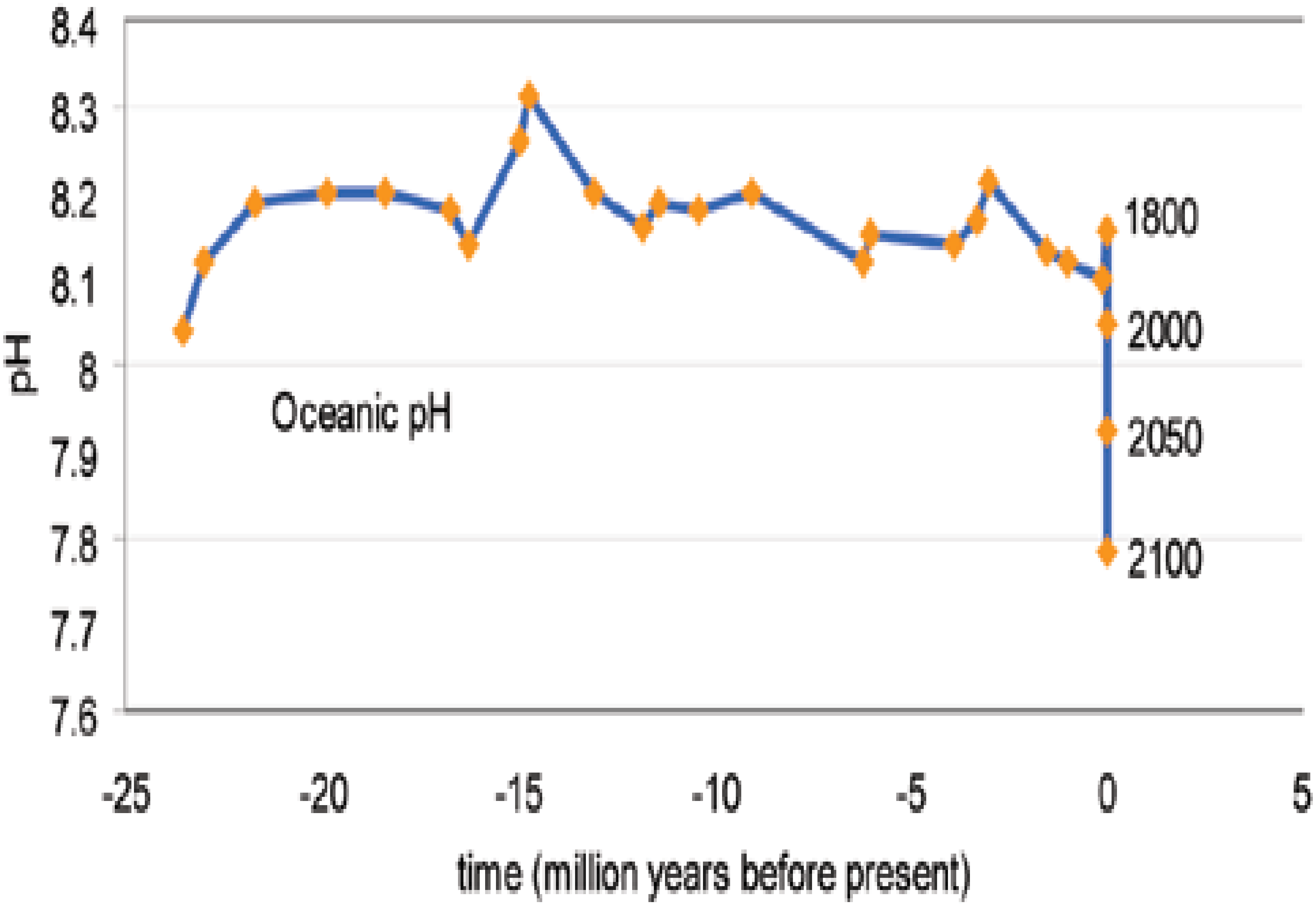

8.4
8.3
8.2
8.1
8
7.9
7.8
7.7
7.6
pH
Oceanic pH
1800
2000
2050
2100
-25
-20
-15
-10
-5
0
5
time (million years before present)

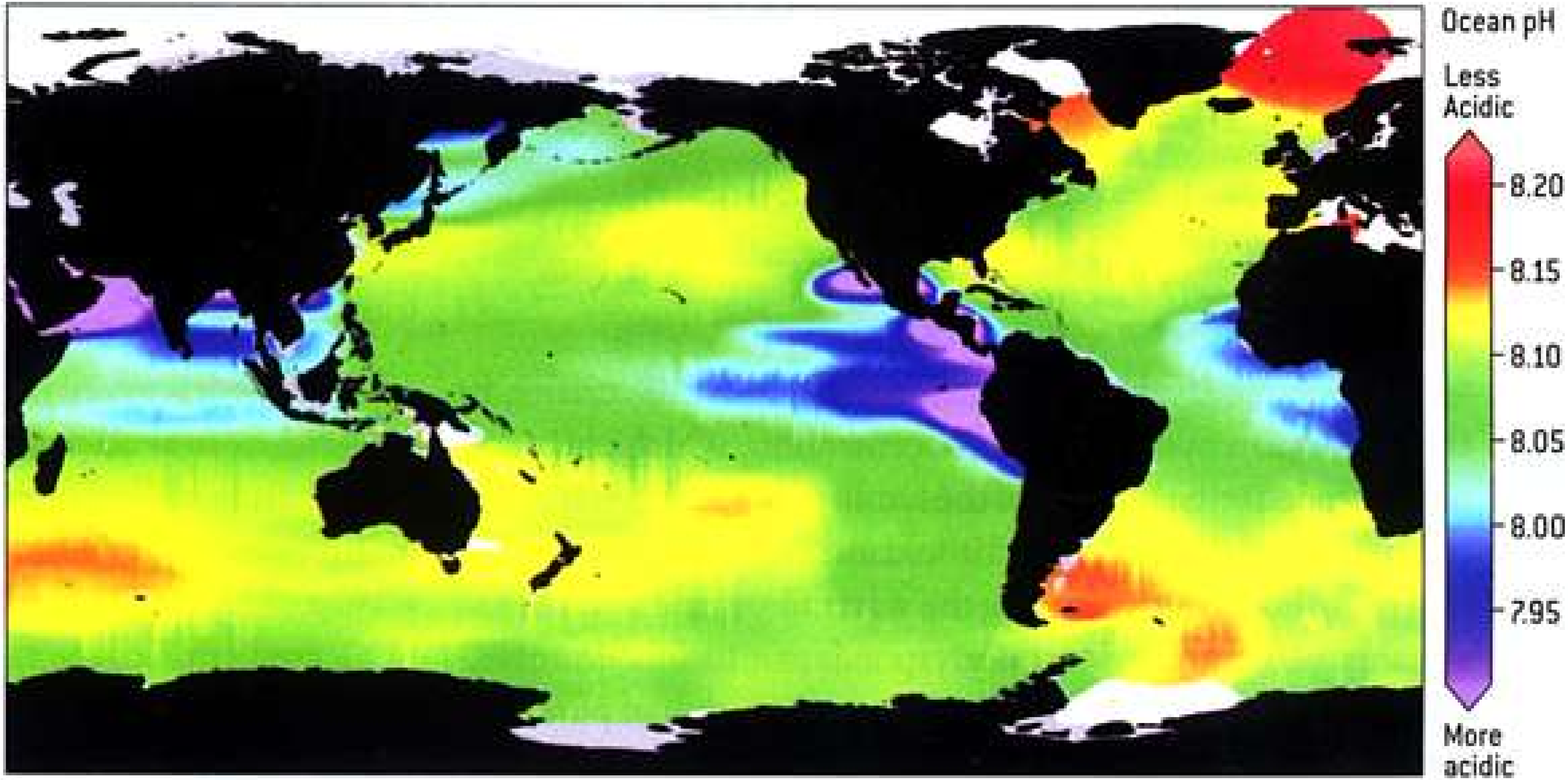

Ocean pH Source: Scott C Doney, SciAm March 2006

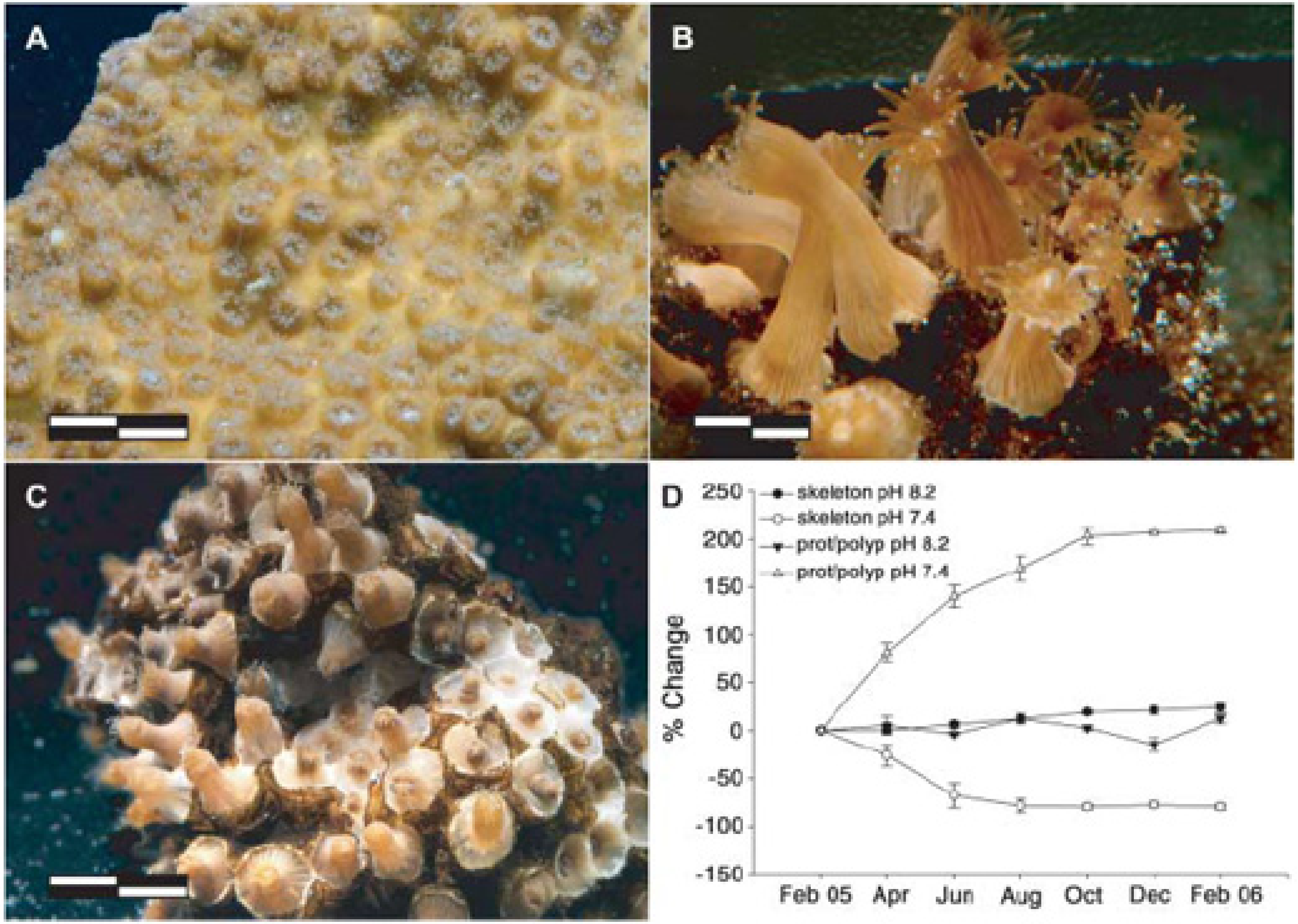
A
B
C
D
skeleton pH 8.2
skeleton pH 7.4
prot/polyp pH 8.2
prot/polyp pH 7.4
% Change
250
200
150
100
50
0
-50
-100
-150
Feb 05
Apr
Jun
Aug
Oct
Dec
Feb 06

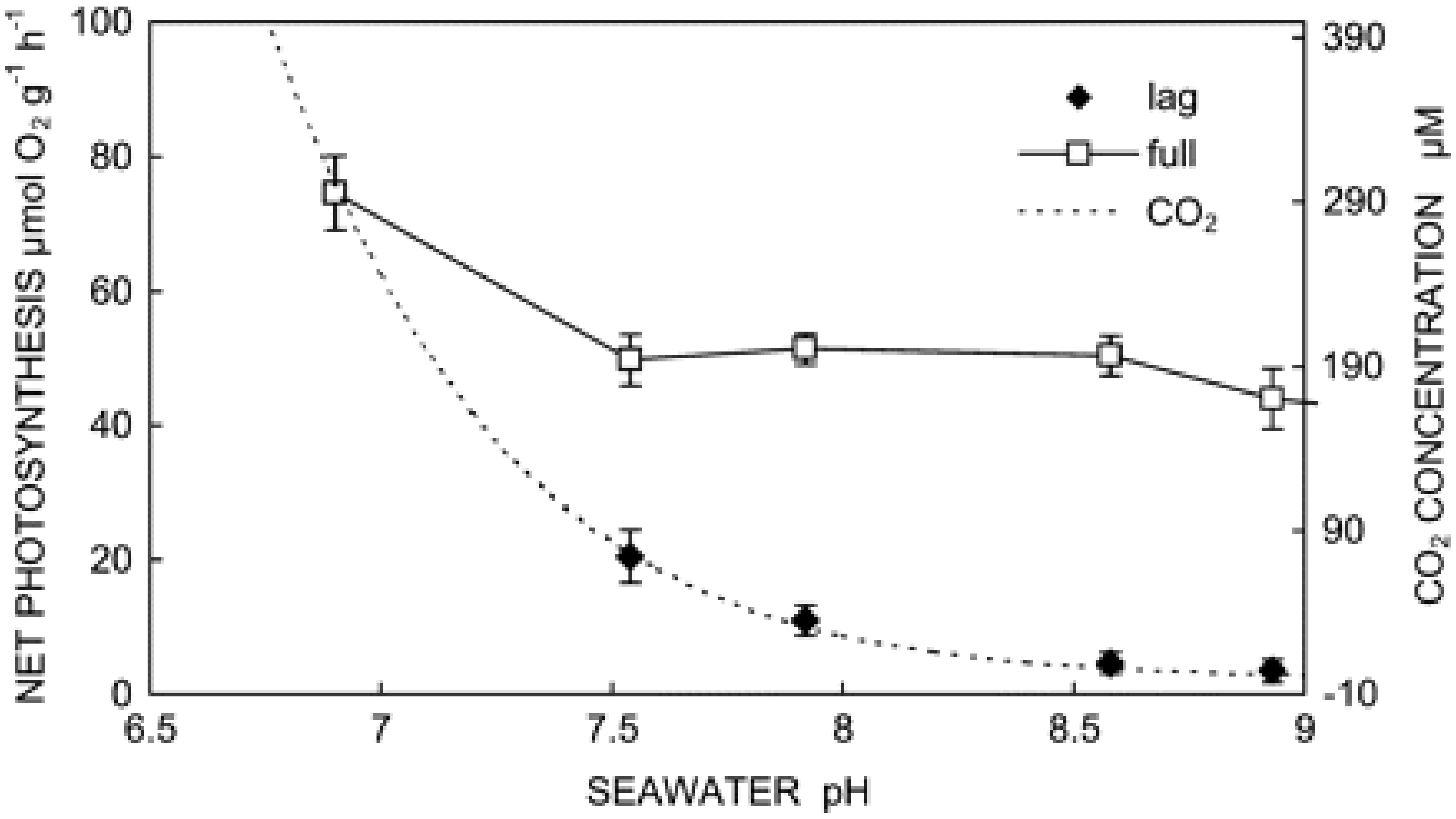

NET PHOTOSYNTHESIS µmol O2 g-1 h-1
CO2 CONCENTRATION µM
SEAWATER pH
lag
full
CO2
0
20
40
60
80
100
6.5
7
7.5
8
8.5
9
-10
90
190
290
390

Why algae
Quantum yield
Areal efficiency
=income

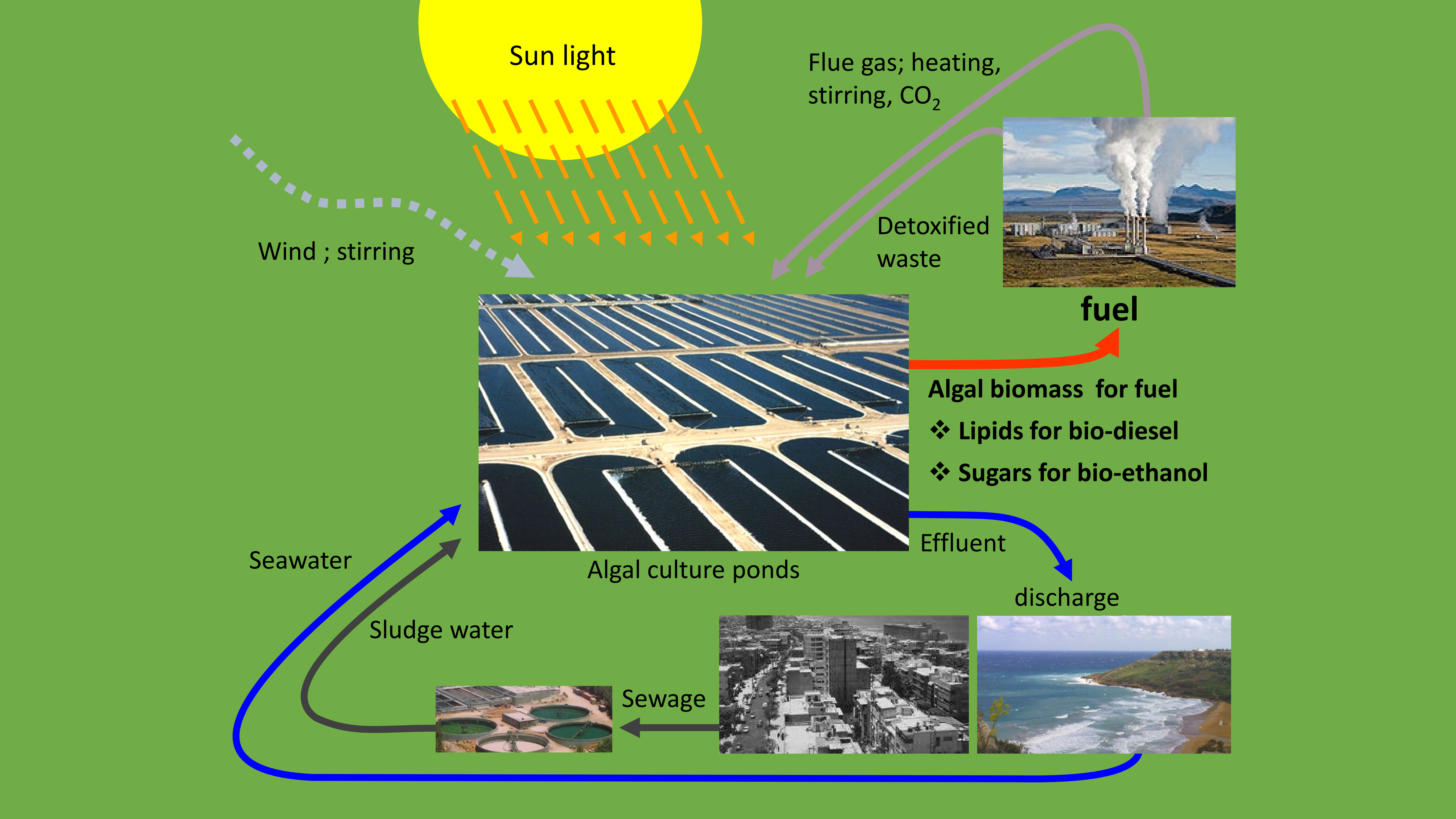
Sun light
Flue gas; heating, stirring, CO_2
Wind ; stirring
Detoxified waste
fuel
Algal biomass for fuel
❖ Lipids for bio-diesel
❖ Sugars for bio-ethanol
Effluent
Algal culture ponds
Seawater
discharge
Sludge water
Sewage

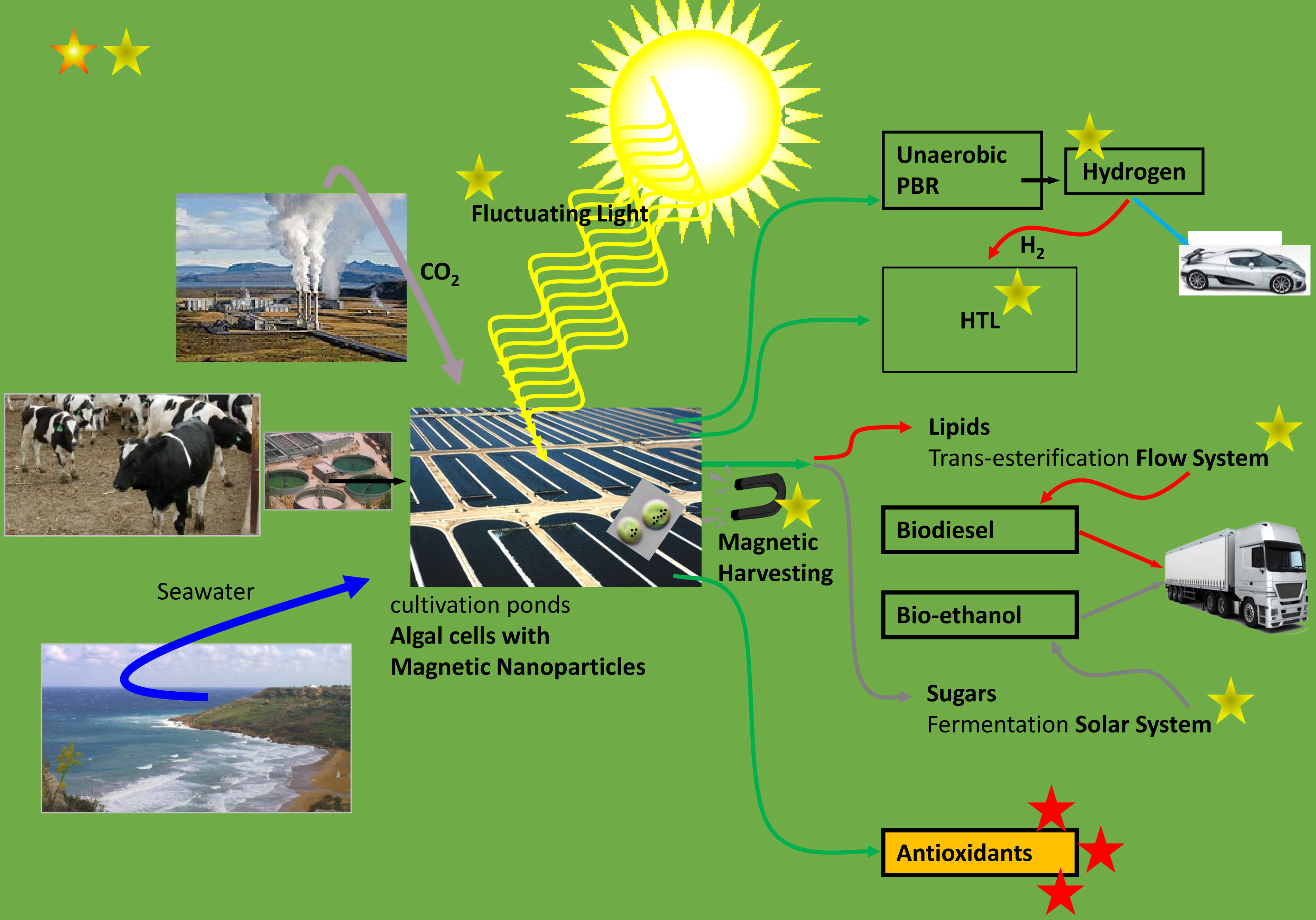

Fluctuating Light
CO2
cultivation ponds
Algal cells with
Magnetic Nanoparticles
Seawater
Magnetic
Harvesting
Unaerobic
PBR
Hydrogen
H2
HTL
Lipids
Trans-esterification Flow System
Biodiesel
Bio-ethanol
Sugars
Fermentation Solar System
Antioxidants

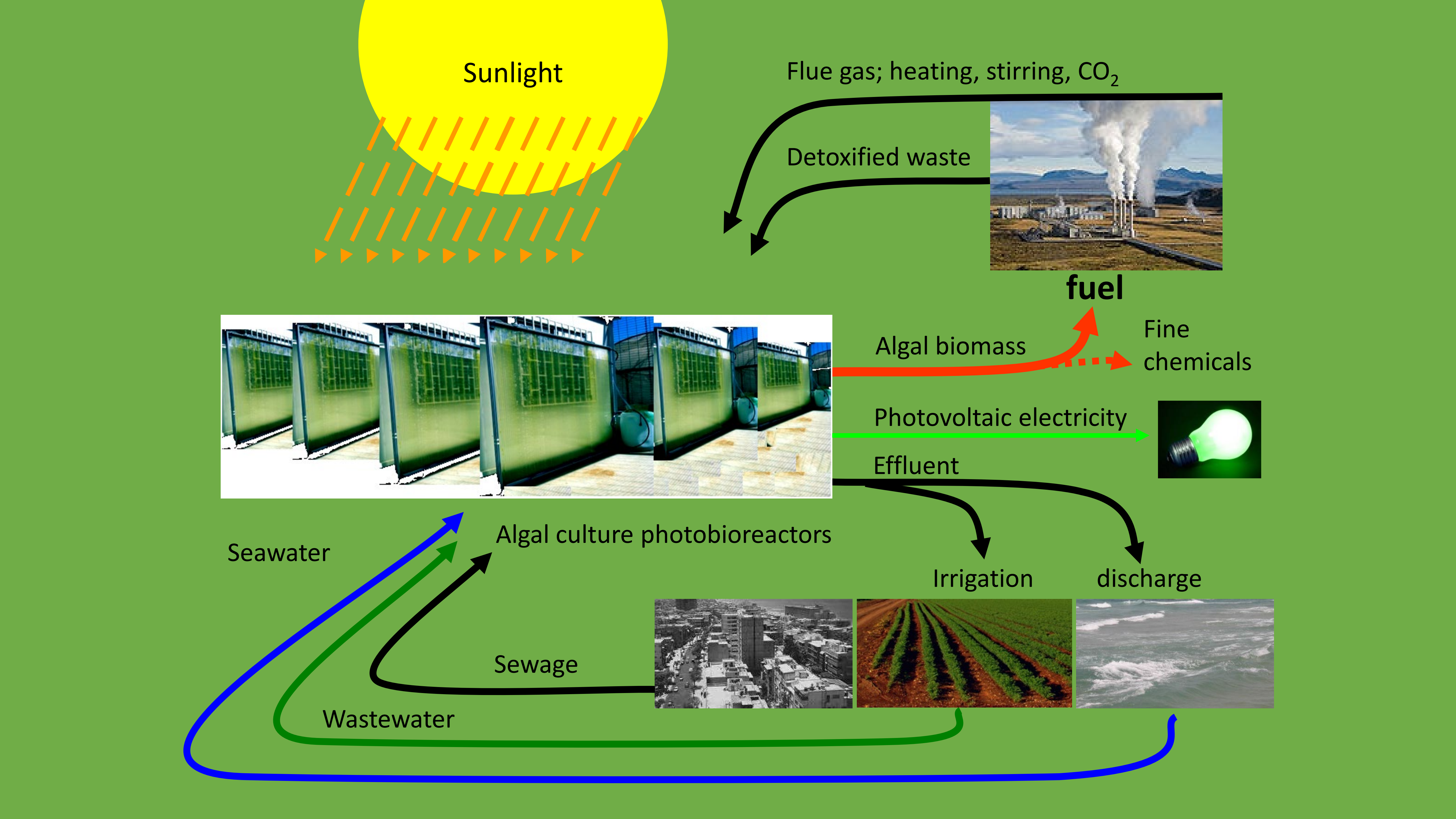
Sunlight
Flue gas; heating, stirring, CO_2
Detoxified waste
fuel
Algal biomass
Fine chemicals
Photovoltaic electricity
Effluent
Algal culture photobioreactors
Seawater
Irrigation
discharge
Sewage
Wastewater

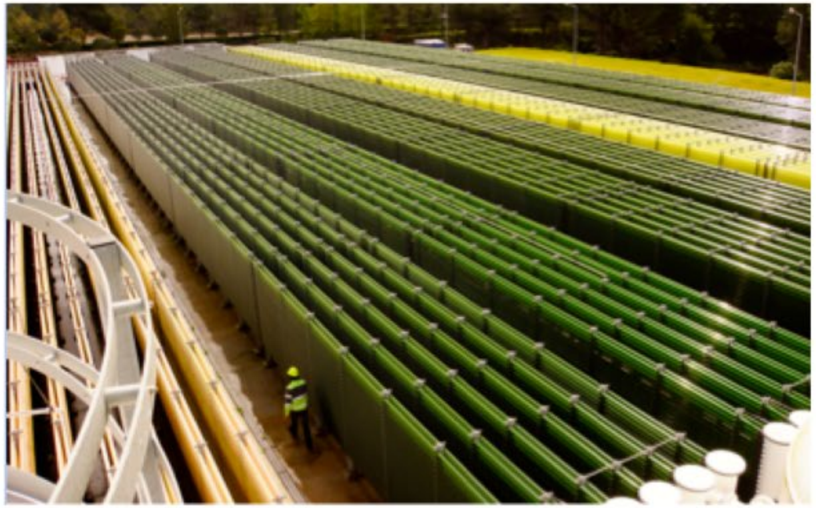

AlgaFarm designed, built, operated by A4F
Tubular Photobioreactors > 1.300 m3

BIOFAT designed, built, operated by A4F
Cascade Raceways > 3.000 m2 - 900 m3

Algal biotechnology unit at Bar Ilan University

Ponds are fully computerized and optimized for the production of biodiesel and fine chemicals, using seawater and brackish water, fertilizer from sewage and CO_2 from industry.

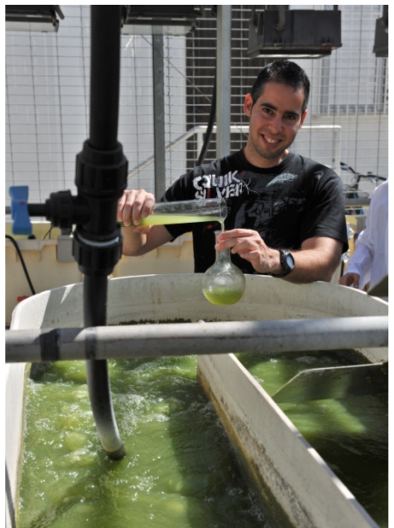

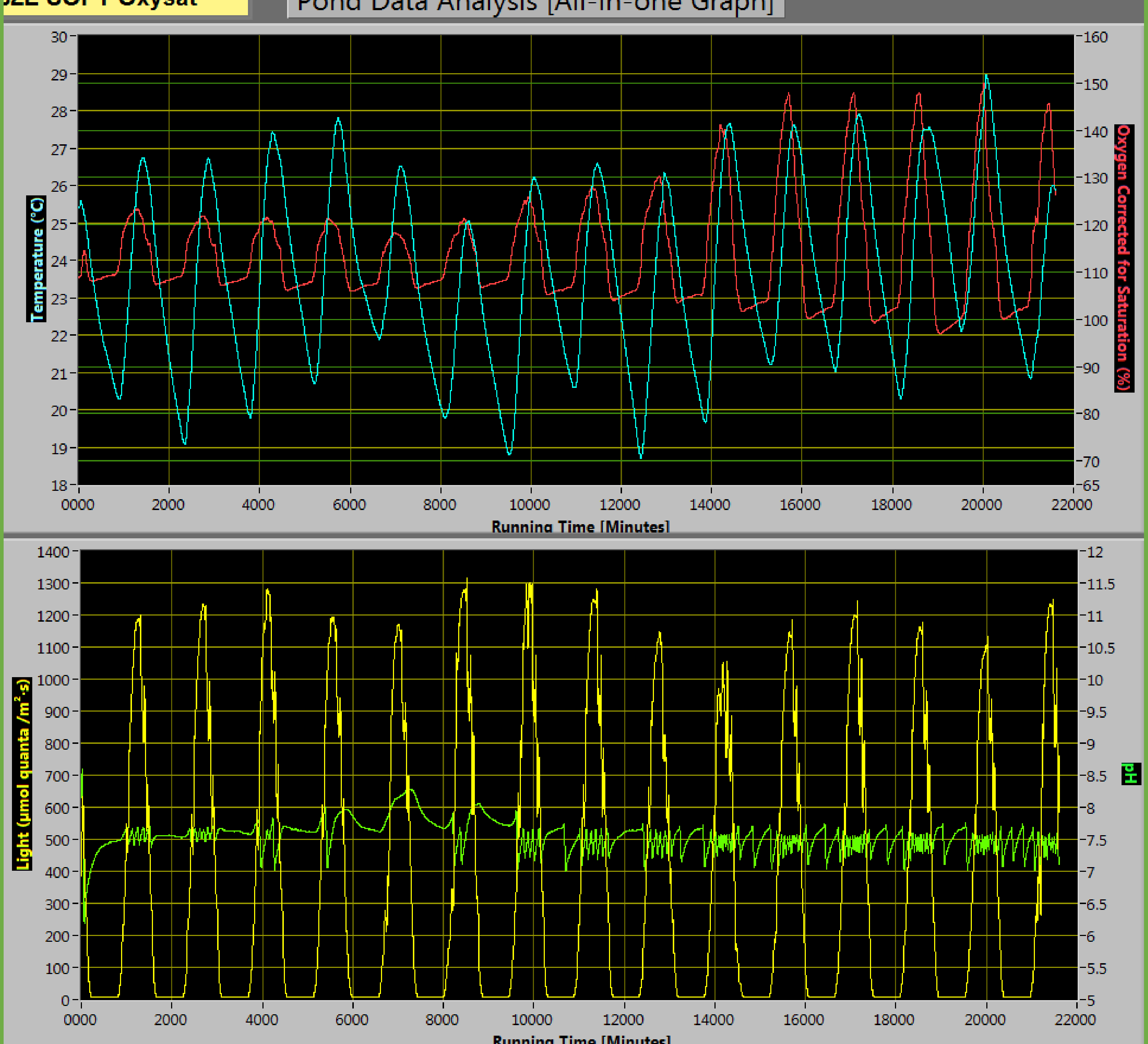

Pond Data Analysis [All-in-one Graph]
Temperature (°C)
Oxygen Corrected for Saturation (%)
Running Time [Minutes]
Light (µmol quanta /m²·s)
pH
Running Time [Minutes]

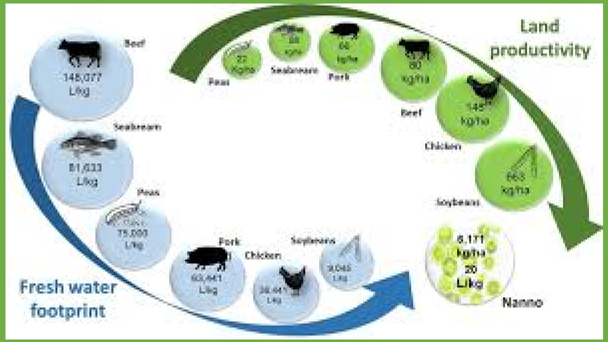
Land
productivity
Beef
Seabream
Peas
Pork
Chicken
Soybeans
Nanno
Fresh water
footprint

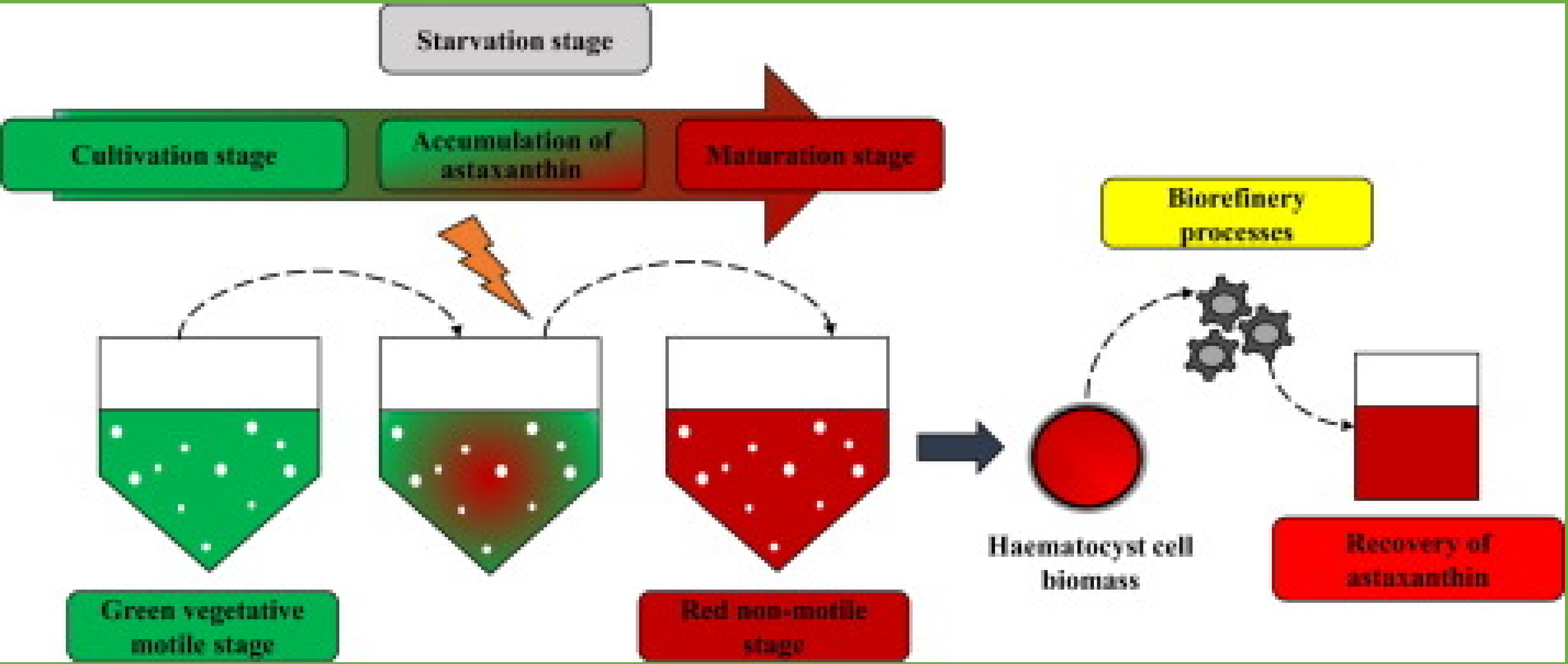
Starvation stage
Cultivation stage
Accumulation of astaxanthin
Maturation stage
Biorefinery processes
Green vegetative motile stage
Red non-motile stage
Haematocyst cell biomass
Recovery of astaxanthin

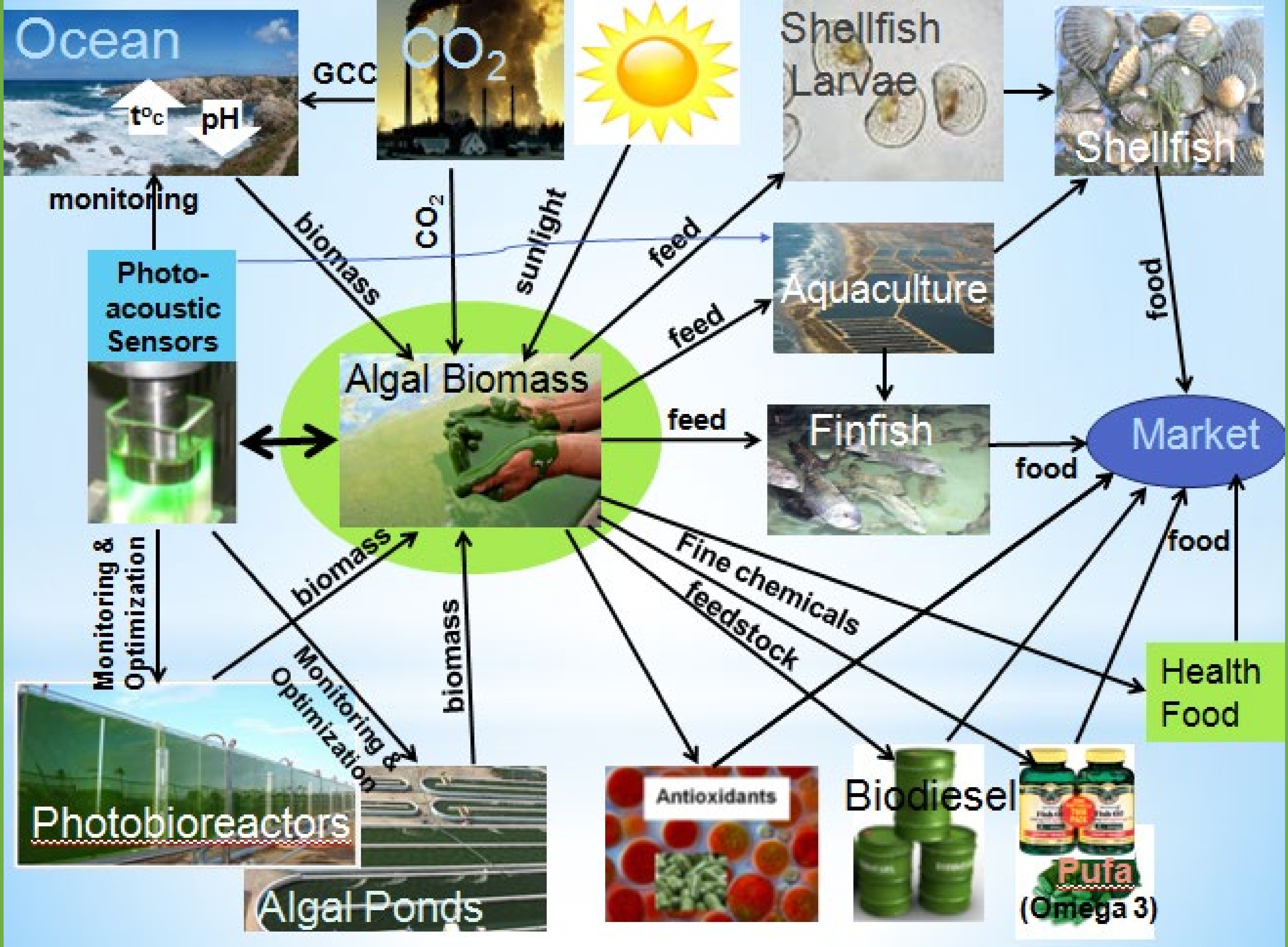
Ocean
t°C
pH
GCC
CO_2
Shellfish Larvae
Shellfish
monitoring
biomass
CO_2
sunlight
feed
Photo-acoustic Sensors
Aquaculture
food
feed
Algal Biomass
feed
Finfish
Market
food
food
Monitoring & Optimization
biomass
Fine chemicals
feedstock
Monitoring & Optimization
biomass
Health Food
Photobioreactors
Algal Ponds
Antioxidants
Biodiesel
Pufa
(Omega 3)

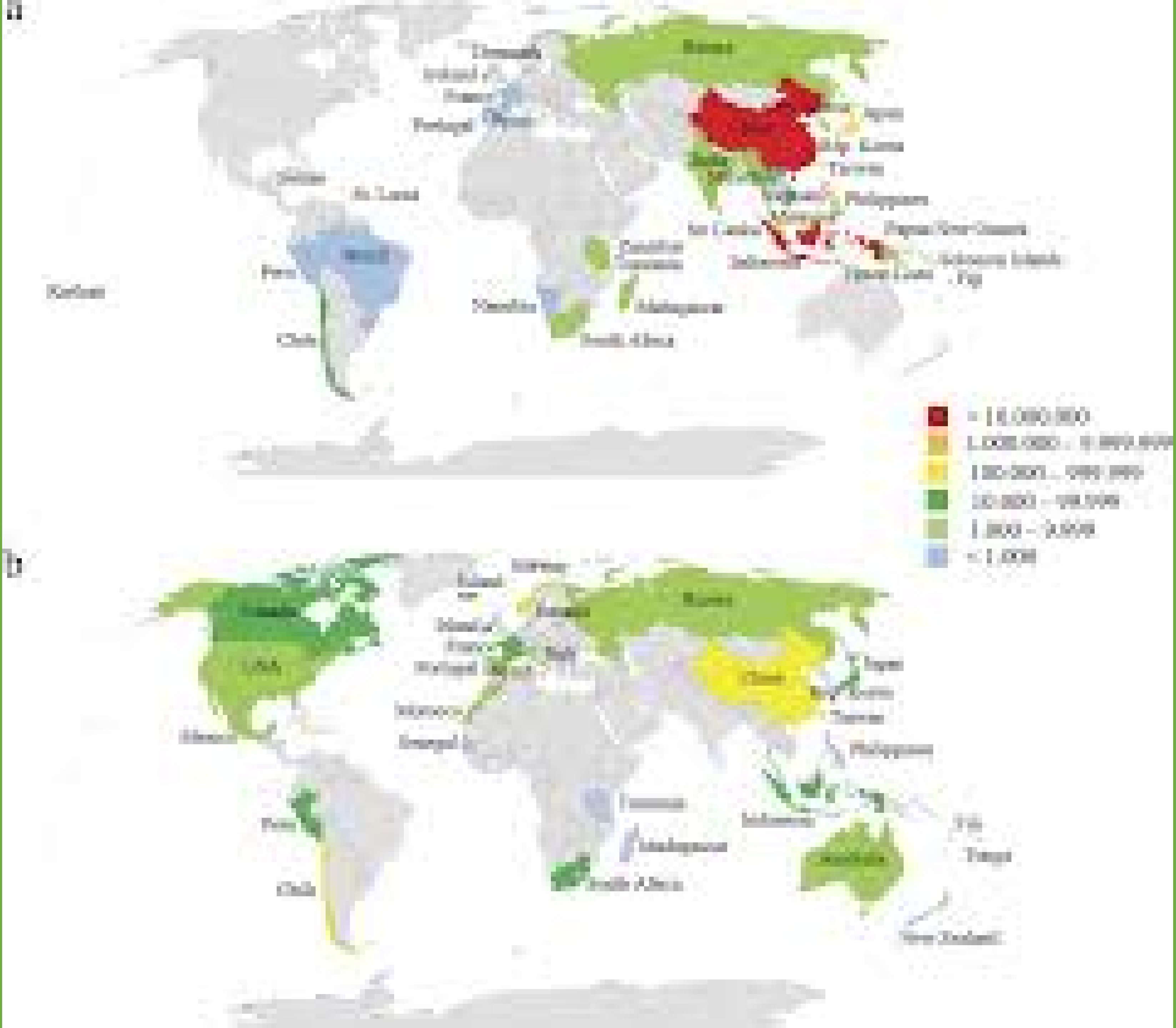
a
Russia
Denmark
Ireland
France
Portugal
Japan
Rep. Korea
Taiwan
Philippines
Sri Lanka
Papua New Guinea
Indonesia
Solomon Islands
Fiji
Brazil
Peru
Namibia
Madagascar
South Africa
Chile
> 10,000,000
1,000,000 – 9,999,999
100,000 – 999,999
10,000 – 99,999
1,000 – 9,999
< 1,000
b
Russia
Canada
USA
France
Portugal
Morocco
Senegal
Mexico
China
Japan
Taiwan
Philippines
Indonesia
Peru
Chile
Madagascar
South Africa
Australia
Fiji
Tonga
New Zealand

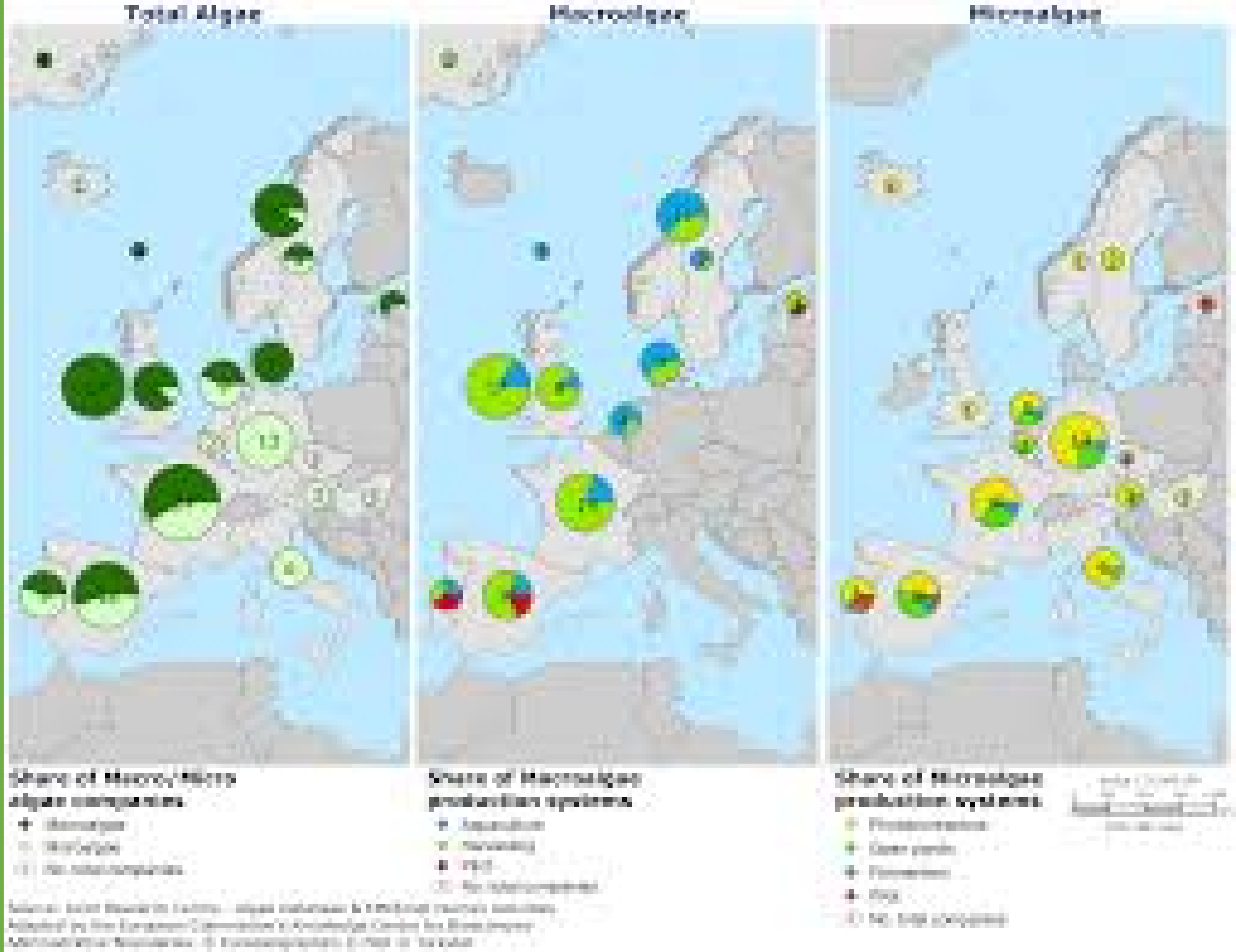

Total Algae
Macroalgae
Microalgae
Share of Macro/Micro algae companies
Share of Macroalgae production systems
Share of Microalgae production systems

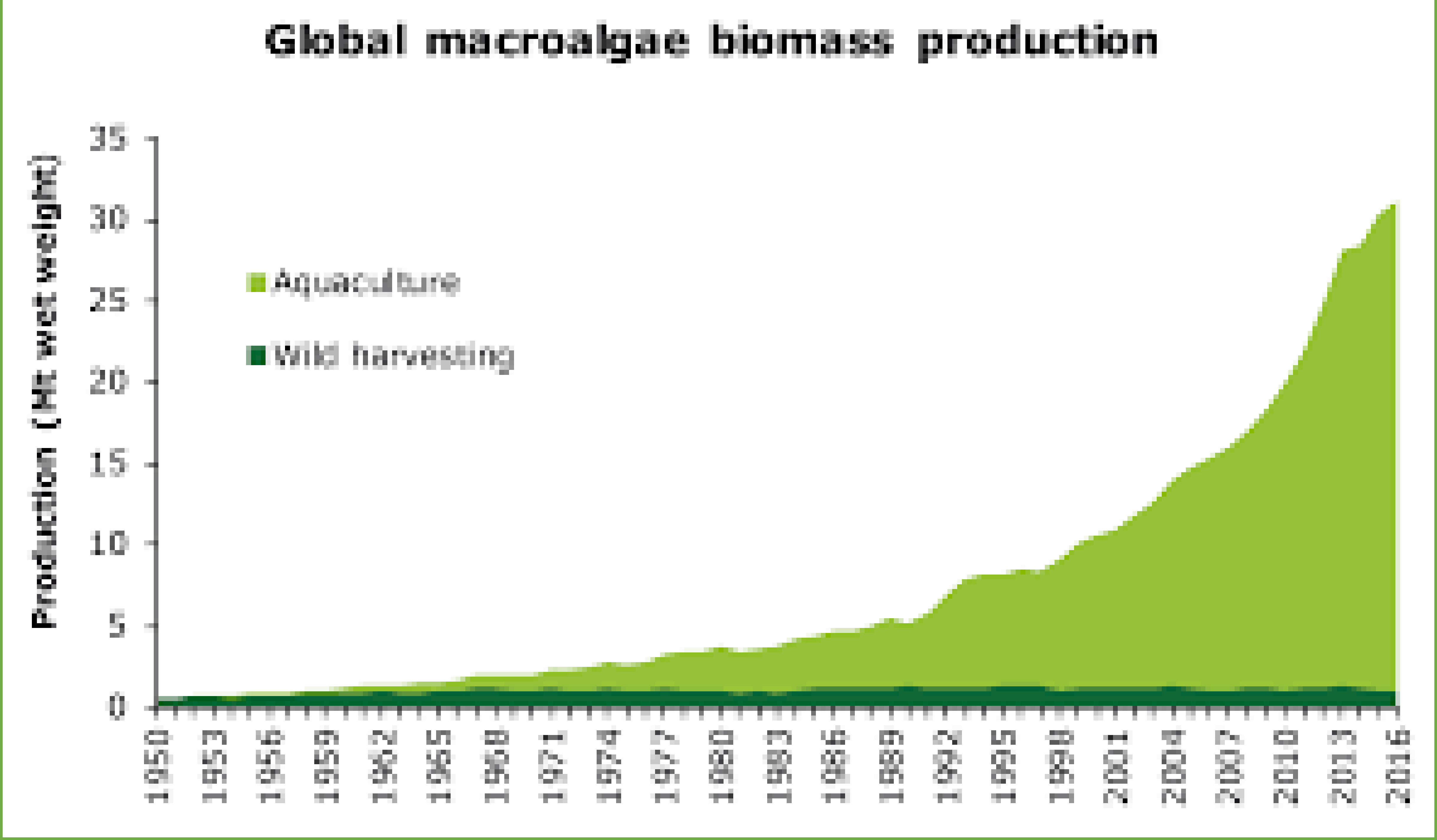

Global macroalgae biomass production
Production (Mt wet weight)
35
30
25
20
15
10
5
0
Aquaculture
Wild harvesting
1950
1953
1956
1959
1962
1965
1968
1971
1974
1977
1980
1983
1986
1989
1992
1995
1998
2001
2004
2007
2010
2013
2016

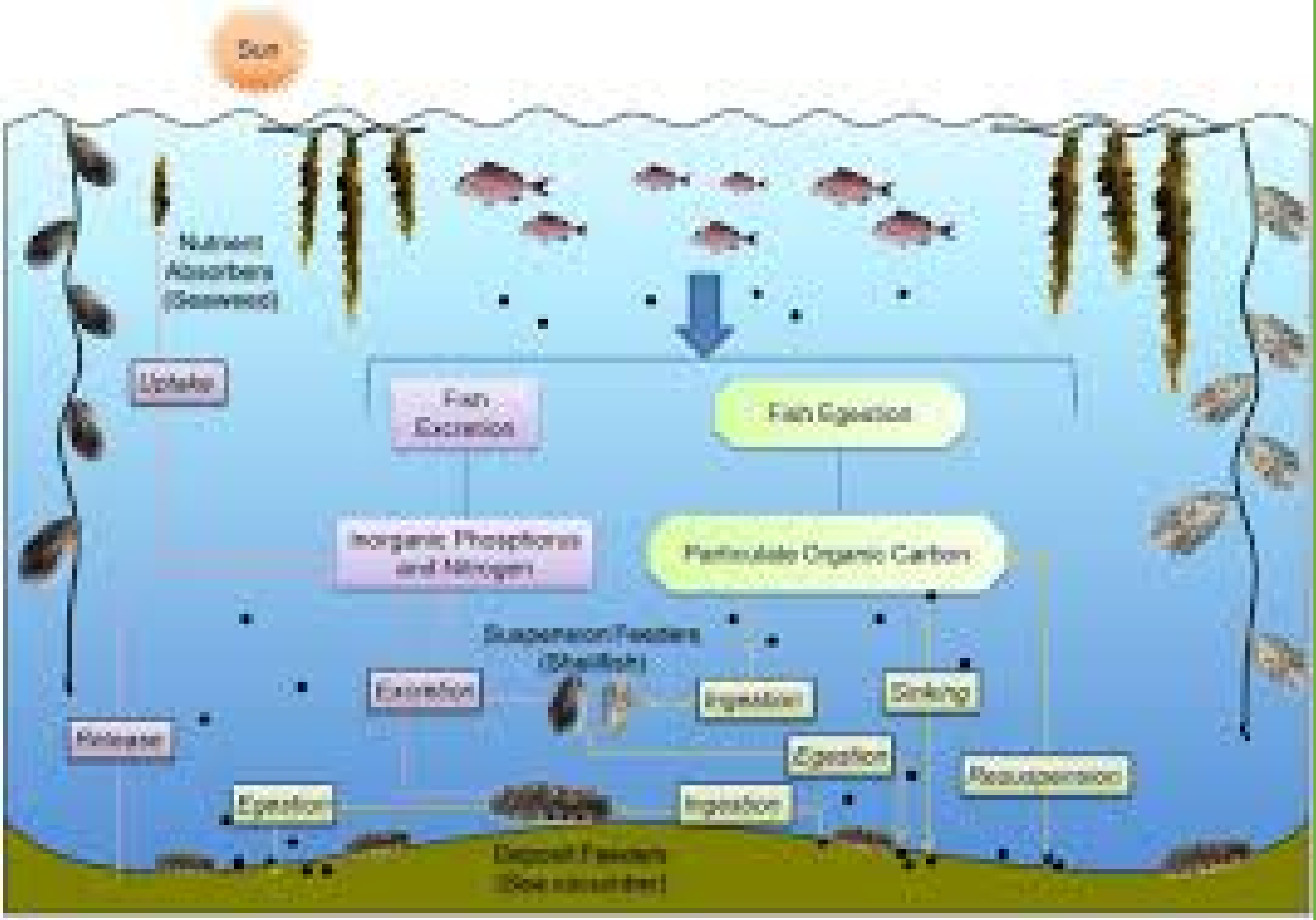
Sun
Nutrient Absorbers (Seaweed)
Uptake
Fish Excretion
Fish Egestion
Inorganic Phosphorus and Nitrogen
Particulate Organic Carbon
Suspension Feeders (Shellfish)
Excretion
Ingestion
Sinking
Release
Egestion
Resuspension
Egestion
Ingestion
Deposit Feeders (Sea cucumber)

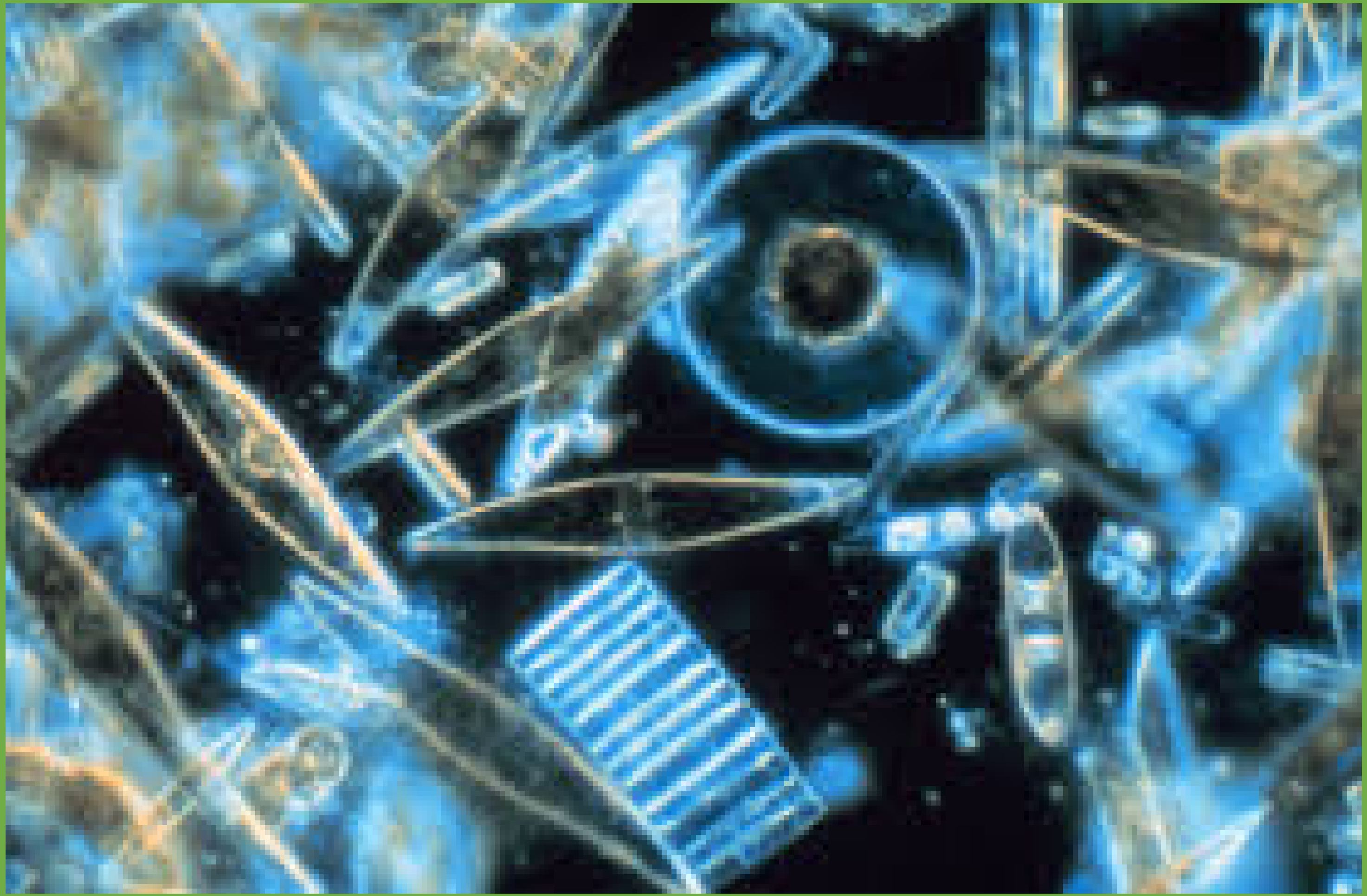

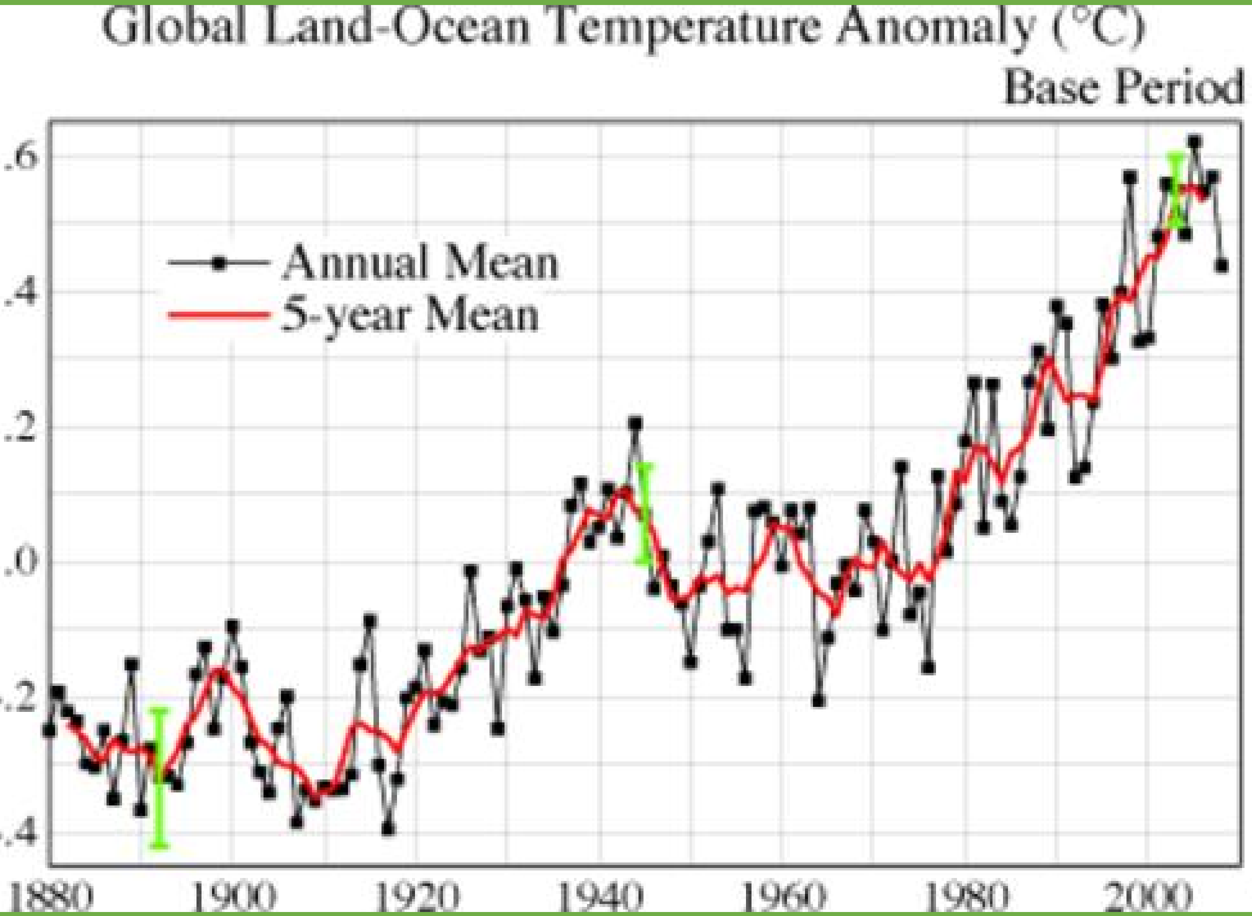

Base Period = 1951-1980

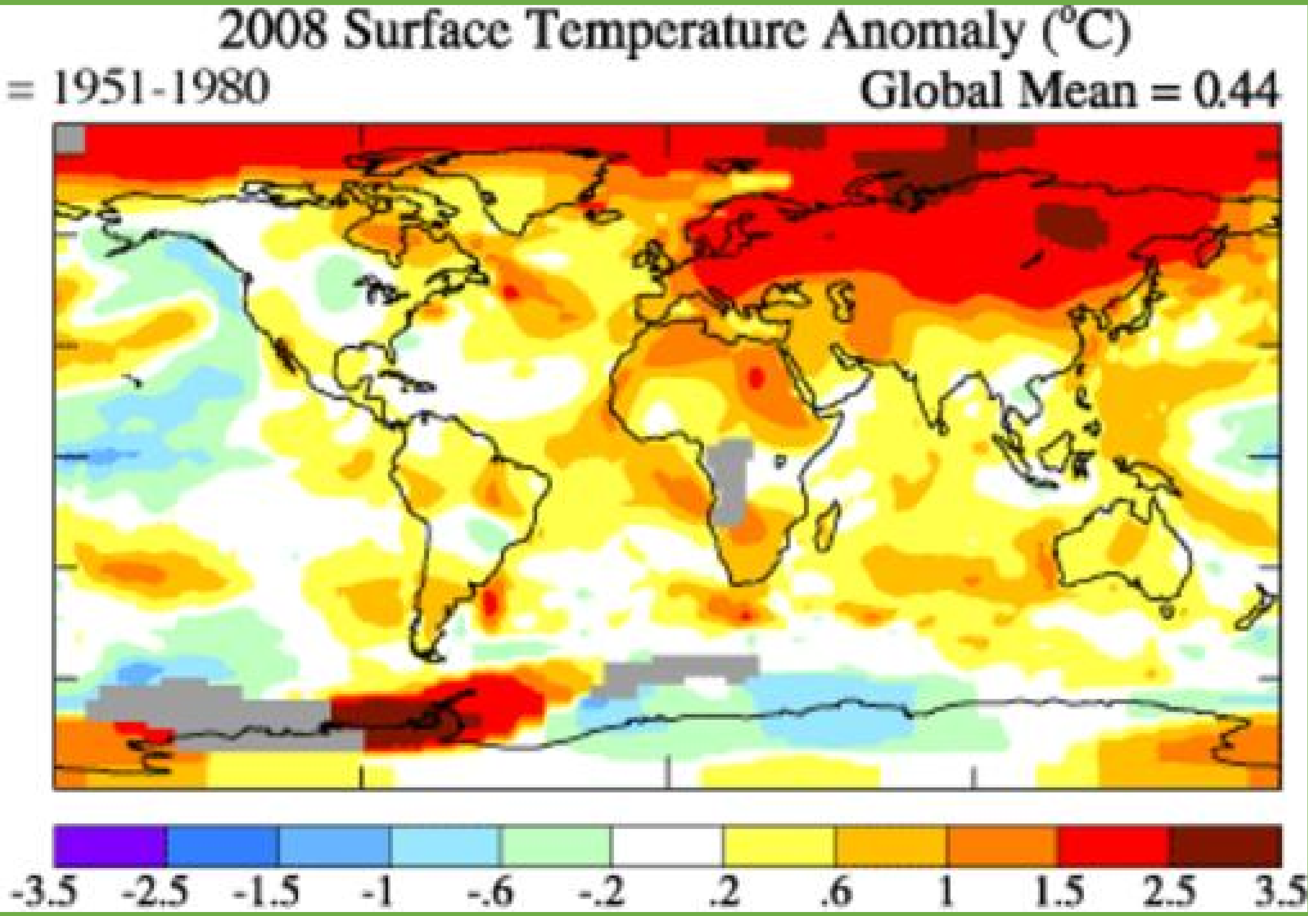

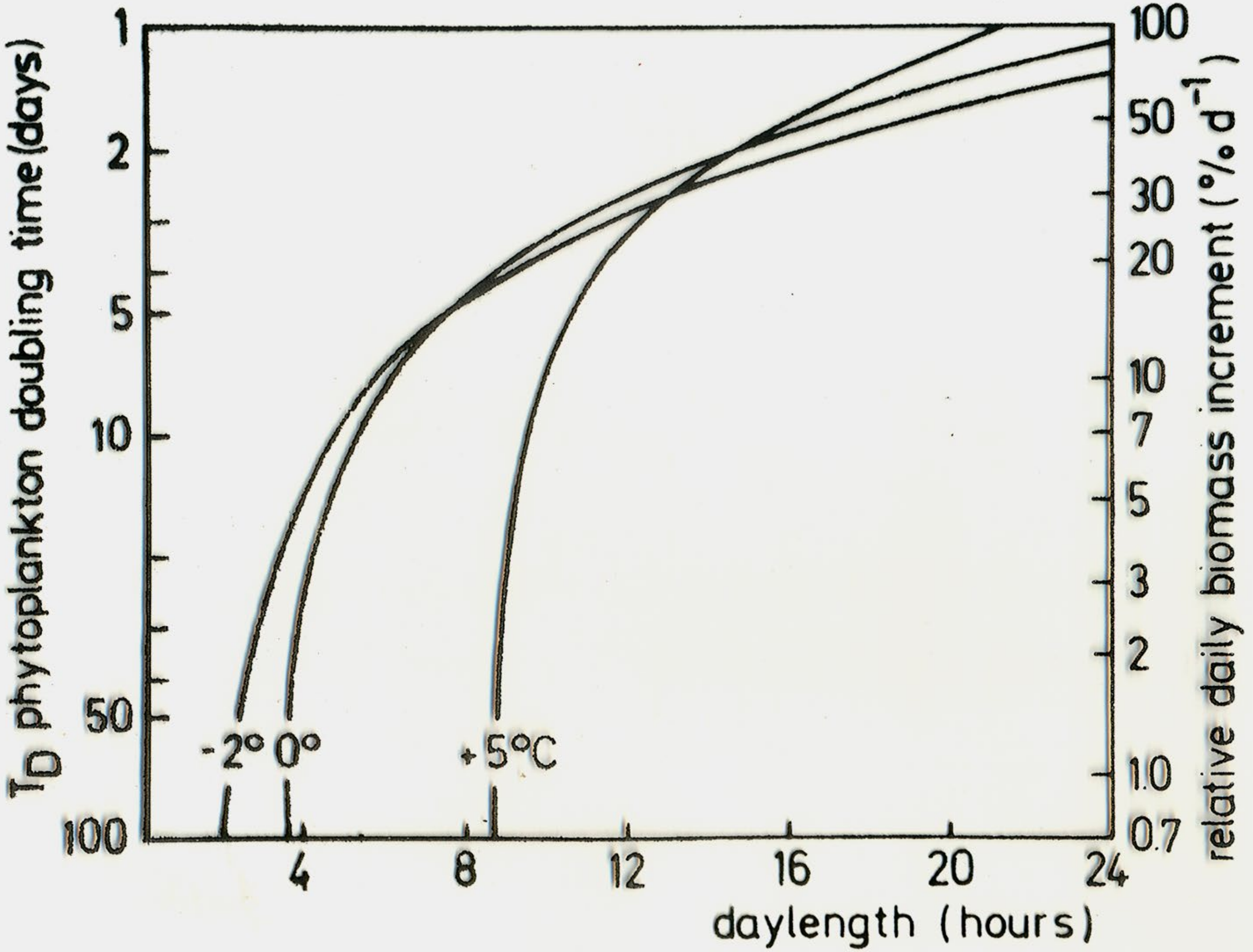

T_D phytoplankton doubling time (days)
1
2
5
10
50
100
relative daily biomass increment (%.d^{-1})
100
50
30
20
10
7
5
3
2
1.0
0.7
-2° 0°
+5°C
4
8
12
16
20
24
daylength (hours)

h i g h l i g h t s

Aim: To realize the energy inputs of the LCA to produce oil-rich algal biomass for biodiesel.

We considered recent technologies and main bottlenecks in algal biomass production.

We calculated and compared the energy requirements of the algal cultivation systems.

Lowest energy input for a complete harvesting process requires 4 MJ per m^3 algal suspension.

We propose the best scenario to grow microalgae for biodiesel.

g r a p h i c a l a b s t r a c t

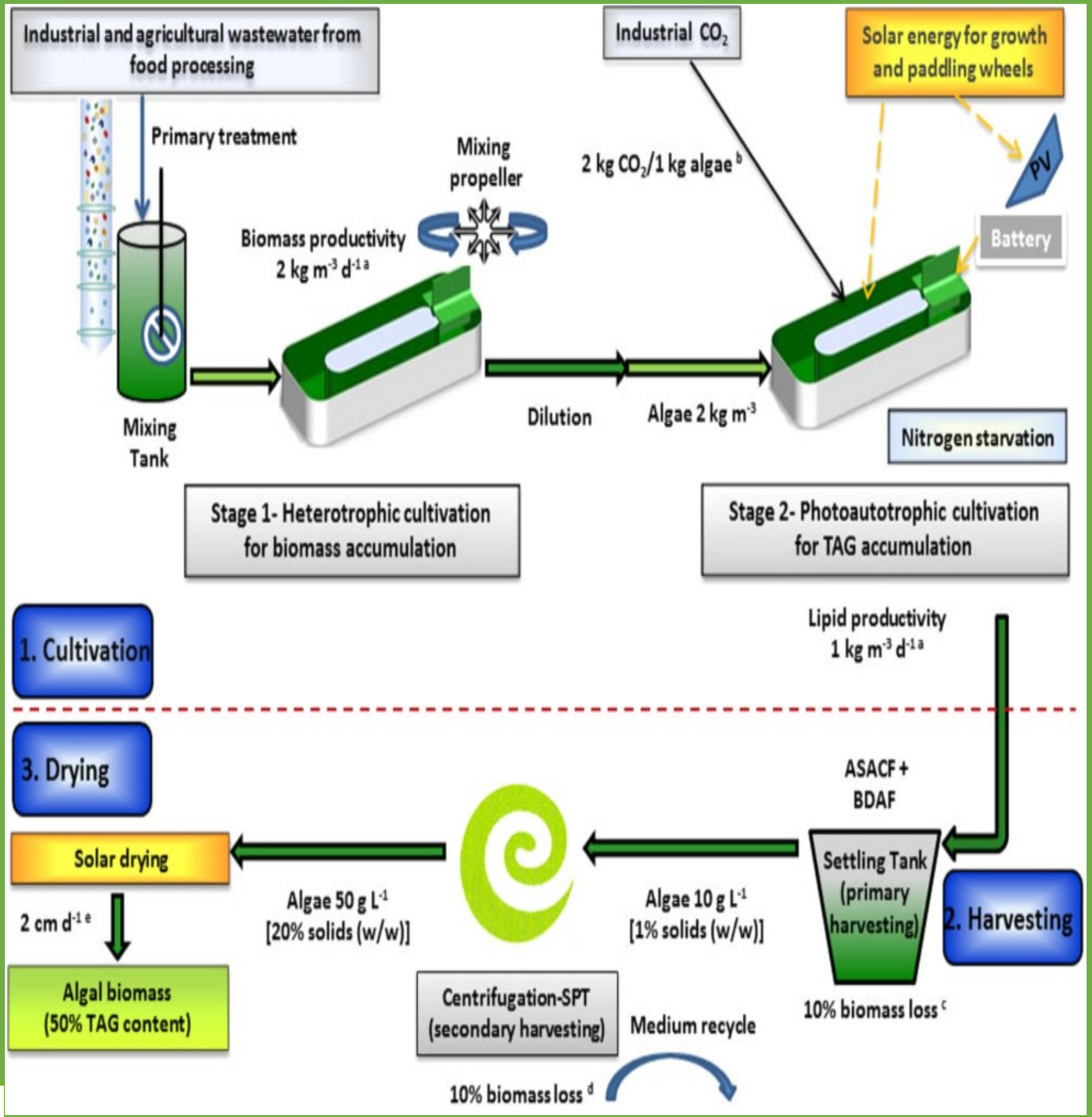

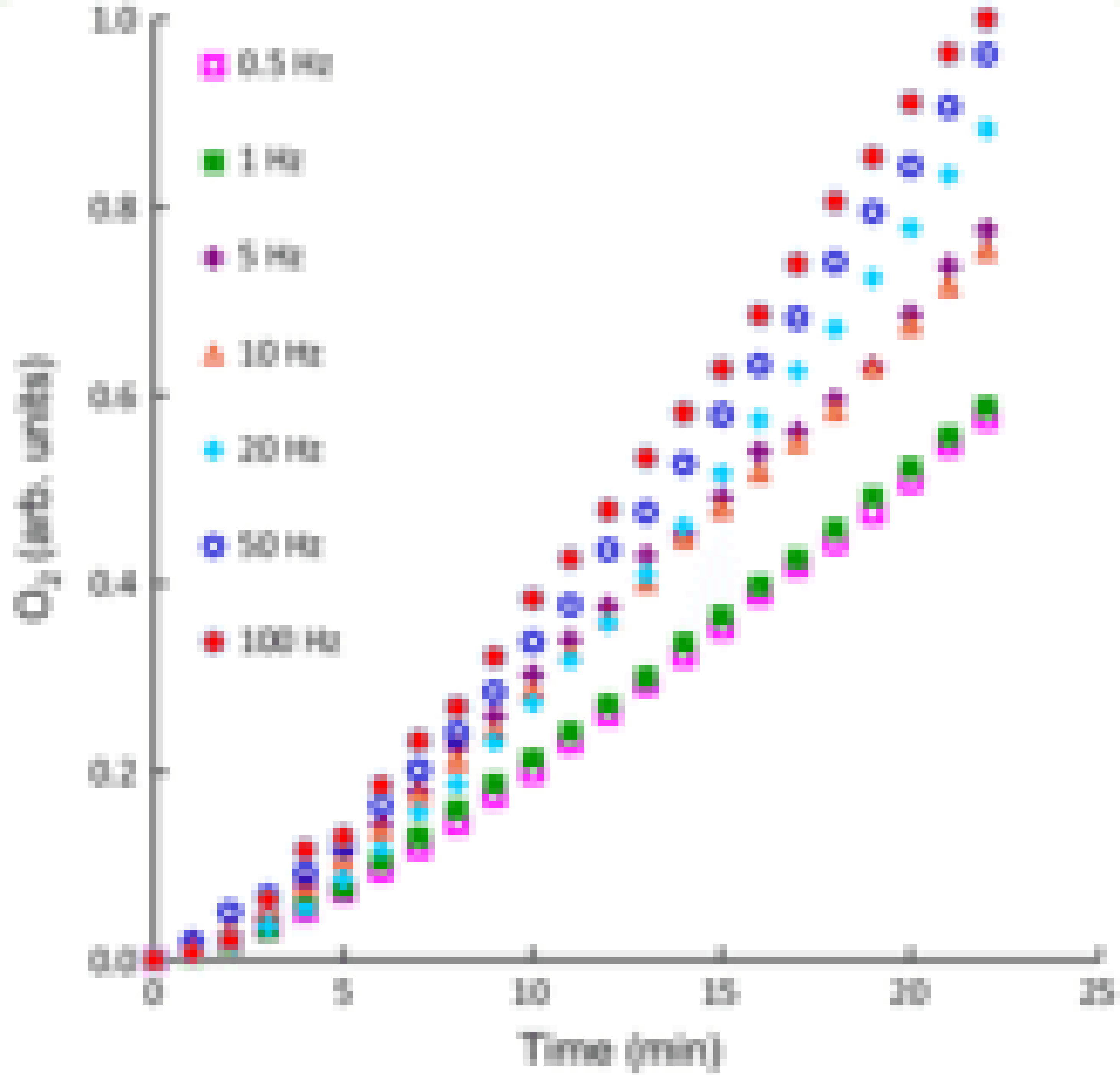

0.5 Hz
1 Hz
5 Hz
10 Hz
20 Hz
50 Hz
100 Hz
1.0
0.8
0.6
0.4
0.2
0.0
0
5
10
15
20
25
Time (min)


The end